SCATTERING
OF
EVANESCENT WAVES
BY REFLECTORS

A THESIS SUBMITTED TO
THE GRADUATE SCHOOL OF NATURAL AND APPLIED SCIENCES
OF
ÇANKAYA UNIVERSITY

BY

MUSTAFA KARA

IN PARTIAL FULFILLMENT OF THE REQUIREMENTS
FOR
THE DEGREE OF
DOCTOR OF PHILOSOPHY
IN

ELECTRONIC AND COMMUNICATION ENGINEERING
DEPARTMENT

JULY 2017

Title of the Thesis: Scattering of evanescent waves by reflectors

Submitted by : Mustafa Kara

Approval of the Graduate School of Natural and Applied Sciences, Çankaya University

Prof. Dr. Can ÇOĞUN
Director

I certify that this thesis satisfies all the requirements as a thesis for the degree of Doctor of Philosophy.

Prof. Dr. Hüseyin Selçuk Geçim
Head of Department

This is to certify that we have read this thesis and that in our opinion it is fully adequate, in scope and quality, as a thesis for the degree of Doctor of Philosophy.

Prof. Dr. Yusuf Ziya Umul
Supervisor

Examination Date: July 7, 2017

Examining Committee Members:

Prof. Dr. Yusuf Ziya UMUL (Çankaya University)

Assoc. Prof. Dr. Nursel AKÇAM (Gazi University)

Assoc. Prof. Dr. Uğur YALÇIN (Uludağ University)

Assist. Prof. Dr. Göker ŞENER (Çankaya University)

Assist. Prof. Dr. Emre SERMUTLU (Çankaya University)

STATEMENT OF NON PLAGIARISM

I hereby declare that all information in this document has been obtained and presented in accordance with academic rules and ethical conduct. I also declare that, as required by these rules and conduct, I have fully cited and referenced all material and results that are not original to this work.

Name, Last Name : Mustafa KARA

Signature :

Date : 07.07.2017

ABSTRACT

SCATTERING OF EVANESCENT WAVES BY REFLECTORS

KARA, Mustafa

Ph. D., Electronic and Communication Engineering Department

Supervisor: Prof. Dr.Yusuf Ziya Umul

July 2017, 121 pages

In this thesis, the scattering integral of electromagnetic incident waves scattered by a cylindrical parabolic perfectly electric conducting reflector is evaluated asymptotically. For the determination of the reflected fields the method of stationary phase, and for the diffracted fields the edge point method, whose details are given in appendix, are employed. A plane wave with an arbitrary angle is assumed as incident on the reflector. The evaluated reflected and diffracted fields are examined numerically for any observation point. In the evaluation of diffracted fields, the non-uniform diffracted field expression encountered is overcome by means of Fresnel function. For the numerical analysis, basically two cases are taken into consideration. One of them is the incident angle being real, and the other is the complex value of it. For these values, the effects of all possible combinations including the complex conjugates are examined and plotted numerically.

Keywords: Scattering, Reflection, Diffraction, Evanescent Waves.

ÖZ

EVANESENT DALGALARIN REFLEKTÖRLER TARAFINDAN SAÇINIMI

KARA, Mustafa

Doktora, Elektronik ve Haberleşme Mühendisliği Anabilim Dalı

Tez Yöneticisi: Prof. Dr. Yusuf Ziya Umul

Temmuz 2017, 121 sayfa

Bu tezde silindirik parabolik mükemmel elektriksel iletken bir reflektör tarafından saçınıma uğrayan gelen elektromanyetik dalgaların saçınım integrali asimptotik olarak hesaplanmıştır. Yansıyan alanların belirlenmesi için , ayrıntıları appendix'te verilen, stasyoner faz hesabı yöntemi, kırınan alanlar için köşe noktası/kırınım yöntemi kullanılmıştır. Bir düzlem dalganın herhangi bir geliş açısıyla reflektöre geldiği kabul edilmiştir. Hesaplanan yansıyan ve kırınan alanlar herhangi bir gözlem noktası için incelenmiştir. Kırınan alanların hesaplanmasında karşılaşılan üniform olmayan ifade Fresnel fonksiyonuyardımıyla düzeltilmiştir.Sayısal analiz için temel olarak iki durum düşünülmüştür. Bunlardan biri geliş açısının reel olması, diğeri kompleks olmasıdır. Bu değerler için kompleks eşlenik de dahil olmak üzere bütün olası durumlar incelenmiş ve sayısal olarak çizdirilmiştir.

Anahtar Kelimeler: Saçılma, Yansıma, Kırınım, Evanescent Dalgalar.

ACKNOWLEDGEMENT

The author wishes to express his deepest gratitude to his supervisor Prof. Dr. Yusuf Ziya UMUL for his guidance, advice, criticism, encouragements and insight throughout the research.

TABLE OF CONTENTS

LIST OF FIGURES

CHAPTER 1

INTRODUCTION

1.1 Background

In the analysis of wave propagation, scattering by the obstacles reflecting or diffracting the waves has a significant place. Exact solutions of the scattered fields are required to satisfy the Helmholtz equation as well as the boundary conditions. Basically, there are three solution methods known as analytic, numerical, and asymptotic. The first two are ray-based and current-based methods. High frequency asymptotic methods are used where the conventional solution methods fail. High frequency asymptotic condition is valid for $k\rho >> 1$, where k is the wave number, and ρ is the distance between source and observation point [1]. Geometrical Optics (GO) is one of the ray based techniques where it is assumed that electromagnetic waves propagate like rays at high frequencies. With this method only incident and reflected fields can be obtained. However, the drawback of this method is that, diffraction is out of its scope. Geometrical Theory of Diffraction (GTD) and Uniform Theory of Diffraction (UTD) are the ray-based techniques interested in investigation of diffracted fields [2-4].

These techniques cannot give a solution to a problem at the caustic regions. Therefore, fields go to infinity at caustic regions. This problem is overcome by the one of the current-based or integral-based techniques. One of the integral-based technique is the Physical Optics (PO) suggested by McDonald [5].

It is based on the integrating current induced on the scatterer surface. It gives accurate results except the edge diffracted fields. UTD analysis of the scattered fields by a Perfectly Electric Conducting (PEC) cylinder, asymptotic evaluation of the edge diffraction in cylindrical parabolic reflector antennas, and asymptotic evaluation for the scattering by a perfectly conducting cylinder are investigated [6-8].

Plane wave scattering by a perfectly conducting circular cylinder near a plane surface [9], and plane wave diffraction by various surfaces are also studied [10-13]. Physical optics (PO) does not consider shadow area contribution which is another lack of this method. Ufimtsev proposed physical theory of diffraction (PTD) method to solve these problems by defining additional correction current and called that non-uniform current and later it was called as fringe current as well. In PTD scattered field consists of uniform and non-uniform field components where the uniform field is obtained by the PO method and the non-uniform field is the result of the fringe current flowing on the discontinuities of the obstacle. Ufimtsev proposed general form of the PTD for electromagnetic edge-waves and eliminated the singularities for electromagnetic wave problems as well as that of acoustic waves [14-19]. A recent method for obtaining the exact solution of diffracted fields from perfectly electric conducting (PEC) surfaces is the modified theory of physical optics (MTPO) that eliminates all mentioned difficulties [20]. This method is applied to the problems of wedge diffraction [21], impedance wedge [22], impedance half plane [23]. Besides, diffraction by a black half plane [24], its uniform version [25], and MTPO based potential function of the boundary diffraction wave theory [26] are the applications of this method. PO theory for the wave diffraction by impedance surfaces [27], for the wave scattering by an impedance strip [28], and a half- plane with different face impedances [29] are also investigated. Physical optics of phase-conjugate mirrors [30], PO theory of resistive surfaces [31], physical optics integral of creeping waves [32] are other studies in this field.

UTD analysis of the scattered fields by a PEC cylinder is carried out by Pathak [33]. Asymptotic expansions of exact solutions for the scattered fields by perfectly conducting cylinder are carried out on a complex plane by Kouyoumjian [34]. A new method for the evaluation of the plane wave scattering by a perfectly conducting circular cylinder near a plane surface is proposed [35]. Diffracted and reflected fields by any convex cylinder are constructed by Keller [36]. The eigen-function solution for electromagnetic scattering by the cylinder, and parabolic cylinder [37, 38], and asymptotic approximation for the current on the illumination side of the cylinder by using the saddle point method are investigated [39]. The first two terms of the asymptotic expansion of the current on the illuminated part of the cylinder is obtained by Riblet [40]. Wetzel studied the high frequency currents on all parts of the cylinder [41], and the current on a parabolic cylinder in the vicinity of the shadow boundary is obtained by Waith [42].

Lawrence and Sarabandi obtained an analytical solution for the electromagnetic scattering by a dielectric cylinder [43] and the examination of the scattering by a conducting cylindrical reflector is carried out by Yalçın [44]. Plane wave scattering by a perfectly conducting circular cylinder near its surface is investigated by Borghi et al. [45]. Büyükaksoy and Uzgören studied the diffraction of waves generated by magnetic line source by the edges of a cylindrically curved surface with different phase impedance [46]. Physical optics integral for a cylinder is obtained as well. [47]. For some impedance and coated structures, equivalent surface currents in a standard general purpose PTD code are implemented [48]. Michaeli worked on the diffracted fields from the smooth convex perfectly conducting surface [49].

Young first proposed the physical meaning of the scattered fields by a knife edge by means of the superposition of the incident and edge diffracted fields [50]. However, his proposal was not able to account for the scattering in all ways. Later, it was replaced by the Fresnel diffraction theory. Moreover, mathematical expressions for the qualitative representation of the Young's idea is derived by means of Kirchhoff's integral [51-52] which has a new representation as well [53]. A work as a modification of Kirchhoff diffraction theory is carried out [54]. The obtained line integrals in the studies of [51] and [52] are the reduction forms of the surface integrals, and their evaluations give the edge diffracted fields. Later, Ganci's works on the half plane indicated that Maggi-Rubinowitz boundary diffraction wave does not give an exact solution, but an approximate solution [55-56].

Ufimtsev improved his theory in his study by reducing his surface integrals for reducing the edge point contributions [57]. Umul solved the corner problem with defining the exact form of the equivalent edge currents by using the axioms of the modified theory of physical optics (MTPO) he proposed [26, 58]. Scattering of the electromagnetic fields by the curved surfaces is studied [59, 60]. Scattering of a line source from a cylindrical parabolic impedance reflector is investigated [61]. Wave scattering by a wedge with perfectly reflecting boundaries is also investigated [62]. Scattering of high-frequency fields by conducting surfaces having cylindrical shapes is also available in the literature

[63-66]. Scattering by a cylindrical reflector which is fed by an offset electrical line source is investigated by Yalçın [67]. Cylindrical reflector antennas have been studied for a long time. Asymptotic evaluation of the reflected field is carried out for plane and cylindrical waves being incident on circular and parabolic cylinders [68]. Circular cylindrical reflectors for scattering of waves are studied as the part of curved shapes [69]. Exact solution of the half-plane problem is obtained for the PEC by Sommerfeld. Ufimtsev's PTD takes this exact solution as a base. Non-uniform fringe fields can be obtained by the subtraction of asymptotic PO fields from asymptotic exact solutions while the uniform fringe fields can be obtained by subtraction of uniform PO fields from uniform exact solutions. Umul pointed out that the values used by Ufimtsev were quite large and not giving the correct results for the fringe fields. According to his work, approximate expressions are not valid in the transition regions. Therefore, the solutions represented by the Fresnel functions must be used for the scattering problems [70]. Syed and Volakis derived PTD formulation for radar cross section (RCS), and for impedance and coated structures [71]. However, in their study, fringe field expressions are not studied analytically and numerically. Also, the work does not include the uniform field expressions. In the literature, there are several of applications on the diffraction analysis for impedance surfaces [72-75]. Studies in the scattering of inhomogeneous waves are keeping pace with the other classes of works in electromagnetic scattering phenomena [76-80]. Inhomogeneous waves are studied by using the method of complex rays that are calculated by the solution of the high frequency Luneberg-Kline expansion of the electromagnetic field having complex-valued amplitude and phase functions [81-85]. Scattering of evanescent waves by cylindrical structures is also studied [86].

In this thesis, scattering of a plane wave incident with an arbitrary complex angle on the cylindrical parabolic reflector is investigated. This study is the first to contribute the investigations in wave scattering. A time factor of exp (jωt) is assumed and suppressed throughout the study.

1.2 Objectives

The aim of this thesis is to investigate the behavior of evanescent waves. For this goal, inhomogeneous plane waves and Gaussian beams that are known as the members of evanescent waves will be studied. Inhomogeneous plane wave will be derived and its scattering behavior will be observed and discussed. Similarly, Gaussian beam will be taken into consideration. As a third attempt, scattering expressions of a HOMOGENEOUS plane wave by a cylindrical parabolic PEC reflector will be obtained. To do that, for the asymptotic evaluation of the scattering integral, reflected field will be obtained by means of stationary phase point method. Then edge point method will be used to obtain the diffracted field. The obtained fields will be plotted numerically for both homogeneous and inhomogeneous plane waves.

1.3 Organization of the Thesis

This thesis is composed of six chapters.

Chapter 1, which is the introduction, is a brief history of the works on electromagnetic scattering that have been carried out so far.

Chapter 2 explains the diffraction theory. Geometrical theory of diffraction (GTD) and Kirchhoff's diffraction theory are described. Also, Fresnel function that is used in obtaining a uniform fields by exploiting its asymptotic property is introduced.

Chapter 3 is an introduction to evanescent waves. For this aspect, as the subclasses of evanescent waves, inhomogeneous waves and Gaussian beams are described. Theoretical deductions are verified by the graphical representations.

In Chapter 4, mathematical expressions of Modified Theory of Physical Optics article [20] on which the scattering integral we started to evaluate asymptotically is based are clarified.

Chapter 5scattering of homogeneous and inhomogeneous plane waves by a cylindrical parabolic perfectly electric conducting reflector is investigated.

Chapter 6 is the conclusion section.

Appendix describes the Stationary Phase Point Method and Edge Point Method used for the asymptotic evaluation of integrals.

CHAPTER 2

DIFFRACTION THEORY

2.1 The geometrical theory of diffraction [2]

This theory was developed by Keller for homogeneous isotropic media but it has also been extended to inhomogeneous, anisotropic and to media such as warm plasma supporting several wave types. The simple ray solutions can be utilized for complicated high-frequency scattering problems by using the geometrical theory of diffraction. The theory says that the scattered field at any observation point is combination of geometrically reflected or refracted, and diffracted rays. The incident field is represented by rays which are scattered when striking an obstacle. The nature of these scattered rays around the scatterer surface depends on the surface and medium properties.

A ray striking a flat obstacle is reflected or refracted according to the plane-wave reflection or refraction law. It is propagated with an amplitude which is determined by the plane-wave reflection coefficient.

A ray striking a curved obstacle is reflected as from a plane which is tangent to the surface at the striking point, but the intensity along its path is determined by a "divergence coefficient," due to the surface curvature. The radius of curvature explains the spreading of the energy contained in a narrow ray bundle. Here we assume that the radius of curvature is always much greater than the wavelength of the incoming rays. The reflected and refracted rays are encountered in the geometrical optics of isotropic and anisotropic media.

A ray incident normally on an edge creates "edge-diffracted" rays that emerge in all directions in the plane that is perpendicular to the edge at the striking point. The intensity along an edge-diffracted ray decreases like $\rho^{1/2}$, where ρ is the distance from the edge.

The edge-diffracted rays due to an obliquely incident ray lie on a cone that has a semi-angle at the apex equal to the angle between the incident ray and the edge. The incident and diffracted rays lie on opposite sides of the perpendicular plane through the striking point.

A ray striking on a conical tip or a corner is scattered in all directions. The intensity along a "tip-diffracted" ray decreases like 1/r, where r is the distance from the tip.

A ray incident tangentially on a curved object creates a creeping ray traveling along the obstacle surface into the shadow region. Its amplitude along the surface decays exponentially with distance.

If there is an interface between two media, an incident ray at the critical angle θc from the optically denser medium launches a lateral ray that travels along the interface in the optically thinner medium and sheds energy back to the denser medium by refraction. The decay of the lateral ray amplitude due to energy leakage is found to be algebraic.

The trajectories of the reflected and diffracted rays are in accord with Fermat's principle of least propagation time, and the variation behavior of the field, both in amplitude and phase, along a reflected or diffracted ray can often be predicted from simple geometrical considerations.

The initial amplitude and phase along a diffracted ray cannot be determined from the geometrical theory but it must be taken from the asymptotic solution for a simple canonical scatterer whose contour at the diffraction point is identical to that of the obstacle.

After satisfying this condition, the scattered field for the canonical object agrees with the asymptotic form of the rigorous solution as the wave number goes to infinity. The geometrical theory of diffraction has important features such as conceptual simplicity and broad range of applicability in homogeneous and inhomogeneous, isotropic or anisotropic regions. The drawback of the theory is that it is based on some postulates whose validity have not been proved so far. Therefore, it is necessary to verify the theory by using the asymptotic expansions of the problems. However, it is important to note that the geometrical theory of diffraction is capable of predicting at least the dominant effects of high-frequency scattering for relatively arbitrary conditions. By using space-time rays instead of time-harmonic rays this theory has also been applied to transient problems in dispersive media.

Generally, it is necessary to solve the scattering problems of the canonical form for specification of initial field values on diffracted rays. However, certain general observations can be made for the multiplicity and orientation of diffracted rays created by an incident ray.

For example, when using a lowest order of approximation, an incident ray on a slowly curved edge in a slowly varying medium creates the same scattered field as a plane wave in a homogeneous medium that is incident on a straight edge extended along the tangent at the striking point.

2.2 Kirchhoff's diffraction theory

$$\nabla^2 u + k^2 = 0. \tag{2.1}$$

This indicates that there is no any source inside the volume because the wave equation is equal to zero.

$$\nabla^2 G + k^2 G = -4\pi\delta(r - r'), \tag{2.2}$$

where G is the Green function.

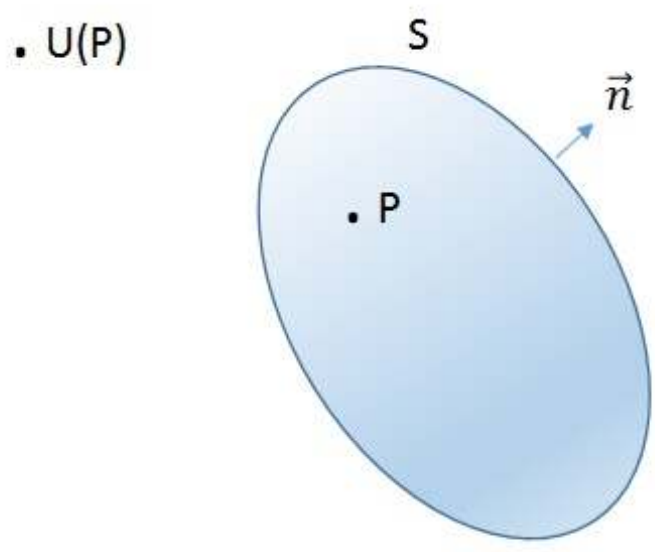

Figure 1 Source enclosed by S and observation point outside S.

The term in the right side of the equation shows that there is a point which is a source somewhere into the space. We can write that,

$$\nabla(u\nabla G - G\nabla u) = u\nabla^2 G - G\nabla^2 u. \tag{2.3}$$

Taking the volume integral of both sides we write,

$$\iiint \nabla(u\nabla G - G\nabla u)dV' = \iiint (u\nabla^2 G - G\nabla^2 u)dV'. \tag{2.4}$$

Left hand side of the equation is reduced to surface integral as,

$$\oint\!\!\!\oint (u\nabla G - G\nabla u).\vec{n}\, dS = \iiint (u\nabla^2 G - G\nabla^2 u) dV'. \tag{2.5}$$

Using Eq. (2.2) we can write,

$$\oint\!\!\!\oint (u\nabla G - G\nabla u).\vec{n}\, dS = k^2 G u - 4\pi\delta(r - r')u + k^2 G u, \tag{2.6}$$

$$\oint\!\!\!\oint (u\nabla G - G\nabla u).\vec{n}\, dS = -4\pi\delta(r - r')u(\vec{r}). \tag{2.7}$$

Finally,

$$u(P) = -\frac{1}{4\pi}\oint\!\!\!\oint (u\nabla G - G\nabla u).\vec{n}\, dS, \tag{2.8}$$

which is the Huygens-Helmholtz theorem. As a result,

$$\oint\!\!\!\oint (u\nabla G - G\nabla u).\vec{n}\, dS = \begin{cases} -4\pi u(P)\,, & P \in V \\ 0\,, & otherwise \end{cases}. \tag{2.9}$$

If the observation point is carried out of the volume (body), the Green function is zero inside the body but nonzero outside of it.

$$u(P) = -\frac{1}{4\pi}\oint\!\!\!\oint \left(u\frac{\partial G}{\partial n} - G\frac{\partial u}{\partial n}\right) dS. \tag{2.10}$$

Eq.(2.10) is known as Kirchhoff's diffraction integral.

Letting the body be transparent we draw Fig. 2 below.

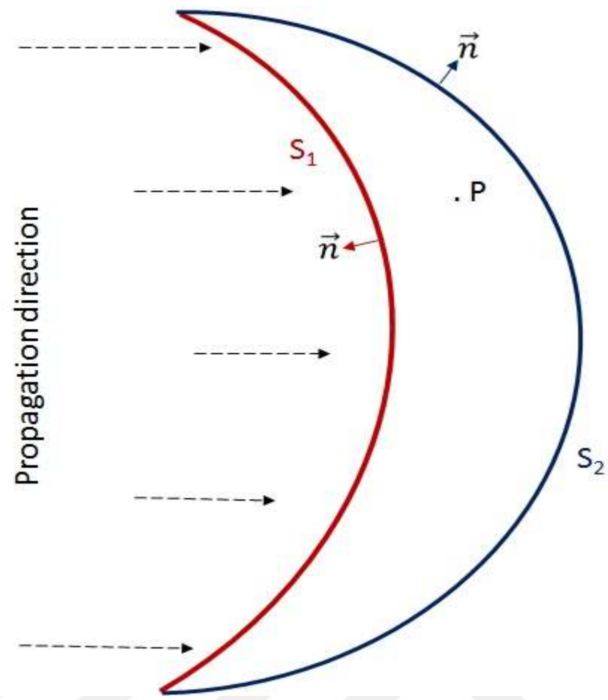

Figure 2 Possible diffraction geometry.

In this case we write,

$$\int_{S_1+S_2}(u\nabla G - G\nabla u).\vec{n}dS = -4\pi u(P), \tag{2.11}$$

which can be rewritten as,

$$\int_{S_1}(u\nabla G - G\nabla u).\vec{n}dS + \int_{S_2}(u\nabla G - G\nabla u).\vec{n}dS = -4\pi u(P). \tag{2.12}$$

In Fig. 3 diffraction problem is separated into three regions as shown.

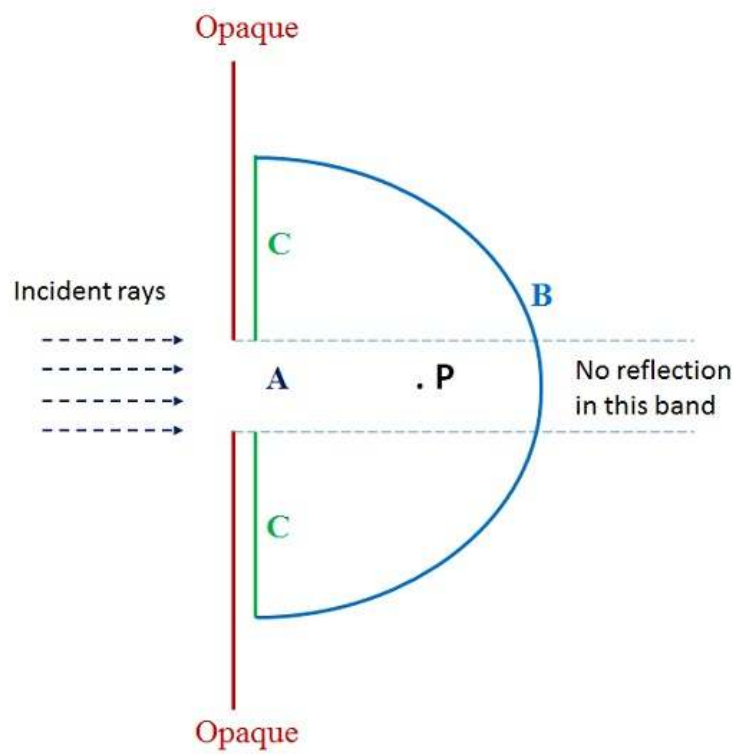

Figure 3 Diffraction geometry. Incident rays represent the source region. Parts A, B, and C represent the diffraction regions.

Transmitted and reflected electric and magnetic fields are needed by means of incident ones. For this situation, the properties of the boundary are also taken into account. On the surface of the opaque sheet the boundary conditions must be satisfied. The diffraction integral for S_2 in Fig.2 vanishes inversely as the hemisphere radius goes to infinity [87].

The Kirchhoff's approximation is based on two assumptions:

1. ψ and its normal derivative on the surface ($\frac{\partial \psi}{\partial n}$) vanish everywhere on S_1 but not in the opening(s).

2. The values of ψ and $\frac{\partial \psi}{\partial n}$ in the openings are equal to the values of the incident wave.

Therefore, there are A, and C parts left.

$$\int_{A+B+C}(u\nabla G - G\nabla u).\vec{n}dS = -4\pi u(P), \quad (2.13)$$

$$\mathrm{u(P)} = -\frac{1}{4\pi}\iint_{\mathrm{A}} \left(\mathrm{u}\frac{\partial \mathrm{G}}{\partial \mathrm{n}} - \mathrm{G}\frac{\partial \mathrm{u}}{\partial \mathrm{n}}\right)\mathrm{dS}, \quad (2.14)$$

or

$$u(P) = -\frac{1}{4\pi}\iint_{A} \left(u_i\frac{\partial G}{\partial n} - G\frac{\partial u_i}{\partial n}\right)dS. \quad (2.15)$$

2.3 Fresnel function

When the field expressions approach to infinity at the reflection and transmission boundaries for the scattering problems, field expressions are needed to be finite for these points. For these cases asymptotic property of the Fresnel function can be used [88]. Fresnel integral function can be given as,

$$F[x] = \frac{\exp{(j\pi/4)}}{\sqrt{\pi}}\int_{x}^{\infty} exp(-jt^2)dt. \quad (2.16)$$

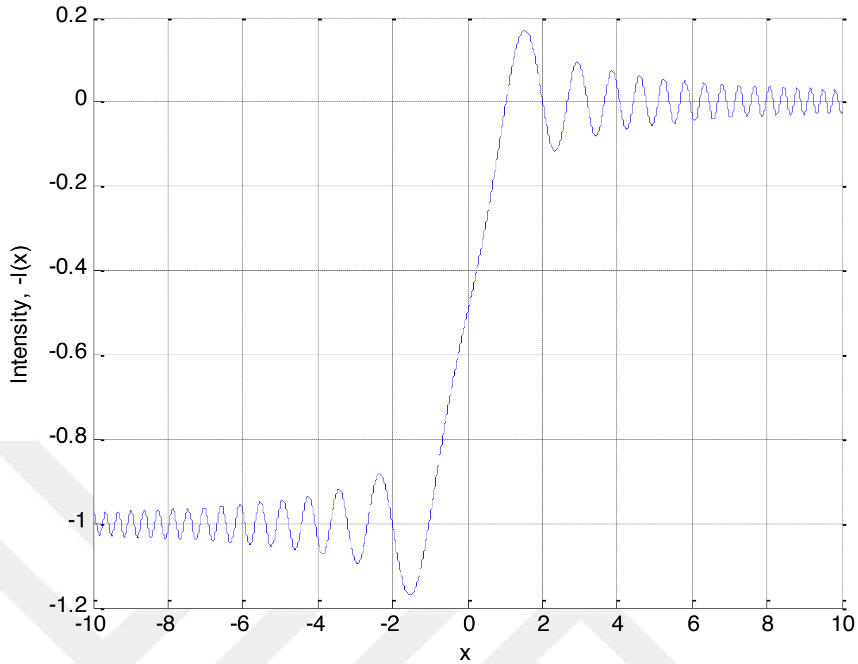

Figure 4 Plot of Fresnel function, -I(x).

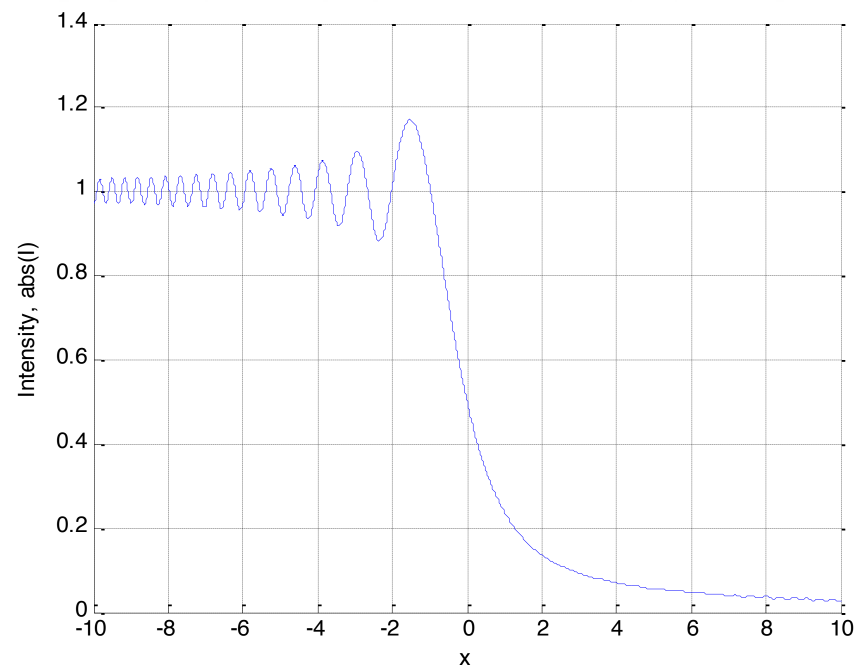

Figure 5 Plot of Fresnel function, abs (I).

We know that,

$$F[x] - u(-x) = \begin{cases} F[x] - 1, & x < 0 \\ F[x], & x > 0 \end{cases}, \tag{2.17}$$

and

$$\int_{-\infty}^{\infty} exp(-jt^2)dt = 1. \tag{2.18}$$

Eq. (2.16) can be rewritten as,

$$F[x] - 1 = \frac{\exp(j\pi/4)}{\sqrt{\pi}} \int_x^{\infty} exp(-jt^2)dt - 1\,, \tag{2.19}$$

$$F[x] - 1 = \frac{\exp(j\pi/4)}{\sqrt{\pi}} \left[\int_x^{\infty} exp(-jt^2)dt - \int_{-\infty}^{\infty} exp(-jt^2)dt\right], \tag{2.20}$$

$$F[x] - 1 = \frac{\exp(j\pi/4)}{\sqrt{\pi}} \left[\int_x^{\infty} exp(-jt^2)dt - \left(\int_{-\infty}^{x} exp(-jt^2)dt + \int_x^{\infty} exp(-jt^2)dt\right)\right].$$

(2.2

As a result,

$$F[x] - 1 = \frac{\exp(j\pi/4)}{\sqrt{\pi}} \left[-\int_{-\infty}^{x} exp(-jt^2)dt\right]. \tag{2.22}$$

Letting $t = -p$, for the lower and upper limits of the integral in Eq. (2.22) we write

$$t = -\infty \xrightarrow{yields} p = \infty\,, \tag{2.23}$$

$$t = x \xrightarrow{yields} p = -x\,, \tag{2.24}$$

Eq. (2.22) becomes as,

$$F[x] - 1 = -\frac{\exp(j\pi/4)}{\sqrt{\pi}} \int_{\infty}^{-x} \exp(-jp^2)(-dp). \quad (2.25)$$

Applying change of variable again,

let $t = -p$, then $dt = -dp$,

$$p = \infty \xrightarrow{yields} t = -\infty \, , \quad (2.26)$$

$$p = -x \xrightarrow{yields} t = x \, , \quad (2.27)$$

Eq. (2.25) becomes as,

$$F[x] - 1 = \frac{\exp(j\pi/4)}{\sqrt{\pi}} \int_{-\infty}^{x} \exp(-jt^2)(-dt) \, , \quad (2.28)$$

from which it can be written that,

$$\int_{-\infty}^{x} \exp(-jt^2)(-dt) = \int_{-x}^{\infty} \exp(-jt^2)(-dt). \quad (2.29)$$

Finally,

$$F[x] - 1 = -\frac{\exp(j\pi/4)}{\sqrt{\pi}} \int_{-x}^{\infty} \exp(-jt^2)dt \, , \quad (2.30)$$

$$F[x] - u(-x) = \begin{cases} -\frac{exp(j\pi/4)}{\sqrt{\pi}} \int_{-x}^{\infty} exp(-jt^2)dt\,, & x < 0 \\ \frac{exp(j\pi/4)}{\sqrt{\pi}} \int_{x}^{\infty} exp(-jt^2)dt\,, & x > 0 \end{cases}, \qquad (2.31)$$

by combining these two cases we get,

$$F[x] - u(-x) = sign(x) \int_{|x|}^{\infty} exp(-jt^2)dt, \qquad (2.32)$$

we obtain,

$$F[x] - u(-x) = sign(x)F[|x|]. \qquad (2.33)$$

Another result can be found as,

$$sign(x)F[|x|] \approx \frac{exp(-j\pi/4)}{2\sqrt{\pi}} \frac{exp(-jx^2)}{x} \qquad (2.34)$$

The plot of Eq. (2.33) is shown in Fig. 6 below.

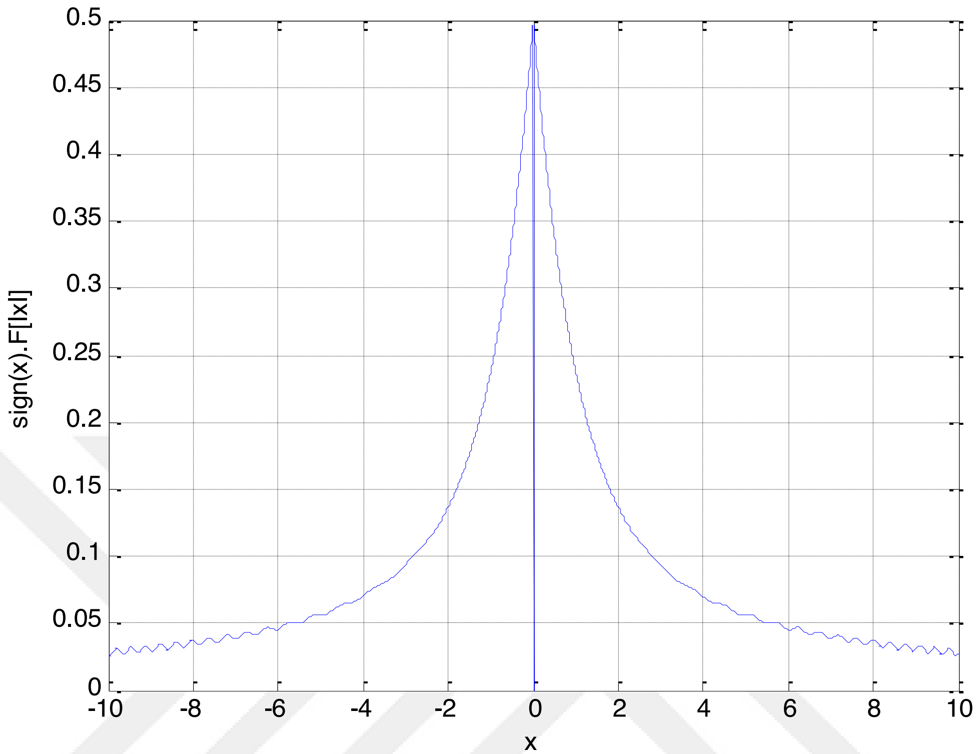

Figure 6 Plot of F[x]-u(-x).

Fresnel sine and integral is given as,

$$S(u) = \int_0^u \sin\left(\frac{1}{2}\pi x^2\right) dx, \tag{2.35}$$

and its plot is given in Fig. 7.

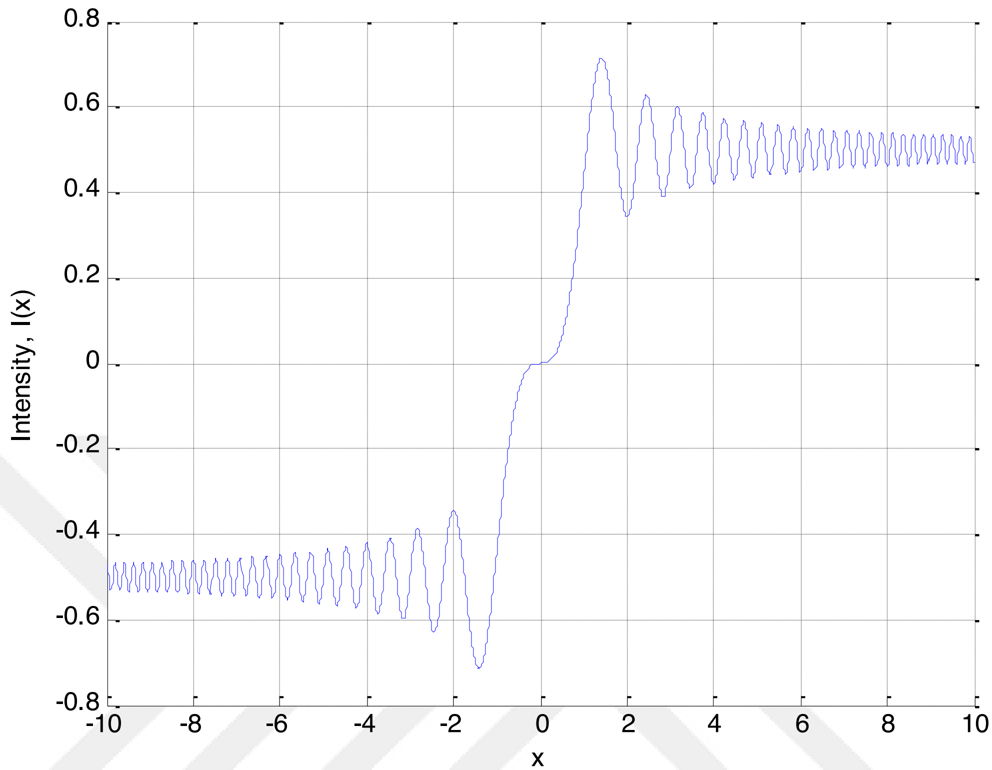

Figure 7 Plot of Fresnel sine function.

Fresnel cosine function is given in Eq. (2.35), and its plot is given in Fig. 8.

$$C(u) = \int_0^u \cos\left(\frac{1}{2}\pi x^2\right) dx. \tag{2.36}$$

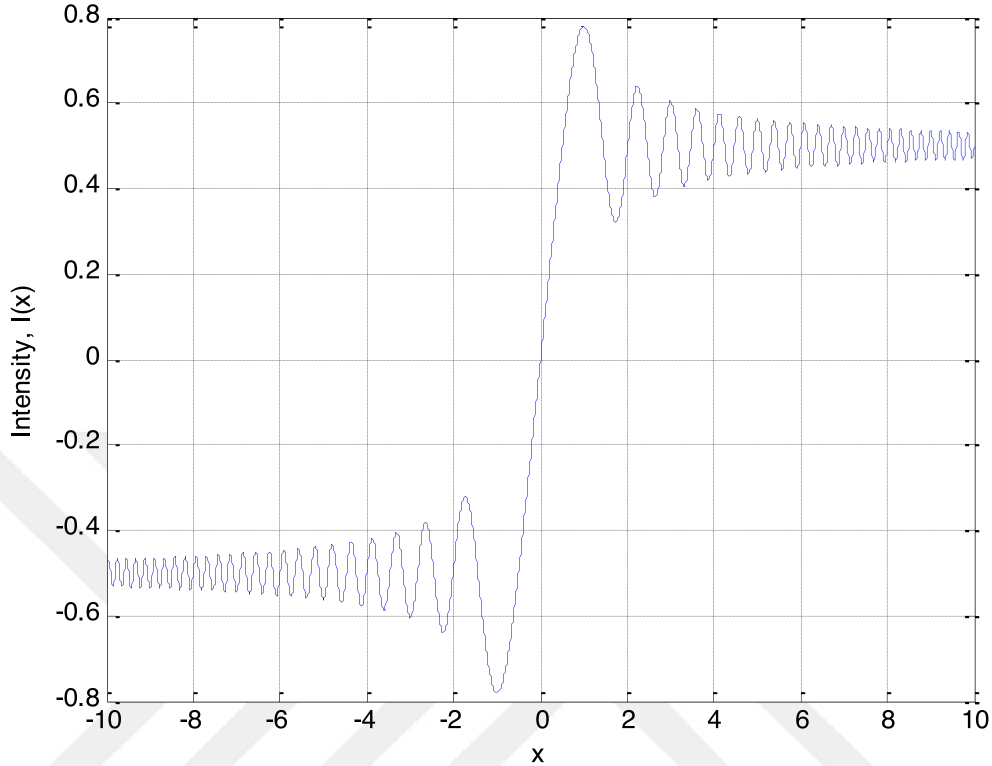

Figure 8 Plot of Fresnel cosine function.

Fresnel integral function is the combination of Fresnel cosine and sine functions as,

$$F[x] = C(u) + j\,S(u). \quad (2.37)$$

CHAPTER 3

EVANESCENT WAVES

For the wave propagation concepts evanescent waves have been in the secondary place due to the nonevanescent waves coming first. Their contribution to the total field is in the near field but they can be ignored in the far field due to their negligible amplitudes. However, if they are the only waves representing the entire field they must be expressed according to their parameters. They are investigated for the cases such as the surface wave structures of slab or rod dielectric to which evanescent waves are exterior. Also they are concerned when there are two media one of which is denser than the other, and when total reflection occurs. They take place on the dark side of the caustics as well [84].

After the development of laser sources evanescent waves have been a very popular research area of optics. They comprise the inhomogeneous plane waves and the Gaussian beams [85]. The characteristics of these waves is that their amplitudes decay in a direction that is different from propagation direction. Studies on evanescent waves are carried out by the complex-rays method in which the eikonal and transport equations are obtained by the solution of the high frequency Luneberg-Kline expansion of the electromagnetic field for complex-valued amplitude and phase functions. [84, 85]. Solution of these functions are used to calculate the complex rays.

In this chapter we will discuss the Gaussian beams and inhomogeneous plane waves that are the members of these waves.

3.1 Derivation of an inhomogeneous wave expression from a plane wave

To obtain an inhomogeneous wave we can start with a plane wave as in Eq. (3.1).

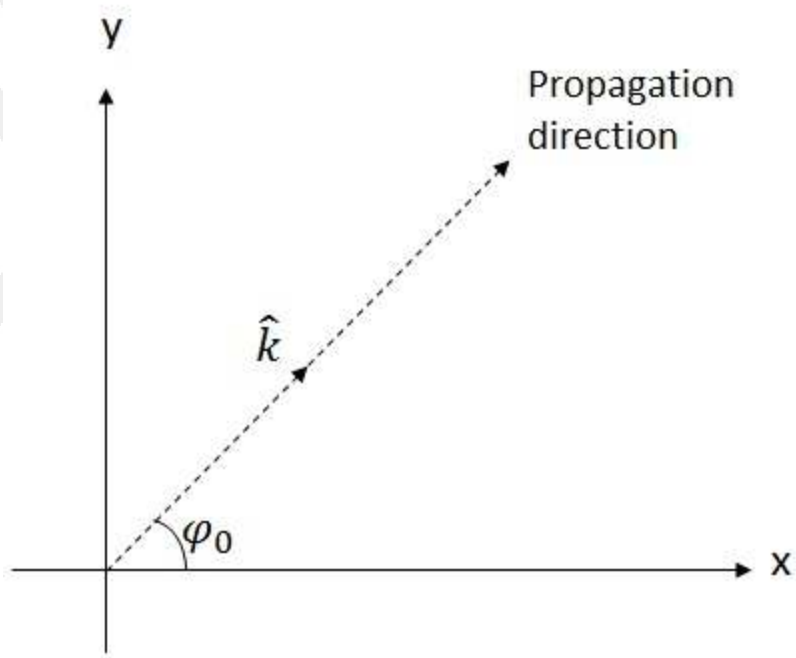

Figure 9 Plane wave propagation.

$$u = \hat{e}_z exp\left(-j\vec{k}.\vec{r}\right), \tag{3.1}$$

where

$$\vec{r} = x\hat{e}_x + y\hat{e}_y + z\hat{e}_z \ , \tag{3.2}$$

and

$$\vec{k} = k\big(cos\,\varphi_0\,\hat{e}_x + sin\,\varphi_0\,\hat{e}_y\big). \tag{3.3}$$

Here φ_0 is the angle of incidence, k is the wave number expressed as $2\pi/\lambda$. The dot product of $\vec{k}$ and $\vec{r}$ is written as,

$$k\,xcos\,\varphi_0 + ky\,sin\,\varphi_0. \tag{3.4}$$

Substituting Eq. (3.4) into Eq. (3.1) the wave becomes,

$$u = exp\big(-jk(xcos\,\varphi_0 + y\,sin\,\varphi_0)\big). \tag{3.5}$$

In Cartesian coordinates. It can be written in cylindrical coordinates by using,

$$x = \rho cos\,\varphi\ , \tag{3.6}$$

and

$$y = \rho sin\,\varphi\ . \tag{3.7}$$

Eq. (3.5) is written as,

$$u = exp\big(-jk(\rho cos\varphi cos\,\varphi_0 + \rho sin\varphi\,sin\,\varphi_0)\big). \tag{3.8}$$

As a result,

$$u = exp\big(-jk\rho cos(\varphi - \varphi_0)\big)\ , \tag{3.9}$$

is obtained for an outgoing wave. Now, we can conclude that for an incoming wave, its expression will be as,

$$u = exp\big(jk\rho cos(\varphi - \varphi_0)\big). \tag{3.10}$$

If we use this expression to obtain an inhomogeneous plane wave, we need to take the angle of incidence as complex parameter.

Assuming,

$$\varphi_0 = \varphi_r + j\varphi_i \ , \tag{3.11}$$

Eq. (3.10) can be rewritten as,

$$u = exp\big(jk\rho cos(\varphi - \varphi_r - \varphi_i)\big) \ , \tag{3.12}$$

which can be arranged as,

$$u = exp(jk\rho cos(\varphi - \varphi_r)\, cosh\, \varphi_i - k\rho\, sin(\varphi - \varphi_r)\, sinh\, \varphi_i). \tag{3.13}$$

By letting,

$$k_1 = k\, cosh\, \varphi_i \ , \tag{3.14}$$

and

$$k_2 = k\, sinh\, \varphi_i \ , \tag{3.15}$$

u can be expressed as,

$$u = exp\big(jk_1\rho cos(\varphi - \varphi_r)\big)exp\big(-k_2\rho sin(\varphi - \varphi_r)\big), \tag{3.16}$$

or

$$u = exp[jk_1(xcos\varphi_r + ysin\varphi_r)]exp[-k_2(xsin\varphi_r - ycos\varphi_r)]. \quad (3.17)$$

This equation is an inhomogeneous plane wave in which the first exponential term determines the propagation direction and the second one identifies the amplitude of the wave. Amplitude of this wave attenuates in a way that is perpendicular to the propagation direction in a homogeneous medium [89].

3.2 Numerical results

The following figures are plotted for λ=0.1m, ρ =3λ and $0 \leq \varphi \leq 2\pi$.

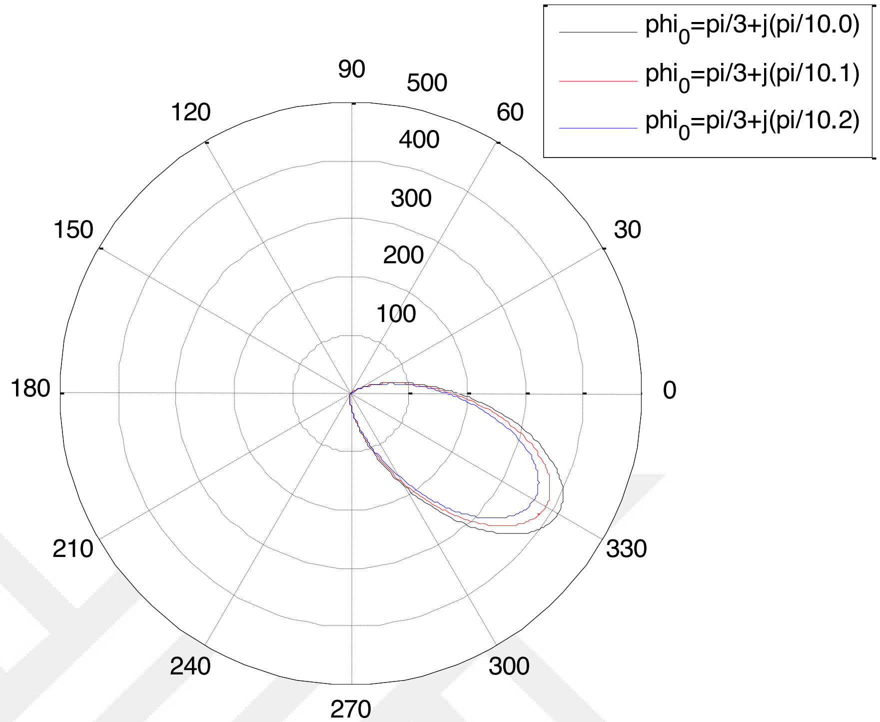

Figure 10 Inhomogeneous wave for various φ_i values of incident angle.

In Fig. 10 incident angle has a real component φ_r of $\pi/3$ radians, which is 60 degrees, and the beam direction is in $-\pi/6$ radians. This verifies the fact that the beam decays in the direction that is perpendicular to the direction of propagation. In Fig. 11 amplitude of the beam versus φ graph is given that validates our conclusion we did for the Fig. 10.

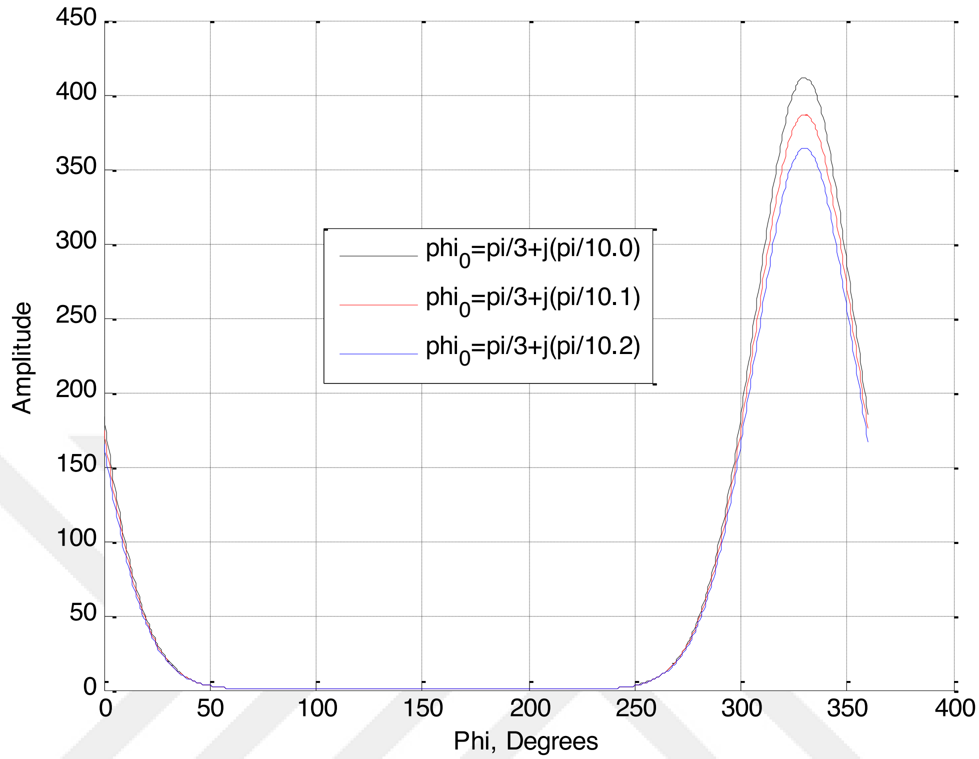

Figure 11 Inhomogeneous wave for various φ_i values of incident angle.

As we can see from the figures above, if the imaginary component φ_i of the incident angle increases, amplitude of the wave increases as well. Complex conjugate of incident angle yields the field that is opposite of the first one. That is, incident angle and its complex conjugate result in the fields that are 180 degrees out of phase. In Fig. 12 and Fig. 13, incident angles given are the complex conjugates of the ones given in Fig. 10 and Fig. 11, and the fields obtained are in opposite directions between these two groups.

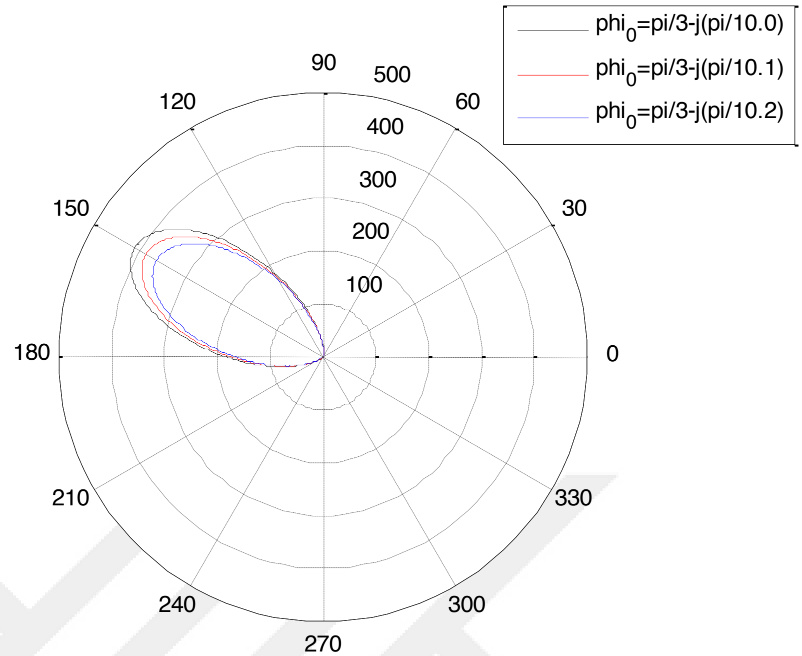

Figure 12 Inhomogeneous wave for various φ_i values of incident angle.

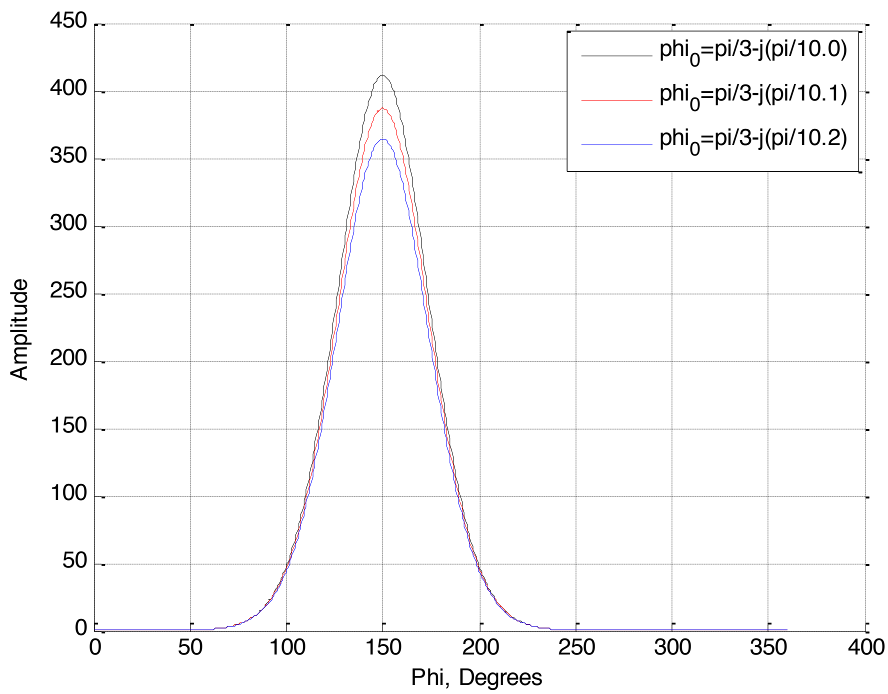

Figure 13 Inhomogeneous wave for various φ_i values of incident angle.

If the φ_r is decreased, this results in a phase shift in the beam only. That is, the beam shift occurs but the beam magnitude/amplitude is not affected. In any case, the attenuation direction is always perpendicular to the real part of the incident angle.

When φ_r is equal to zero, one possible radiation pattern becomes as in Fig. 14. In that figure beam is directed to -90 degrees. However, if the φ_i is taken as negative, beam direction is directed to +90 degrees that is the opposite direction of the former one as shown in Fig. 15.

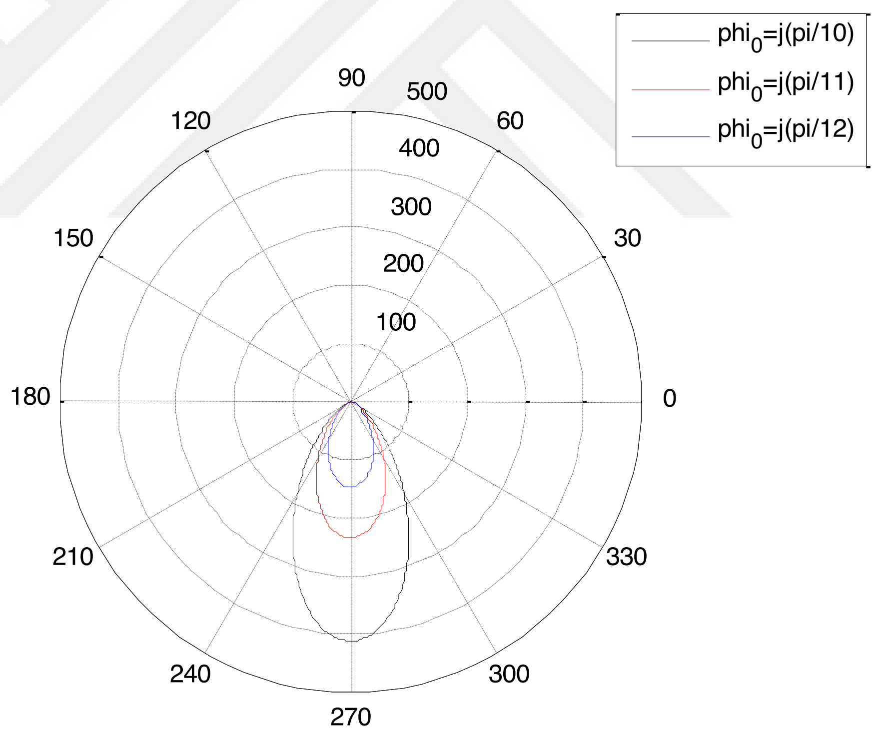

Figure 14 Inhomogeneous wave for incident angles with only positive φ_i.

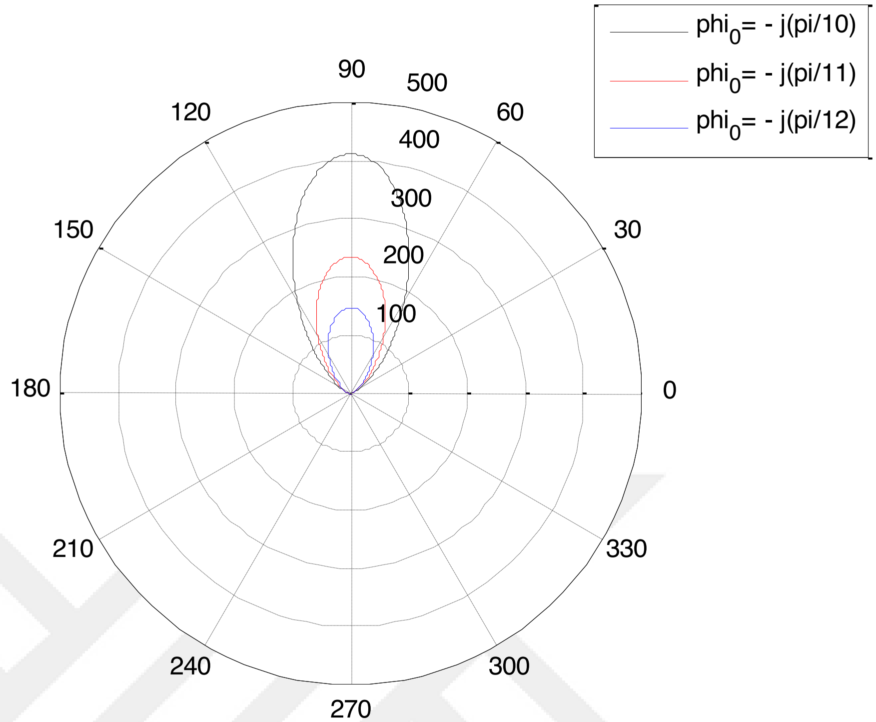

Figure 15 Inhomogeneous wave for incident angles with only negative φ_i.

If the incident angle has a nonzero real component but zero imaginary component, inhomogeneous wave, denoted by “u” in Fig. 16, turns out to be a plane wave.

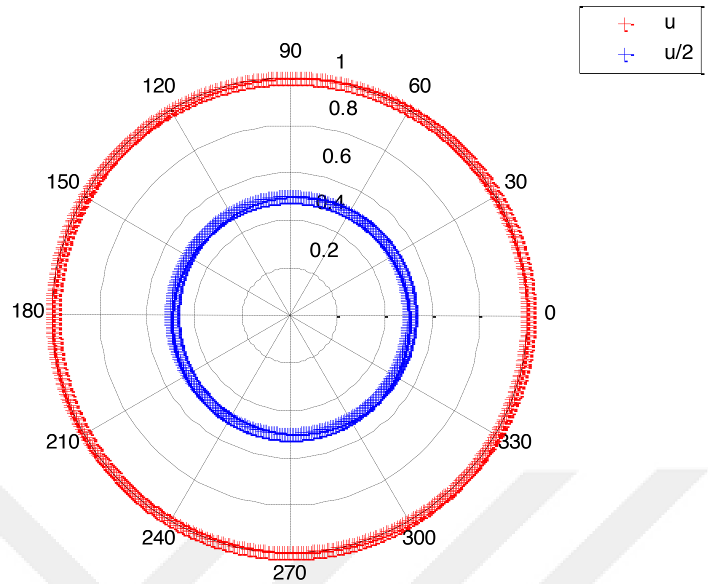

Figure 16 Inhomogeneous wave for incident angles with only real parts.

Fig. 17 - Fig. 20 illustrate the phase shift effect of φ_r . Phase shift in φ_r causes the same amount of phase shift in the field.

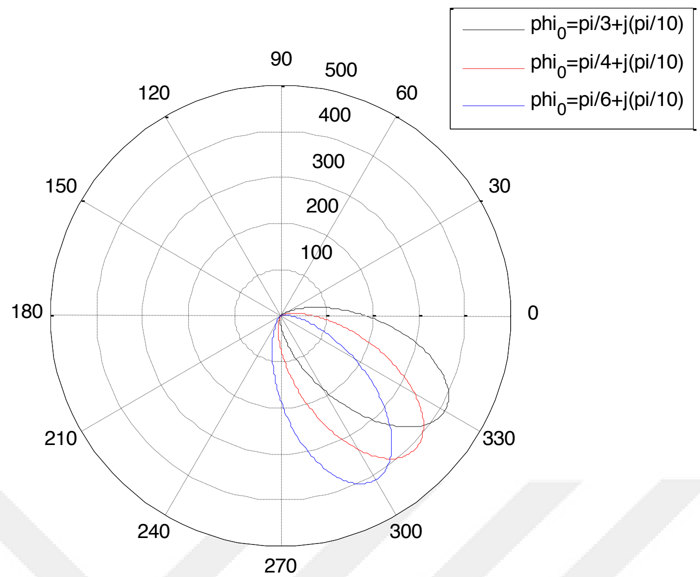

Figure 17 Inhomogeneous wave for complex incident angles having various real, but constant imaginary components.

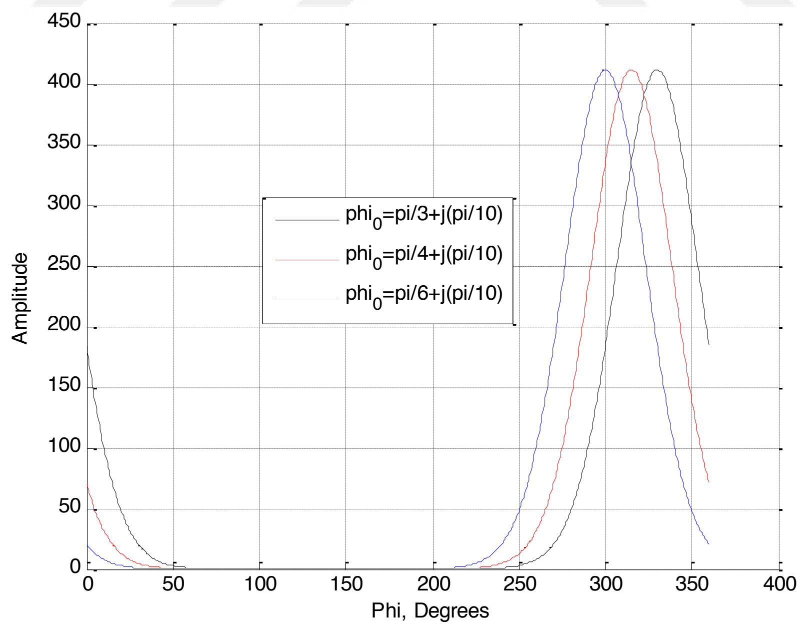

Figure 18 Inhomogeneous wave for complex incident angles having various real, but constant imaginary components.

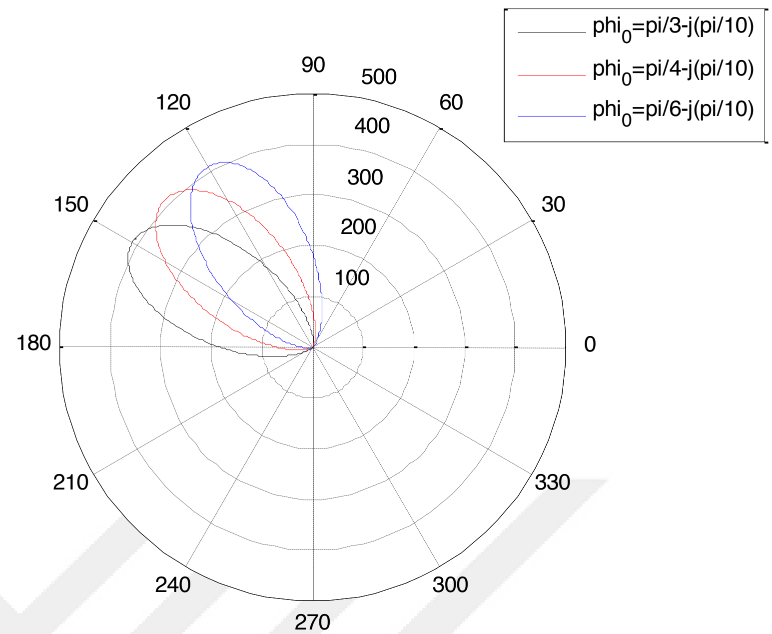

Figure 19 Inhomogeneous wave for complex incident angles having various real parts.

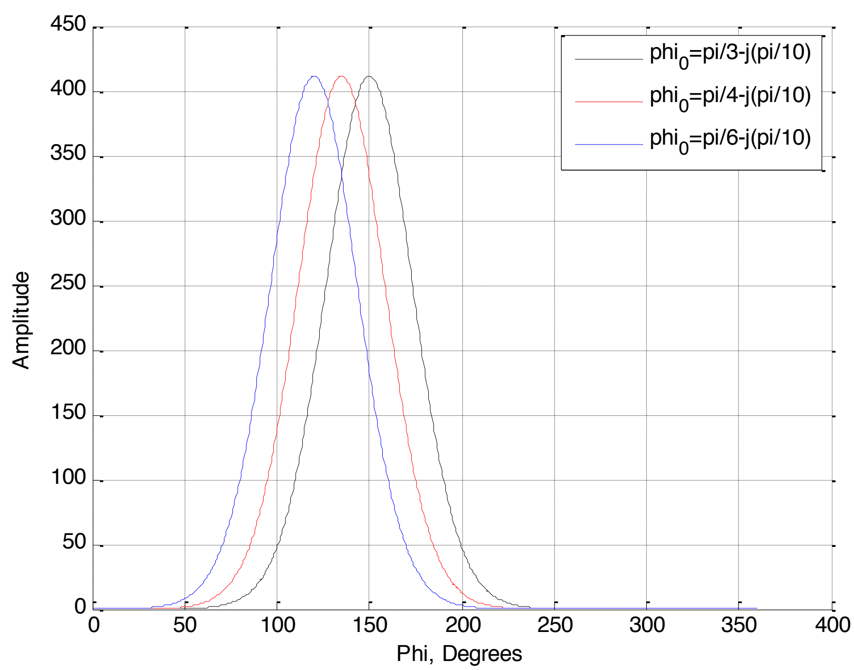

Figure 20 Inhomogeneous wave for complex incident angles having various real parts.

3.3 Gaussian beams

Light can be restricted in the form of beams which approximate to spatially localized and nondiverging waves. Examples of this kind of angular and spatial bounding are the plane waves and the spherical waves. The wavefront normals of a plane wave are in the same direction as the propagation direction and angular spread is not observed. However, the energy extends spatially all over the space. Spherical waves are originated from a single point whose wavefront normals diverge in all directions.

Gaussian beams have become very important after the development of laser sources and their applications in fiber optics and microwave acoustics. In recent decades the use of laser beams has become widespread. Lasers have been increasingly used in the fields such as spectroscopical analysis and bar-code reading.

Although Gaussian beams are generally studied by plane wave spectral analysis, they are actually evanescent waves mentioned in previous section [84].

The beam power of a Gaussian profile concentrates in a small cylinder surrounding the beam axis. The intensity distribution in any transverse plane is a circularly symmetrical around the beam axis. The width of the Gaussian function is minimum at the beam waist and it increases as the distance from the waist is increased in both directions. The wavefronts tend to be planar near the beam waist, gradually curve as the distance from the waist increases, and tend to be spherical far from the waist [90].

In this section we will derive an expression for Gaussian beam. For a two-dimensional beam propagating parallel to y axis with no variation along x-axis, and the electric field is polarized along z-axis, the electric field produced by a line source can be given as,

$$E \cong E_0 \frac{exp(-jkR-j\pi/4)}{\sqrt{kR}} \hat{e}_z \ , \tag{3.18}$$

which is a cylindrical wave. We need to assign complex values to the source coordinates to obtain a Gaussian beam [91]. For the source coordinates we assume,

$$(x, y) = (-x_0, -y_0 + jb), \tag{3.19}$$

and R can be expressed in the paraxial region as,

$$R = [(x + x_0)^2 + (y - y_0 - jb)^2]^{\frac{1}{2}} \ , \tag{3.20}$$

which can be rewritten as,

$$R = (y + y_0 - jb)\left[1 + \frac{(x+x_0)^2}{(y+y_0-jb)^2}\right]^{\frac{1}{2}}. \tag{3.21}$$

To rearrange R, we can use the binomial expansion which is expressed as,

$$(1 \pm x)^n \cong 1 \pm nx \ \text{ for x<<1.} \tag{3.22}$$

When the inequality in Eq. (3.23) is satisfied,

$$(x + x_0)^2 \ll (y + y_0 - jb)^2, \tag{3.23}$$

R can be rewritten as,

$$R = (y + y_0 - jb)\left[1 + \frac{1}{2}\frac{(x+x_0)^2}{(y+y_0-jb)^2}\right], \tag{3.24}$$

and

$$E \cong E_0 \frac{exp(-j\pi/4)}{\sqrt{k(y+y_0-jb)}} exp[-jk(y+y_0-jb)] exp\left[-j\frac{k}{2}\frac{(x+x_0)^2}{(y+y_0-jb)}\right], \tag{3.25}$$

which has the form of Gaussian beam.

Letting $E_0 = 1,\ x + x_0 = x'$, and $y + y_0 = y'$, Gaussian beam is obtained as,

$$E \cong \frac{exp(-j\pi/4)}{\sqrt{k(y'-jb)}} exp[-jk(y'-jb)] exp\left[-j\frac{k}{2}\frac{x'^2}{(y'-jb)}\right]. \tag{3.26}$$

As “y+y_0” goes to zero, this location is called as the beam throat. When considering the far field, “b” becomes very small with respect to y’ (b<<y’), and the beam diverges. In that case we can say that the beam’s source is a line source whose origin is (-x_0, -y_0) of the beam throat.

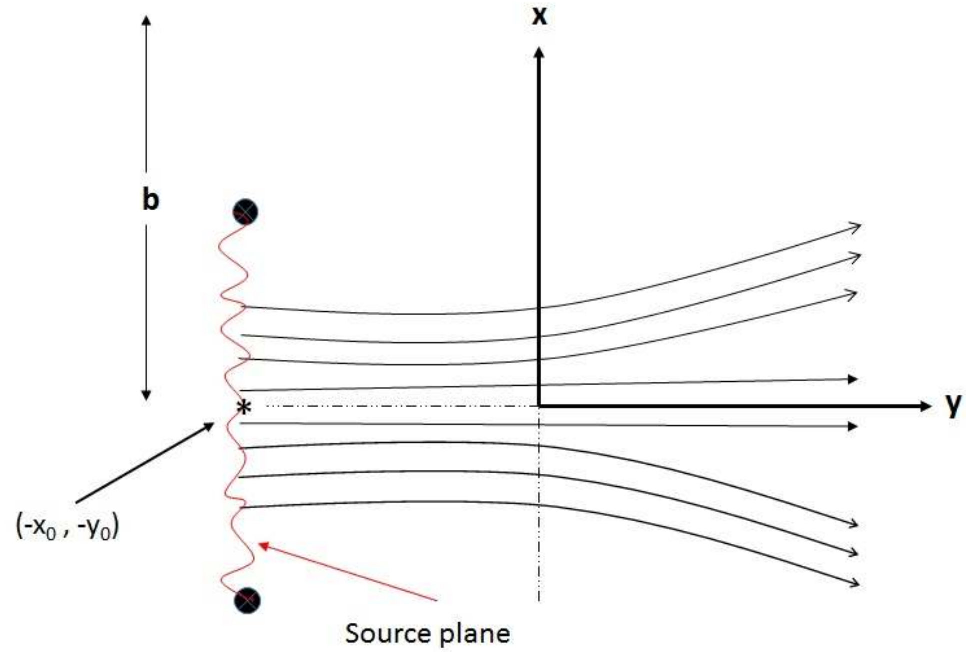

Figure 21 Gaussian beam cast by complex line source.

3.4 Numerical results

Various Gaussian beams are obtained in the following figures for λ=0.1m, ρ =3λ. The beam amplitude and 'b' are inversely proportional as shown in Fig. 22 and Fig. 23.

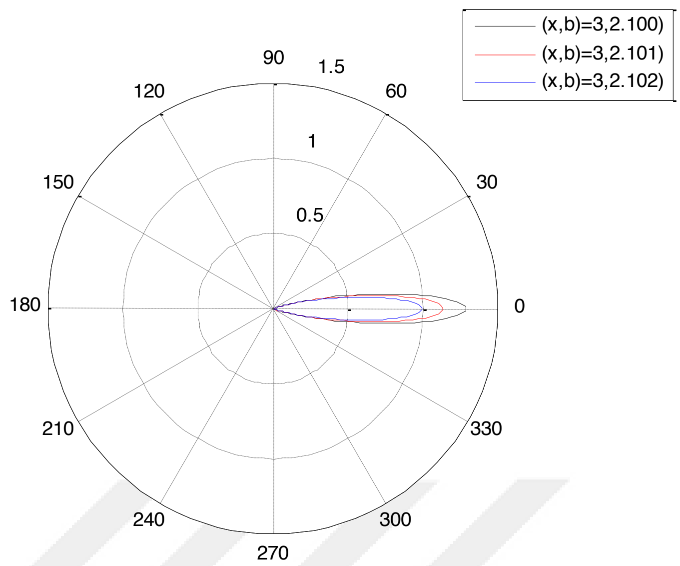

Figure 22 Gaussian beam amplitude variation for some "b" values.

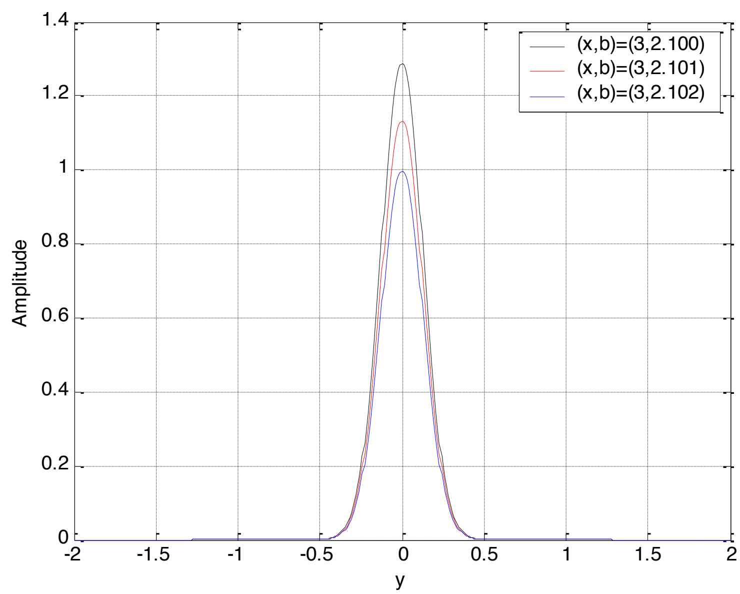

Figure 23 Gaussian beam amplitude variations for some "b" values.

The beam amplitude and x are directly proportional as shown the Fig.24 and Fig.25.

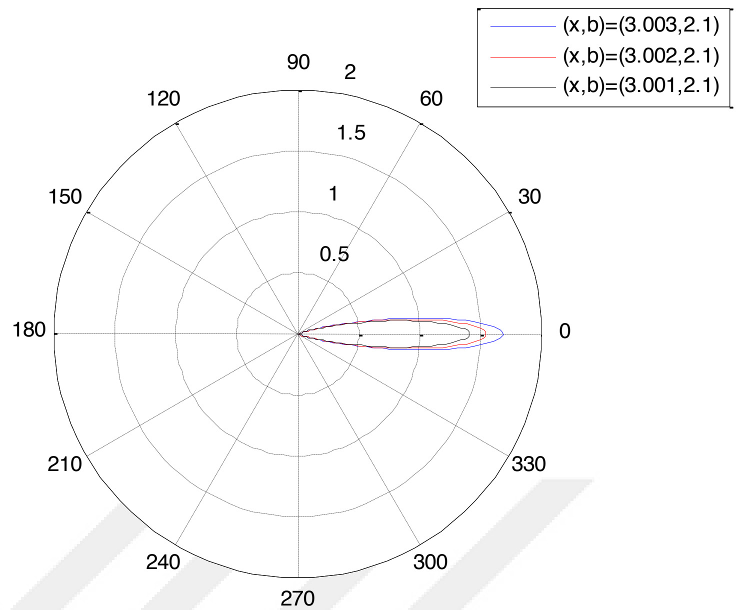

Figure 24 Gaussian beam amplitude variation for some “x”values.

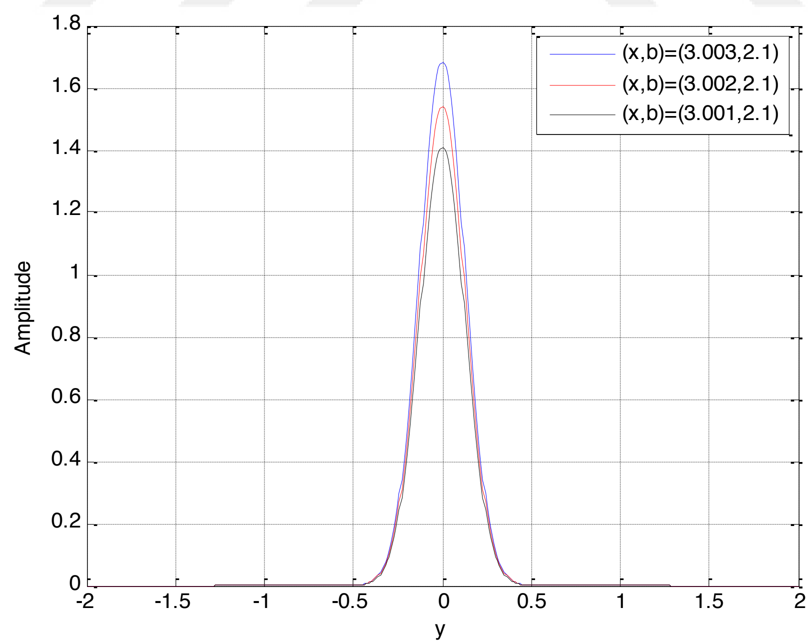

Figure 25 Gaussian beam amplitude variation for some “x” values.

CHAPTER 4

DERIVATION OF SCATTERING FIELD EXPRESSIONS BY MEANS OF MTPO METHOD FOR A PEC HALF PLANE [20]

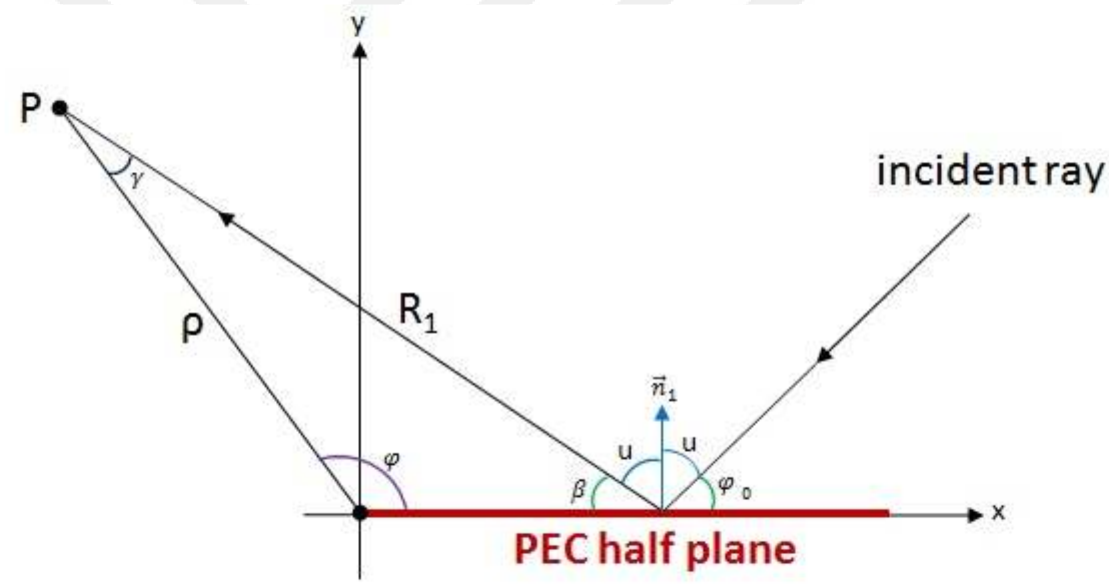

Figure 26 Geometry of reflection from a PEC half plane.

We will find reflected scattered and incident scattered fields for this problem. Firstly, reflected field is taken into consideration. Let us begin with the incident plane wave. That is,

$$\vec{E}_i = \hat{e}_z E_i e^{jk(xcos\varphi_0 + y\sin\varphi_0)}. \tag{4.1}$$

By letting,

$$\psi = e^{jk(xcos\varphi_0 + y\sin\varphi_0)}, \tag{4.2}$$

incident magnetic field can be given as,

$$\vec{H}_i = \frac{1}{j\omega\mu_0}\begin{vmatrix} \hat{e}_x & \hat{e}_y & \hat{e}_z \\ \frac{\partial}{\partial x} & \frac{\partial}{\partial y} & \frac{\partial}{\partial z} \\ 0 & 0 & -E_i\psi \end{vmatrix}. \tag{4.3}$$

As a result,

$$\vec{H}_i = \frac{E_i}{Z_0}\left(\hat{e}_x sin\varphi_0 - \hat{e}_y cos\varphi_0\right)\psi. \tag{4.4}$$

Using the boundary condition on the PEC surface,

$$\vec{n}_1 \times \left(\vec{E}_i + \vec{E}_r\right)\Big|_{S_1} = 0, \tag{4.5}$$

where

$$\vec{n}_1 = \cos(u + \varphi_0)\hat{e}_x + \sin(u + \varphi_0)\,\hat{e}_y\ , \tag{4.6}$$

and

$$u = \frac{\pi}{2} - \frac{\beta + \varphi_0}{2}\ , \tag{4.7}$$

we write,

$$\vec{n}_1 \times \left(\hat{e}_z E_i e^{jk(xcos\varphi_0 + y\sin\varphi_0)} + \vec{E}_r\right) = 0. \tag{4.8}$$

Using the relations of,

$$\vec{k} = -cos\beta\hat{e}_x + sin\beta\hat{e}_y\ , \tag{4.9}$$

and

$$\vec{r} = x\hat{e}_x + y\hat{e}_y + z\hat{e}_z\ , \tag{4.10}$$

we obtain,

$$\vec{k}.\vec{r} = xcos\beta - ysin\beta. \tag{4.11}$$

Substituting Eq. (4.11) into Eq. (4.12), reflected field is obtained as,

$$\vec{E}_r = -\hat{e}_z E_i e^{-j\vec{k}.\vec{r}}, \tag{4.12}$$

$$\vec{E}_r = -\hat{e}_z E_i e^{jk(xcos\beta - y\sin\beta)}. \tag{4.13}$$

For the reflected magnetic field, we write,

$$\vec{H}_r = \frac{1}{j\omega\mu_0}\nabla\times\vec{E}_r\ . \tag{4.14}$$

Letting,

$$\eta = e^{jk(xcos\beta - y\sin\beta)}, \tag{4.15}$$

reflected magnetic field is expressed as,

$$\vec{H}_r = \frac{1}{j\omega\mu_0}\begin{vmatrix} \hat{e}_x & \hat{e}_y & \hat{e}_z \\ \frac{\partial}{\partial x} & \frac{\partial}{\partial y} & \frac{\partial}{\partial z} \\ 0 & 0 & -E_i\eta \end{vmatrix}, \tag{4.16}$$

and,

$$\vec{H}_r = \frac{1}{j\omega\mu_0}\left(\hat{e}_x \frac{\partial}{\partial y} E_i\eta - \hat{e}_y \frac{\partial}{\partial x} E_i\eta\right). \tag{4.17}$$

Finally, substituting Eq. (4.15) into Eq. (4. 17), Eq. (4.18) is obtained as in below.

$$\vec{H}_r = -\frac{E_i}{Z_0}\left(sin\beta\hat{e}_x + cos\beta\hat{e}_y\right)e^{jk(xcos\beta - y\,sin\,\beta)}. \tag{4.18}$$

The surface current J is written as,

$$J = \vec{n}_1 \times \left(\vec{H}_i + \vec{H}_r\right). \tag{4.19}$$

We write,

$$\vec{n}_1 \times \vec{H}_i = \hat{e}_z \frac{E_i}{Z_0} cosue^{jk(xcos\varphi_0 + ysin\varphi_0)}, \tag{4.20}$$

and

$$\vec{n}_1 \times \vec{H}_r = -\hat{e}_z \frac{E_i}{Z_0} cos\,(u + \varphi_0 + \beta)e^{jk(xcos\beta - y\,sin\,\beta)}. \tag{4.21}$$

As a result, for the MTPO surface current of the PEC surface we write,

$$\vec{J}_{MTPO} = \hat{e}_z \frac{E_i}{Z_0}\left(cosu - cos(u + \varphi_0 + \beta)\right)e^{jkx'cos\varphi_0}, \tag{4.22}$$

and,

$$\vec{J}_{MTPO}\Big|_{S_1} = -\hat{e}_z \frac{2E_i}{Z_0} cos(u + \beta + \varphi_0) e^{jkx\prime cos\varphi_0} \ . \qquad (4.22)$$

From the geometry in Fig. 26 we can write that,

$$cosu - cos(u + \beta + \varphi_0) = -2cos(u + \beta + \varphi_0) \ . \qquad (4.23)$$

Using the relation of,

$$u = \frac{\pi-(\beta+\varphi_0)}{2} = \frac{\pi}{2} - \frac{\beta+\varphi_0}{2} \ , \qquad (4.24)$$

into Eq. (5.23) we get,

$$\vec{J}_{MTPO}\Big|_{S_1} = \hat{e}_z \frac{2E_i}{Z_0} sin\left(\frac{\beta+\varphi_0}{2}\right) e^{jkx\prime cos\varphi_0} \ . \qquad (4.25)$$

Reflected scattered field,

$$E_{rs} = -\frac{j\omega\mu_0}{4\pi} \iint_{S_1} J_{MTPO}|_{S_1} \frac{e^{-jkR_1}}{R_1} dx'dz', \qquad (4.26)$$

$$E_{rs} = -\frac{j\omega\mu_0}{4\pi} \frac{2E_i}{Z_0} \int_{x'=0}^{\infty} \int_{-\infty}^{\infty} e^{jkx\prime cos\varphi_0} \, sin\left(\frac{\beta+\varphi_0}{2}\right) \frac{e^{-jkR_1}}{R_1} dx'dz', \qquad (4.27)$$

$$\vec{E}_{rs} = -\hat{e}_z \frac{j2\omega\mu_0 E_i}{4\pi Z_0} \int_0^{\infty} \int_{-\infty}^{\infty} sin\left(\frac{\beta+\varphi_0}{2}\right) \frac{e^{-jkR_1}}{R_1} e^{jkx\prime cos\varphi_0} dz'dx', \qquad (4.28)$$

$$\vec{E}_{rs} = -\hat{e}_z \frac{jkE_i}{2\pi} \int_0^{\infty} \int_{-\infty}^{\infty} sin\left(\frac{\beta+\varphi_0}{2}\right) \frac{e^{-jkR_1}}{R_1} e^{jkx\prime cos\varphi_0} dz'dx', \qquad (4.29)$$

$$\vec{E}_{rs} = -\hat{e}_z \frac{jkE_i}{2\pi} \int_0^\infty sin\left(\frac{\beta+\varphi_0}{2}\right) e^{jkx\prime cos\varphi_0} dx' \int_{-\infty}^{\infty} \frac{e^{-jkR_1}}{R_1} dz', \tag{4.30}$$

is obtained. Here the wave number k is,

$$k = \frac{\omega\mu_0}{Z_0}. \tag{4.31}$$

Letting,

$$z - z' = R\, sinh\, \alpha, \tag{4.32}$$

we get,

$$dz' = R\, cosh\, \alpha\, d\alpha, \tag{4.33}$$

and

$$\sqrt{R^2 + (z - z')^2} = R\, cosh\, \alpha. \tag{4.34}$$

The incident-scattered electric field becomes as,

$$\vec{E}_{rs} = -\hat{e}_z \frac{jkE_i}{2\pi} \int_0^\infty sin\left(\frac{\beta+\varphi_0}{2}\right) e^{jkx\prime cos\varphi_0} dx' \int_C e^{jkR\, cosh\, \alpha} d\alpha, \tag{4.35}$$

where

$$\int_C e^{jkR\, cosh\, \alpha} d\alpha = \frac{\pi}{j} H_0^{(2)}(kR). \tag{4.36}$$

$H_0^{(2)}(kR)$ is the zero-order Hankel function of the second kind that can approximately be written as,

$$H_0^{(2)}(kR) \cong \sqrt{\frac{2}{\pi}} e^{j\left(\frac{\pi}{4}\right)} \frac{e^{-jkR}}{\sqrt{kR}}. \tag{4.37}$$

Using Eq. (4.36) in Eq. (4.35) we write,

$$\vec{E}_{rs} = -\hat{e}_z \frac{jkE_i}{2\pi} \int_0^{\infty} sin\left(\frac{\beta+\varphi_0}{2}\right) e^{jkx\prime cos\varphi_0} dx' \frac{\pi}{j} H_0^{(2)}(kR). \tag{4.38}$$

Using Eq. (4.37) in Eq. (4.38) E_{rs} becomes,

$$\vec{E}_{rs} = -\hat{e}_z \frac{jkE_i}{2\pi} \frac{\pi}{j} \sqrt{\frac{2}{\pi}} e^{j\left(\frac{\pi}{4}\right)} \int_0^{\infty} sin\left(\frac{\beta+\varphi_0}{2}\right) \frac{e^{-jkR}}{\sqrt{kR}} e^{jkx\prime cos\varphi_0} dx', \tag{4.39}$$

and

$$\vec{E}_{rs} = -\hat{e}_z \frac{kE_i}{\sqrt{2\pi}} e^{j\left(\frac{\pi}{4}\right)} \int_0^{\infty} sin\left(\frac{\beta+\varphi_0}{2}\right) \frac{e^{-jkR}}{\sqrt{kR}} e^{jkx\prime cos\varphi_0} dx'. \tag{4.40}$$

For the incident scattered field, we use the equivalent source that is shown in Fig. 27 below.

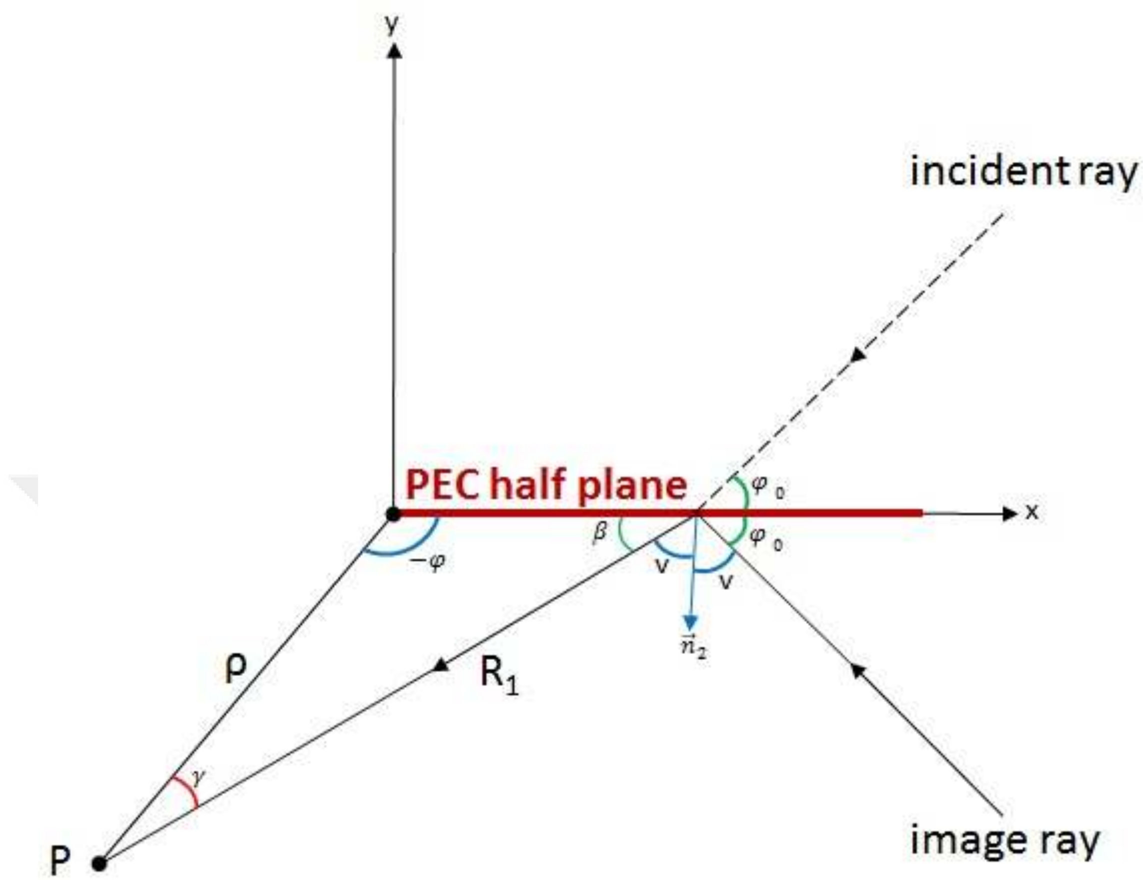

Figure 27 Geometry considered for the evaluation of the incident scattered field.

Incident equivalent electric field can be expressed as,

$$\vec{E}_{i_{eq}} = -\hat{e}_z E_i e^{jk(x\cos\varphi_0 - y\sin\varphi_0)}. \tag{4.41}$$

Letting,

$$\chi = e^{jk(x\cos\varphi_0 - y\sin\varphi_0)}, \tag{4.42}$$

equivalent magnetic field is written as,

$$\vec{H}_{i_{eq}} = \frac{1}{j\omega\mu_0}\nabla\times(E_i)_{eq} \ , \tag{4.43}$$

$$\vec{H}_{i_{eq}} = \frac{1}{j\omega\mu_0}\begin{vmatrix} \hat{e}_x & \hat{e}_y & \hat{e}_z \\ \frac{\partial}{\partial x} & \frac{\partial}{\partial y} & \frac{\partial}{\partial z} \\ 0 & 0 & -E_i\chi \end{vmatrix}, \tag{4.44}$$

$$\vec{H}_{i_{eq}} = \frac{1}{j\omega\mu_0}\left(\hat{e}_x\frac{\partial}{\partial y}E_i\chi - \hat{e}_y\frac{\partial}{\partial x}E_i\chi\right), \tag{4.45}$$

$$\vec{H}_{i_{eq}} = \frac{1}{j\omega\mu_0}\left(-jkE_i(-sin\varphi_0)\hat{e}_x - (-jkE_i)cos\varphi_0\hat{e}_y\right)\chi, \tag{4.46}$$

$$\vec{H}_{i_{eq}} = \frac{jkE_i}{j\omega\mu_0}\left(sin\,\varphi_0\,\hat{e}_x + cos\,\varphi_0\,\hat{e}_y\right)e^{jk(xcos\varphi_0 - y\,sin\,\varphi_0)}, \tag{4.47}$$

finally, we obtain the magnetic equivalent field as,

$$\vec{H}_{i_{eq}} = \frac{E_i}{Z_0}\left(sin\,\varphi_0\,\hat{e}_x + cos\,\varphi_0\,\hat{e}_y\right)e^{jk(xcos\varphi_0 - y\,sin\,\varphi_0)} \ , \tag{4.48}$$

where

$$\frac{k}{\omega\mu_0} = \frac{1}{Z_0} \ . \tag{4.49}$$

For the surface current we write,

$$\vec{n}_2\times\vec{H}_{t_{eq}} = J_{MTPO}, \tag{4.50}$$

where,

$$\vec{H}_{t_{eq}} = \vec{H}_{i_{eq}} + \vec{H}_{r_{eq}} \ , \tag{4.51}$$

and, $\vec{H}_{i_{eq}}$ and $\vec{H}_{r_{eq}}$ are the equivalent incident and reflected magnetic fields respectively. We can write that,

$$\vec{E}_{r_{eq}} = \hat{e}_z E_i e^{jk(x\cos\beta + y\sin\beta)}. \tag{4.52}$$

Letting,

$$\xi = e^{jk(x\cos\beta + y\sin\beta)}, \tag{4.53}$$

we write,

$$\vec{H}_{r_{eq}} = \frac{1}{j\omega\mu_0} \nabla \times \vec{E}_{r_{eq}} \ , \tag{4.54}$$

$$\vec{H}_{r_{eq}} = \frac{1}{j\omega\mu_0} \begin{vmatrix} \hat{e}_x & \hat{e}_y & \hat{e}_z \\ \frac{\partial}{\partial x} & \frac{\partial}{\partial y} & \frac{\partial}{\partial z} \\ 0 & 0 & E_i\xi \end{vmatrix}, \tag{4.55}$$

$$\vec{H}_{r_{eq}} = \frac{1}{j\omega\mu_0} \left(\hat{e}_x \frac{\partial}{\partial y} E_i\xi - \hat{e}_y \frac{\partial}{\partial x} E_i\xi \right), \tag{4.56}$$

$$\vec{H}_{r_{eq}} = \frac{jkE_i}{j\omega\mu_0}\left(\hat{e}_x \sin\beta - \hat{e}_y \cos\beta\right)\xi \ , \tag{4.57}$$

finally, we obtain,

$$\vec{H}_{r_{eq}} = \frac{E_i}{Z_0}\left(\hat{e}_x \sin\beta - \hat{e}_y \cos\beta\right)e^{jk(x\cos\beta + y\sin\beta)}. \tag{4.58}$$

By using,

$$\vec{n}_2 = \cos(v+\varphi_0)\hat{e}_x - \sin(v+\varphi_0)\,\hat{e}_y \ , \tag{4.59}$$

we write,

$$\vec{n}_2 \times \vec{H}_{t_{eq}} = \vec{n}_2 \times \vec{H}_{i_{eq}} + \vec{n}_2 \times \vec{H}_{r_{eq}} \ . \tag{4.60}$$

For the first term of the summation of the right hand side of Eq. (4.60) we write,

$$\vec{n}_2 \times \vec{H}_{i_{eq}} = \cos(v+\varphi_0)\cos\varphi_0\,\hat{e}_z + \sin(v+\varphi_0)\sin\varphi_0\,\hat{e}_z. \tag{4.61}$$

Finally we obtain,

$$\vec{n}_2 \times \vec{H}_{i_{eq}} = \hat{e}_z \frac{E_i}{Z_0}\cos v. \tag{4.62}$$

For the second term we write,

$$\vec{n}_2 \times \vec{H}_{r_{eq}} = -\hat{e}_z \frac{E_i}{Z_0}\left(-\cos(v+\varphi_0)\cos\beta + \sin(v+\varphi_0)\sin\beta\right),$$

And we obtain, (4.63)

$$\vec{n}_2 \times \vec{H}_{r_{eq}} = \hat{e}_z \frac{E_i}{Z_0}\cos(v+\varphi_0+\beta). \tag{4.64}$$

To obtain the surface current we write,

$$J_{MTPO} = \vec{n}_2 \times \vec{H}_{t_{eq}} \,, \tag{4.65}$$

and

$$J_{MTPO} = \hat{e}_z \frac{E_i}{Z_0}\left(cosv + cos(v + \varphi_0 + \beta)\right)e^{jkx\prime cos\varphi_0}. \tag{4.66}$$

Using the relations of,

$$cosv = -cos(v + \varphi_0 + \beta), \tag{4.67}$$

and

$$v = \frac{\pi}{2} - \frac{\varphi_0 + \beta}{2} \,, \tag{4.68}$$

Surface current can be found as,

$$\vec{J}_{MTPO} = -\hat{e}_z \frac{2E_i}{Z_0} cos\left(\frac{\pi}{2} - \frac{\varphi_0}{2} - \frac{\beta}{2} + \varphi_0 + \beta\right) e^{jkx\prime cos\varphi_0} \,, \tag{4.69}$$

$$\vec{J}_{MTPO} = -\hat{e}_z \frac{2E_i}{Z_0} sin\left(\frac{\varphi_0 + \beta}{2}\right) e^{jkx\prime cos\varphi_0} \,. \tag{4.70}$$

Incident-scattered field,

$$\vec{E}_{is} = \frac{-j\omega\mu_0}{4\pi} \iint_{S_1} \vec{J}_{MTPO} \frac{e^{-jkR_1}}{R_1} dS' \,. \tag{4.71}$$

Substituting Eq. (4.70) into Eq. (4.71) we write,

$$\vec{E}_{is} = \hat{e}_z \frac{j\omega\mu_0}{4\pi} \iint_{S_1} \frac{2E_i}{Z_0} sin\left(\frac{\beta+\varphi_0}{2}\right) \frac{e^{-jkR_1}}{R_1} e^{jkx\prime cos\varphi_0}\, dS' \ , \tag{4.72}$$

$$\vec{E}_{is} = \hat{e}_z \frac{j2\omega\mu_0 E_i}{4\pi Z_0} \iint_{S_1} sin\left(\frac{\beta+\varphi_0}{2}\right) \frac{e^{-jkR_1}}{R_1} e^{jkx\prime cos\varphi_0} dS', \tag{4.73}$$

$$\vec{E}_{is} = \hat{e}_z \frac{jkE_i}{2\pi} \int_{-\infty}^{0} \int_{-\infty}^{\infty} sin\left(\frac{\beta+\varphi_0}{2}\right) \frac{e^{-jkR_1}}{R_1} e^{jkx\prime cos\varphi_0} dz'dx', \tag{4.74}$$

where the wave number k can be written as,

$$k = \frac{\omega\mu_0}{Z_0} \ . \tag{4.75}$$

Incident scattered field can be arranged as,

$$\vec{E}_{is} = \hat{e}_z \frac{jkE_i}{2\pi} \int_{-\infty}^{0} sin\left(\frac{\beta+\varphi_0}{2}\right) e^{jkx\prime cos\varphi_0} dx' \int_{-\infty}^{\infty} \frac{e^{-jkR_1}}{R_1} dz'. \tag{4.76}$$

Letting,

$$z - z' = R\, sinh\, \alpha \ , \tag{4.77}$$

We get,

$$dz' = R\, cosh\, \alpha\, d\alpha, \tag{4.78}$$

and

$$\sqrt{R^2 + (z - z')^2} = R\, cosh\, \alpha. \tag{4.79}$$

The incident-scattered electric field becomes as,

$$\vec{E}_{is} = \hat{e}_z \frac{jkE_i}{2\pi} \int_{-\infty}^{0} sin\left(\frac{\beta+\varphi_0}{2}\right) e^{jkx\prime cos\varphi_0} dx' \int_C \; e^{jkR\, cosh\, \alpha} d\alpha, \tag{4.80}$$

where

$$\int_C \; e^{jkR\, cosh\, \alpha} d\alpha = \frac{\pi}{j} H_0^{(2)}(kR). \tag{4.81}$$

$H_0^{(2)}(kR)$ is the zero-order Hankel function of the second kind that can approximately be written as,

$$H_0^{(2)}(kR) \cong \sqrt{\frac{2}{\pi}} e^{j\left(\frac{\pi}{4}\right)} \frac{e^{-jkR}}{\sqrt{kR}} \; . \tag{4.82}$$

Thus,

$$\vec{E}_{is} = \hat{e}_z \frac{jkE_i}{2\pi} \int_{-\infty}^{0} sin\left(\frac{\beta+\varphi_0}{2}\right) e^{jkx\prime cos\varphi_0} dx' \frac{\pi}{j} H_0^{(2)}(kR). \tag{4.83}$$

If Eq. (4.82) is substituted into Eq. (4.83),

$$\vec{E}_{is} = \hat{e}_z \frac{jkE_i}{2\pi} \frac{\pi}{j} \sqrt{\frac{2}{\pi}} e^{j\left(\frac{\pi}{4}\right)} \int_{-\infty}^{0} sin\left(\frac{\beta+\varphi_0}{2}\right) \frac{e^{-jkR}}{\sqrt{kR}} e^{jkx\prime cos\varphi_0} dx', \tag{4.84}$$

$$\vec{E}_{is} = \hat{e}_z \frac{kE_i}{\sqrt{2\pi}} e^{j\left(\frac{\pi}{4}\right)} \int_{-\infty}^{0} sin\left(\frac{\beta+\varphi_0}{2}\right) \frac{e^{-jkR}}{\sqrt{kR}} e^{jkx\prime cos\varphi_0} dx' \tag{4.85}$$

is obtained. Finally, we can write total scattered field as,

$$\vec{E}_t = \vec{E}_{is} + \vec{E}_{rs} \, , \tag{4.86}$$

$$\vec{E}_t = \hat{e}_z \frac{kE_i}{\sqrt{2\pi}} e^{j\left(\frac{\pi}{4}\right)} \left(\int_{-\infty}^{0} sin\left(\frac{\beta+\varphi_0}{2}\right) \frac{e^{-jkR}}{\sqrt{kR}} e^{jkx\prime cos\varphi_0} dx' - \int_{0}^{\infty} sin\left(\frac{\beta+\varphi_0}{2}\right) \frac{e^{-jkR}}{\sqrt{kR}} e^{jkx\prime cos\varphi_0} dx' \right). \tag{4.87}$$

The first integral, which represents the incident-scattered waves, contains incident, and incident diffracted fields for $\varphi \geq \pi$, and for $\varphi \epsilon [0, 2\pi]$ respectively. The second one contains the reflected and reflected-diffracted waves. Reflected fields are evaluated asymptotically by by the stationary phase method whereas the diffracted fields can be obtained by the edge point method.

CHAPTER 5

SCATTERING OF HOMOGENEOUS AND INHOMOGENEOUS PLANE WAVES BY A CYLINDRICAL PARABOLIC PERFECTLY ELECTRIC CONDUCTING REFLECTOR

5.1 Theory

A cylindrical parabolic reflector whose surface equation is given in Eq. (5.1) is placed on a coordinate system symmetrical with respect to x-axis as shown in Fig. 28.

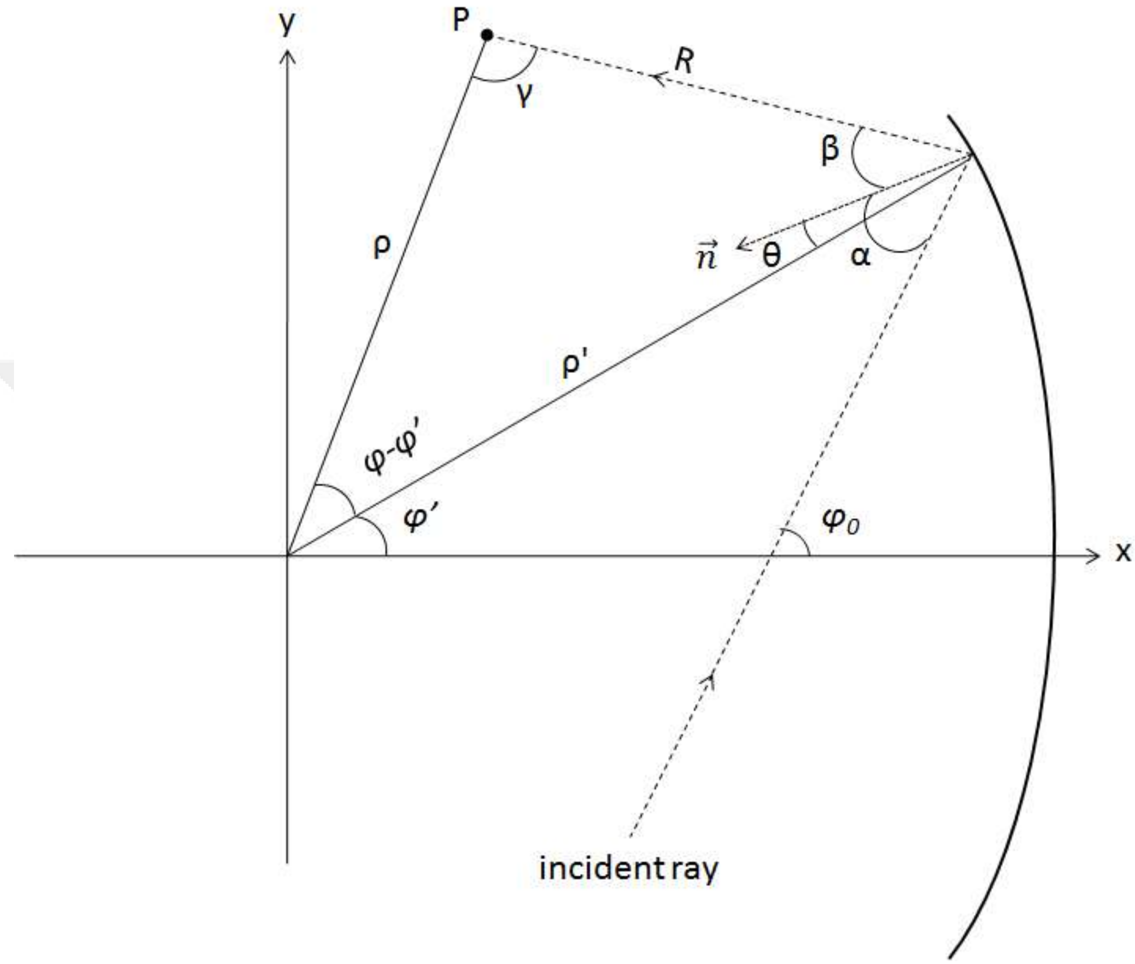

Figure 28 Geometry of the problem

The parabola expression can be written as,

$$\rho' = \frac{f}{\left(\cos\frac{\varphi'}{2}\right)^2}, \tag{5.1}$$

where φ’ and ρ’ are cylindrical coordinates and f is the focus of the parabola whose expression can be rewritten as,

$$f = \rho' cos^2\left(\frac{\varphi'}{2}\right). \tag{5.2}$$

Gradient of " f " in cylindrical coordinates is written as,

$$\vec{\nabla} f = \vec{n} = cos^2\left(\frac{\varphi'}{2}\right)\hat{e}_\rho + \frac{1}{\rho'}\left(-\frac{1}{2}\right)\rho' 2cos\left(\frac{\varphi'}{2}\right)sin\left(\frac{\varphi'}{2}\right)\hat{e}_\varphi\ , \tag{5.3}$$

from which the normal of the parabola is obtained in Eq. (5.4).

$$\vec{n} = cos^2\left(\frac{\varphi'}{2}\right)\hat{e}_\rho - cos\left(\frac{\varphi'}{2}\right)sin\left(\frac{\varphi'}{2}\right)\hat{e}_\varphi = 0. \tag{5.4}$$

Thus, the normal vector of the parabola directing outward is,

$$\vec{n} = cos\left(\frac{\varphi'}{2}\right)\hat{e}_\rho - sin\left(\frac{\varphi'}{2}\right)\hat{e}_\varphi \tag{5.5}$$

Inward vector is the opposite of the Eq. (5.5) as,

$$\vec{n} = -cos\left(\frac{\varphi'}{2}\right)\hat{e}_\rho + sin\left(\frac{\varphi'}{2}\right)\hat{e}_\varphi \tag{5.6}$$

Theta in Fig. (6.1) can be found by means of dot product as,

$$\vec{n}.\hat{e}_\rho = |\hat{n}|\left|\hat{e}_\rho\right|cos\theta, \tag{5.7}$$

$$\left(-cos\left(\frac{\varphi'}{2}\right)\hat{e}_\rho + sin\left(\frac{\varphi'}{2}\right)\hat{e}_\varphi\right).\left(\hat{e}_\rho\right) = cos\theta, \tag{5.8}$$

$$cos\left(\frac{\varphi'}{2}\right) = cos\theta, \tag{5.9}$$

$$\theta = \varphi'/2. \tag{5.10}$$

The scattering integral [92] of MTPO [20] for an impedance surface can be applied to a perfectly electric conducting (PEC) surface as,

$$E_s = \frac{ke^{j\frac{\pi}{4}}}{2\pi}\int_{-\varphi_e}^{\varphi_e} \cos\left(\frac{\beta+\alpha}{2}\right)\frac{e^{-jk[\rho\prime\cos(\varphi'-\varphi_0)+R]}}{\sqrt{kR}}\frac{\rho\prime}{\cos\frac{\varphi\prime}{2}}d\varphi' \;, \tag{5.11}$$

where

$$R = \rho\cos\gamma + \rho'\cos\left(\beta + \frac{\varphi\prime}{2}\right). \tag{5.12}$$

5.2 Asymptotic evaluation of the scattering integral

For the asymptotic evaluation of the scattering integral, to obtain the reflected field we need to use the phase function. The phase function of the scattering integral is,

$$\psi = \rho' cos(\varphi' - \varphi_0) + R \;, \tag{5.13}$$

which can be rewritten as,

$$\psi = \rho' cos(\varphi' - \varphi_0) + \rho' cos\beta + \rho cos\gamma. \tag{5.14}$$

Taking the derivative of both sides with respect to φ' we get,

$$\psi' = \frac{\partial\rho\prime}{\partial\varphi\prime}cos(\varphi' - \varphi_0) - \rho' sin(\varphi' - \varphi_0) + \frac{\partial\rho'}{\partial\varphi'}cos\beta - \rho' sin\beta\frac{\partial\beta}{\partial\varphi'} - \rho sin\gamma\frac{\partial\gamma}{\partial\varphi'} \;, \tag{5.15}$$

where,

$$\frac{\partial\rho'}{\partial\varphi'} = \rho' \frac{\sin\frac{\varphi'}{2}}{\cos\frac{\varphi'}{2}} \ . \tag{5.16}$$

From the geometry in Fig. 28 we write,

$$\frac{\rho'}{\sin\gamma} = \frac{\rho}{\sin\beta} \ , \tag{5.17}$$

and

$$\gamma = \pi - (\varphi - \varphi') - \beta \ , \tag{5.18}$$

from which we get,

$$\frac{\partial\gamma}{\partial\varphi'} = \frac{1}{2} - \frac{\partial\beta}{\partial\varphi'} \tag{5.19}$$

We can rewrite the first derivative of the phase function as,

$$\psi' = \rho' \frac{\sin\frac{\varphi'}{2}}{\cos\frac{\varphi'}{2}} \cos(\varphi' - \varphi_0) - \rho' \sin(\varphi' - \varphi_0) + \rho' \frac{\sin\frac{\varphi'}{2}}{\cos\frac{\varphi'}{2}} \cos\beta - \rho' \sin\beta \left(1 - \frac{\partial\beta}{\partial\varphi'}\right) - \rho' \sin\beta \frac{\partial\beta}{\partial\varphi'} \ , \tag{5.20}$$

$$\psi' = \rho' \frac{\sin\frac{\varphi'}{2}}{\cos\frac{\varphi'}{2}} (\cos(\varphi' - \varphi_0) + \cos\beta) - \rho' \sin(\varphi' - \varphi_0) - \rho' \sin\beta, \tag{5.21}$$

$$\psi' = \frac{\rho'}{\cos\frac{\varphi'}{2}} \left[\sin\frac{\varphi'}{2} \cos(\varphi' - \varphi_0) + \sin\frac{\varphi'}{2} \cos\beta - \sin(\varphi' - \varphi_0) \cos\frac{\varphi'}{2} - \sin\beta \cos\frac{\varphi'}{2}\right] \tag{5.22}$$

$$\psi' = \frac{\rho'}{\cos\frac{\varphi'}{2}} \left[\sin\left(\frac{\varphi'}{2} - \varphi' + \varphi_0\right) + \sin\left(\frac{\varphi'}{2} - \beta\right)\right], \tag{5.23}$$

and its first derivative is found to be,

$$\frac{\partial\psi}{\partial\varphi'} = \frac{\rho'}{cos\frac{\varphi'}{2}}\left[sin\left(\varphi_0 - \frac{\varphi'}{2}\right) - sin\left(\beta - \frac{\varphi'}{2}\right)\right]. \tag{5.24}$$

By equating the first derivative to zero, we obtain the stationary phase point value of β as,

$$\beta_s = \alpha_s = \varphi_0 - \frac{\varphi_s}{2} \ , \tag{5.25}$$

where β_s is the value of β at the stationary point. Now we need to find the second derivative of the phase function.

$$\psi_s'' = \frac{\rho_s\left[\cos\left(\varphi_0 - \frac{\varphi_s}{2}\right)\left(-\frac{1}{2}\right) - \cos\left(\beta_s - \frac{\varphi_s}{2}\right)\left(\frac{\partial\beta}{\partial\varphi'} - \frac{1}{2}\right) - 0\right]}{cos^2\frac{\varphi'}{2}}, \tag{5.26}$$

$$\psi_s'' = \frac{\rho_s}{\cos\frac{\varphi_s}{2}}\left[-\frac{1}{2}\cos\left(\varphi_0 - \frac{\varphi_s}{2}\right) - \cos\left(\varphi_0 - \frac{\varphi_s}{2}\right)\frac{\partial\beta}{\partial\varphi'} + \frac{1}{2}\cos\left(\varphi_0 - \frac{\varphi_s}{2}\right)\right], \tag{5.27}$$

where φ_s , ρ_s are the stationary values of φ'and ρ'respectively. As a result,

$$\psi_s'' = \frac{\rho_s}{\cos\frac{\varphi_s}{2}}\cos\left(\varphi_0 - \frac{\varphi_s}{2}\right)\frac{\partial\beta}{\partial\varphi'} . \tag{5.28}$$

Here the first derivative of β with respect to *φ'* is needed. From the geometry in Fig. 28 we can write,

$$\rho' sin\beta = \rho sin\gamma. \tag{5.29}$$

By taking the first derivative of both sides we write,

$$\rho' \frac{sin\frac{\varphi'}{2}}{cos\frac{\varphi'}{2}} sin\beta + \rho' cos\beta \frac{\partial\beta}{\partial\varphi'} = \rho cos\gamma \frac{\partial\gamma}{\partial\varphi'} . \tag{5.30}$$

Substituting Eq. (5.19) into Eq. (5.30) we arrange the equation as,

$$\rho cos\gamma \left(1 - \frac{\partial\beta}{\partial\varphi'}\right) = \rho' \left(\frac{sin\frac{\varphi'}{2}}{cos\frac{\varphi'}{2}} sin\beta + cos\beta \frac{\partial\beta}{\partial\varphi'}\right), \tag{5.31}$$

$$\rho cos\gamma - \rho' sin\beta \frac{sin\frac{\varphi'}{2}}{cos\frac{\varphi'}{2}} = (\rho cos\gamma + \rho' cos\beta) \frac{\partial\beta}{\partial\varphi'} . \tag{5.32}$$

By using the relation of

$$R = \rho cos\gamma + \rho' cos\beta, \tag{5.33}$$

For Eq. (5.32) we write the following steps as,

$$\rho cos\gamma - \rho' sin\beta \frac{sin\frac{\varphi'}{2}}{cos\frac{\varphi'}{2}} = R \frac{\partial\beta}{\partial\varphi'} \ , \tag{5.34}$$

$$\frac{\partial\beta}{\partial\varphi'} = \frac{\rho cos\gamma - \rho' sin\beta \frac{sin\frac{\varphi'}{2}}{cos\frac{\varphi'}{2}}}{R} , \tag{5.35}$$

$$\frac{\partial\beta}{\partial\varphi'} = \frac{\rho cos\gamma cos\frac{\varphi'}{2} - \rho' sin\beta sin\frac{\varphi'}{2}}{R cos\frac{\varphi'}{2}} , \tag{5.36}$$

$$\frac{\partial\beta}{\partial\varphi'} = \frac{\rho cos\gamma cos\frac{\varphi'}{2} + \rho' cos\beta cos\frac{\varphi'}{2} - \rho' cos\beta cos\frac{\varphi'}{2} - \rho' sin\beta sin\frac{\varphi'}{2}}{R cos\frac{\varphi'}{2}} , \tag{5.37}$$

$$\frac{\partial\beta}{\partial\varphi\prime} = \frac{cos\frac{\varphi'}{2}(\rho cos\gamma+\rho\prime cos\beta)-\rho' cos\beta cos\frac{\varphi'}{2}-\rho' sin\beta sin\frac{\varphi'}{2}}{Rcos\frac{\varphi'}{2}}, \tag{5.38}$$

$$\frac{\partial\beta}{\partial\varphi\prime} = \frac{Rcos\frac{\varphi'}{2}-\rho\prime\left(cos\beta cos\frac{\varphi'}{2}+sin\beta sin\frac{\varphi'}{2}\right)}{Rcos\frac{\varphi'}{2}}, \tag{5.39}$$

$$\frac{\partial\beta}{\partial\varphi\prime} = \frac{Rcos\frac{\varphi'}{2}-\rho\prime cos\left(\beta-\frac{\varphi'}{2}\right)}{Rcos\frac{\varphi'}{2}} \;. \tag{5.40}$$

Substituting Eq. (5.40) into Eq. (5.28) we get,

$$\psi_s'' = \frac{\rho_s}{cos\frac{\varphi_s}{2}}\left[-cos\left(\varphi_0-\frac{\varphi_s}{2}\right)+\frac{\rho_s cos^2\left(\varphi_0-\frac{\varphi_s}{2}\right)}{l\,cos\frac{\varphi_s}{2}}\right], \tag{5.41}$$

or

$$\psi_s'' = \frac{\rho_s}{lcos^2\frac{\varphi_s}{2}} cos\left(\varphi_0-\frac{\varphi_s}{2}\right)\left[lcos\frac{\varphi_s}{2}-\rho_s\, cos\left(\varphi_0-\frac{\varphi_s}{2}\right)\right], \tag{5.42}$$

where l is the stationary value of R. By remembering that the first derivative of the phase function is zero, its Taylor expansion is written as,

$$\psi(\varphi') = \psi(\varphi_s)+\frac{1}{2}\psi''(\varphi_s)(\varphi-\varphi_s)^2, \tag{5.43}$$

which can be written for our problem as,

$$\psi(\varphi') = l + \rho_s + \frac{1}{2}\frac{-\rho_s}{l cos^2\frac{\varphi_s}{2}} cos\left(\varphi_0 - \frac{\varphi_s}{2}\right)\times$$
$$\left[l cos\frac{\varphi_s}{2}\rho_s cos\left(\varphi_0 - \frac{\varphi_s}{2}\right)\right](\varphi' - \varphi_s)^2. \quad (5.44)$$

Reflected field becomes as,

$$E_r = -\frac{k exp(j\pi/4)}{\sqrt{2\pi}} exp\left[-jk\rho_s \cos(\varphi_s - \varphi_0)\frac{\exp(jkl)}{\sqrt{kl}}\right]\times$$
$$\int_{-\infty}^{\infty} exp\left[\frac{jk}{2}\frac{\rho_s}{l cos^2\frac{\varphi_s}{2}} cos\left(\varphi_0 - \frac{\varphi_s}{2}\right)\times\left[l cos\frac{\varphi_s}{2} - \rho_s cos\left(\varphi_0 - \frac{\varphi_s}{2}\right)\right](\varphi' - \varphi_s)^2\right] d\varphi',$$
$$(5.45)$$

$$E_r = f_s e^{-jk\rho_s \cos(\varphi_s - \varphi_0)} e^{-jkl}\times$$
$$\int_{-\infty}^{\infty} e^{-jk\frac{\rho_s \cos\left(\varphi_0 - \frac{\varphi_s}{2}\right)}{2l cos^2\left(\frac{\varphi_s}{2}\right)}\left[\rho_s \cos\left(\varphi_0 - \frac{\varphi_s}{2}\right) - l\cos\frac{\varphi_s}{2}\right](\varphi' - \varphi_s)^2} d\varphi'$$
$$(5.46)$$

where,

$$f_s = \frac{k e^{j\frac{\pi}{4}}}{\sqrt{2\pi}} \cos\left(\varphi_0 - \frac{\varphi_s}{2}\right)\frac{\rho_s}{\sqrt{kl}\cos\frac{\varphi_s}{2}} \;, \quad (5.47)$$

or,

$$f_s = \frac{k e^{j\frac{\pi}{4}}}{\sqrt{2\pi}} cos\left(\frac{\beta_s + \alpha_s}{2}\right)\frac{\rho_s}{\sqrt{kl}\, cos\frac{\varphi_s}{2}} \;, \quad (5.48)$$

Where,

$$\beta_s = \alpha_s = \varphi_0 - \frac{\varphi_s}{2}. \quad (5.49)$$

The integral in Eq. (5.46) has the form of,

$$\int_{-\infty}^{\infty} exp\,(-\frac{y^2}{2})\,dy = \sqrt{2\pi}\,. \tag{5.50}$$

By letting,

$$A = -jk\,\frac{\rho_s\,cos\left(\varphi_0-\frac{\varphi_s}{2}\right)}{l cos^2\left(\frac{\varphi_s}{2}\right)}\left[\rho_s\,cos\left(\varphi_0-\frac{\varphi_s}{2}\right)-l\,cos\,\frac{\varphi_s}{2}\right], \tag{5.51}$$

the integral becomes,

$$\int_{-\infty}^{\infty} exp\,(-A\,\frac{(\varphi'-\varphi_s)^2}{2})d\varphi'. \tag{5.52}$$

Letting,

$$A(\varphi'-\varphi_s)^2 = y^2, \tag{5.53}$$

Then we write,

$$\sqrt{A}(\varphi'-\varphi_s) = y\,, \tag{5.54}$$

and

$$\sqrt{A}d\varphi' = dy. \tag{5.55}$$

By using Eq. (6.53) - Eq. (6.55) into Eq. (6.46), reflected field is reduced to,

$$E_r = e^{-jk\rho_s\,cos(\varphi_s-\varphi_0)}e^{-jkl}\sqrt{\frac{\rho_s\,cos\left(\varphi_0-\frac{\varphi_s}{2}\right)}{\rho_s\,cos\left(\varphi_0-\frac{\varphi_s}{2}\right)-l\,cos\frac{\varphi_s}{2}}}\;. \tag{5.56}$$

5.3 Numerical results for the reflected fields

The following figures Fig. 29 through Fig. 42 are the plots of the reflected field obtained in Eq. (5.56) and related geometry given in Fig. 1. The observation angle ρ is 6λ, where λ is the wavelength and taken as 0.1 meter. The focus of the parabola is 3λ, and k is the wave number which is equal to $2\pi/\lambda$.

In Fig. 29 and Fig. 30 reflected field is plotted for φ_0=pi/3, and $\varphi_s \in$ [-pi/3, pi/3] which means that the cylindrical parabolic reflector is located symmetrical with respect to x-axis.

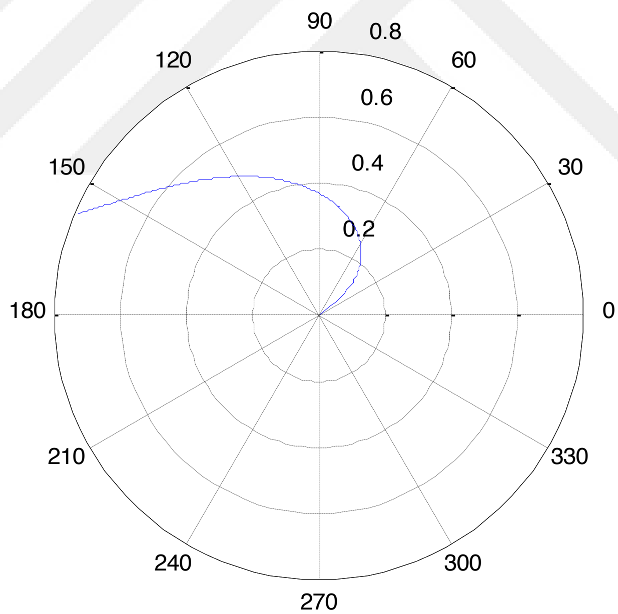

Figure 29 Reflected field variation with respect to φ.

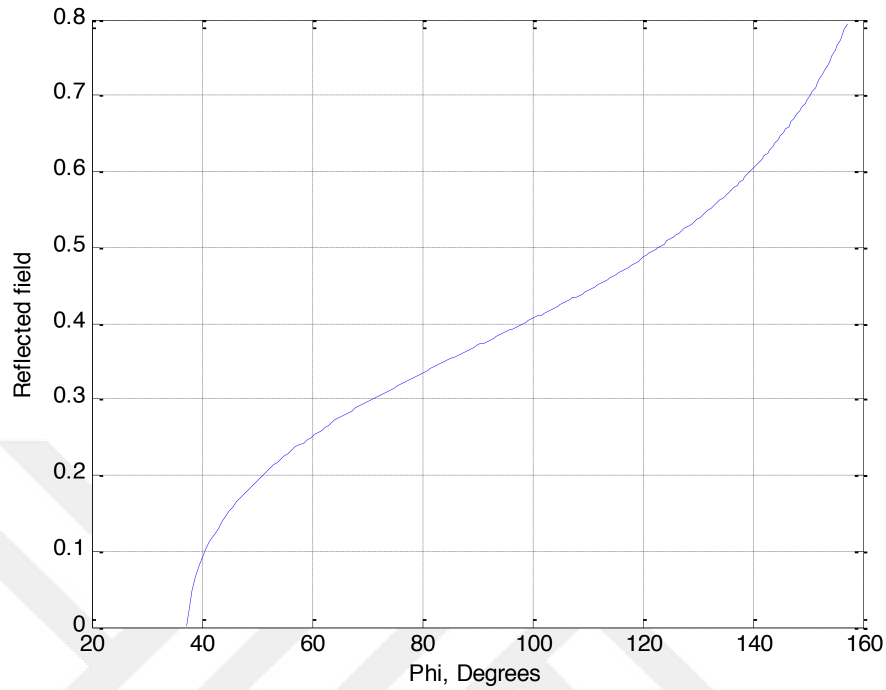

Figure 30 Reflected field variation with respect to φ.

This curve in Fig. 30 describes the variation of reflected field with respect to φ. Since φ is a function of φ_s , it takes the values as shown in Fig. 30.

From Fig. 31 and Fig. 32 we see that as the lower limit of φ_s is increased in magnitude, the reflected field moves clockwise which is reasonable due to the geometry.

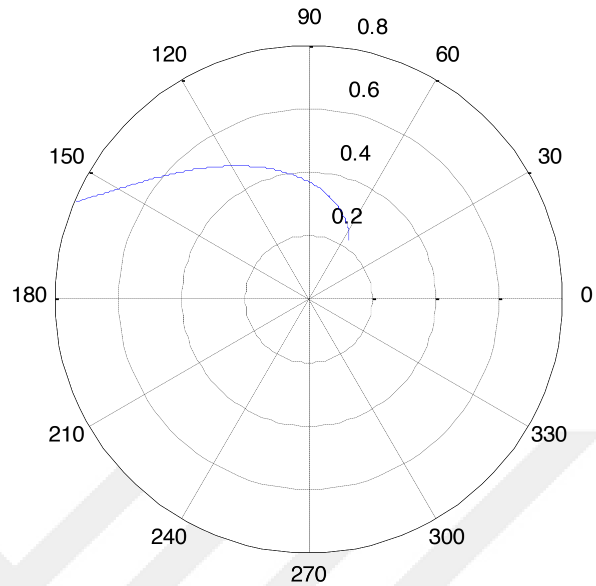

Figure 31 Reflected field variation for φ_0 =pi/3, and φ_s ϵ [-pi/4, pi/3].

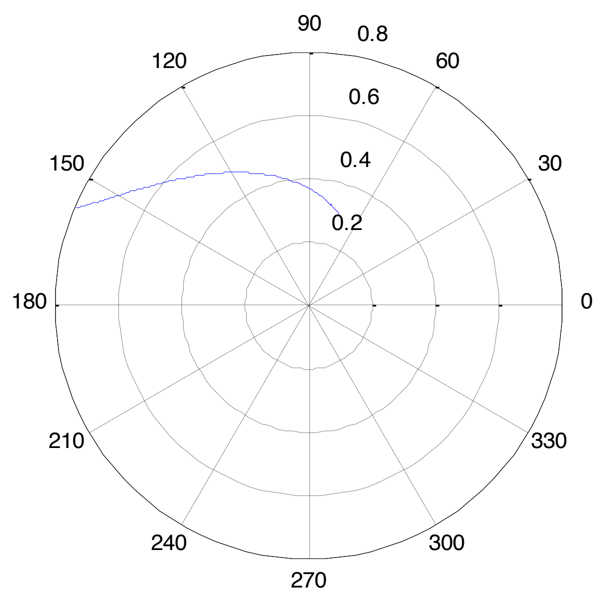

Figure 32 Reflected field variation for φ_0 =pi/3, and φ_s ϵ [-pi/6, pi/3].

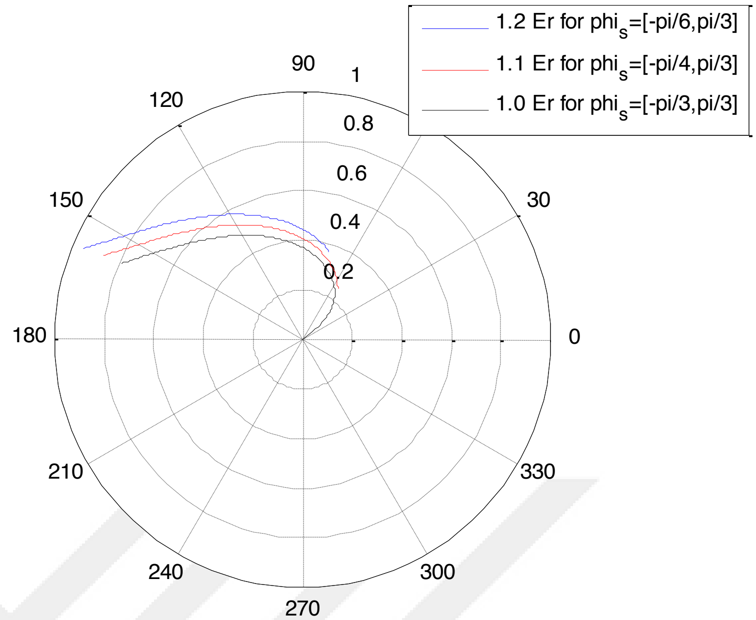

Figure 33 Reflected field variations for φ_0 =pi/3.

Here in Fig. 33 and Fig. 34, all three cases are shown together to verify this phenomenon. In Fig. 33, to avoid coincidences, E_r, 1.1 E_r, and 1.2 E_r are plotted by the colors of black, red, and blue respectively. In Fig. 34, to show the variations clearly, E_r is multiplied by 1.0, 1.05, and 1.1 and these curves are shown in colors of black, red, and blue respectively.

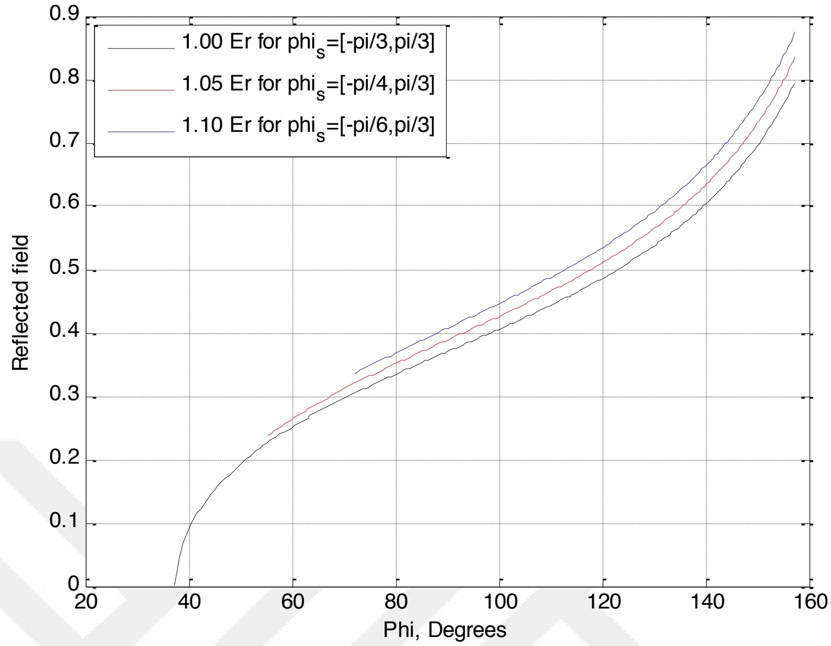

Figure 34 Reflected field for φ_0 =pi/3.

Fig. 35 and Fig. 36 depict the effects of the upper limit variation of the parabola on the reflected field. As can be seen from these figures when the lower limit of φ_s is increased, the reflected field moves counter-clockwise which is also an expected case due to the geometry.

In Fig. 35, to show the variations clearly, E_r is multiplied by 1.0, 1.05, and 1.1 and these curves are shown in colors of black, red, and blue respectively. The same operation is done for Fig. 36.

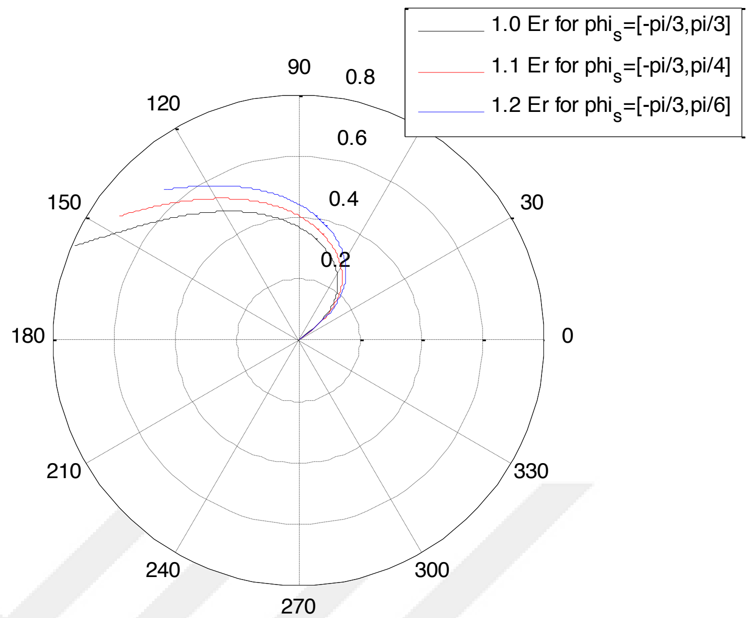

Figure 35 Reflected fields for φ_0 =pi/3.

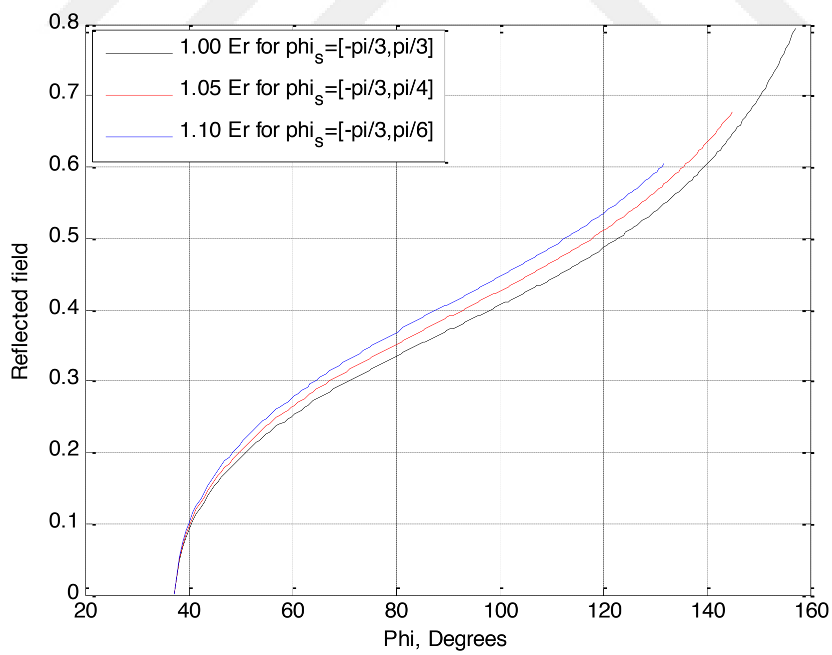

Figure 36 Reflected field versus φ variations.

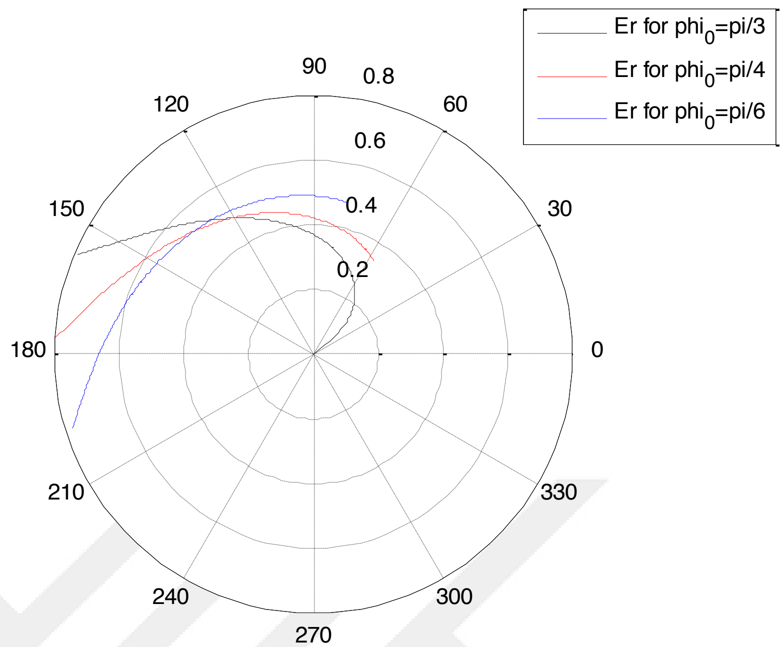

Figure 37 Reflected field variations in the interval of $\varphi_s \in$ [-pi/3, pi/3].

Fig. 37 shows the reflected field variation with respect to incident angle having a real component only. Using the same notation as in Chapter 2, let us call the real component φ_r, and the imaginary component as φ_i of the incident angle φ_0. When the angle is increased beam turns clockwise. Because φ_r determines the phase of the beam which is the feature of inhomogeneous waves.

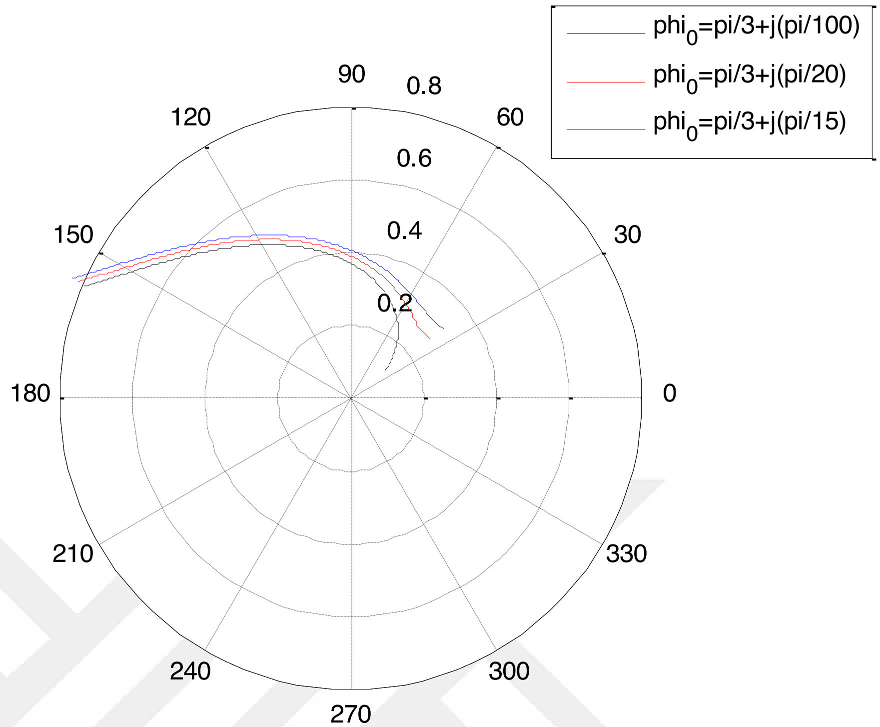

Figure 38 Reflected field variations due to positive φ_i .

In Fig. 38, for $\varphi_s \epsilon$ [-pi/3, pi/3] variation of the reflected field with respect to φ_i is shown. It can be observed that the field intensity and the φ_i are directly proportional. Complex conjugate of the incident angle does not affect the results as shown in Fig. 39 below.

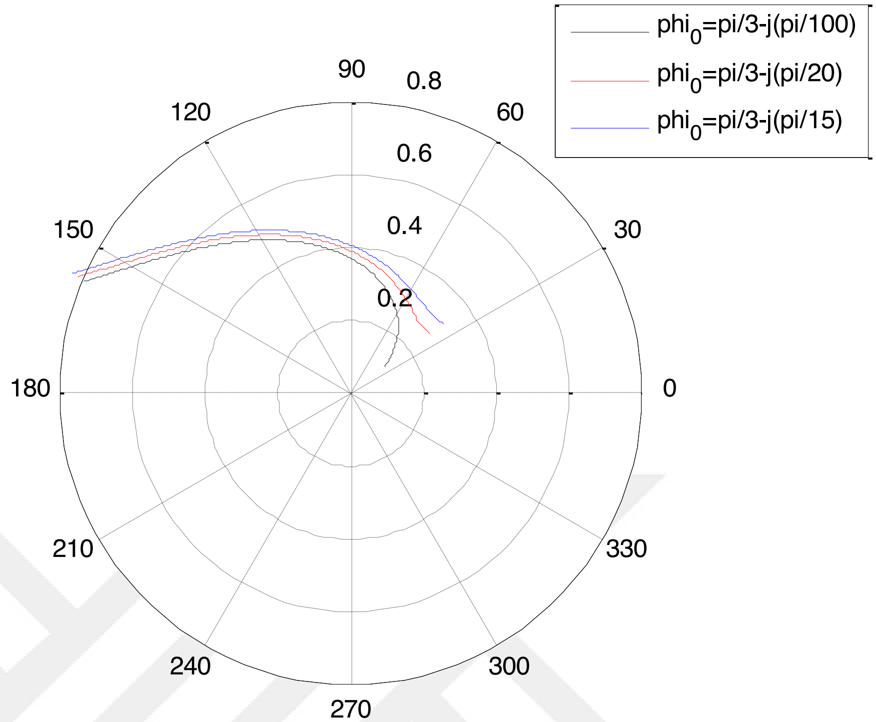

Figure 39 Reflected field variations due to φi, for φ_s ϵ [-pi/3, pi/3].

From Fig. 28 we can write,

$$\beta = \cos^{-1}\left(\frac{(R^2+(\rho\prime)^2-\rho^2)}{(2\rho R)}\right) - \frac{\varphi\prime}{2}. \tag{5.58}$$

The plot of β with respect to φ is given in Fig. 40.

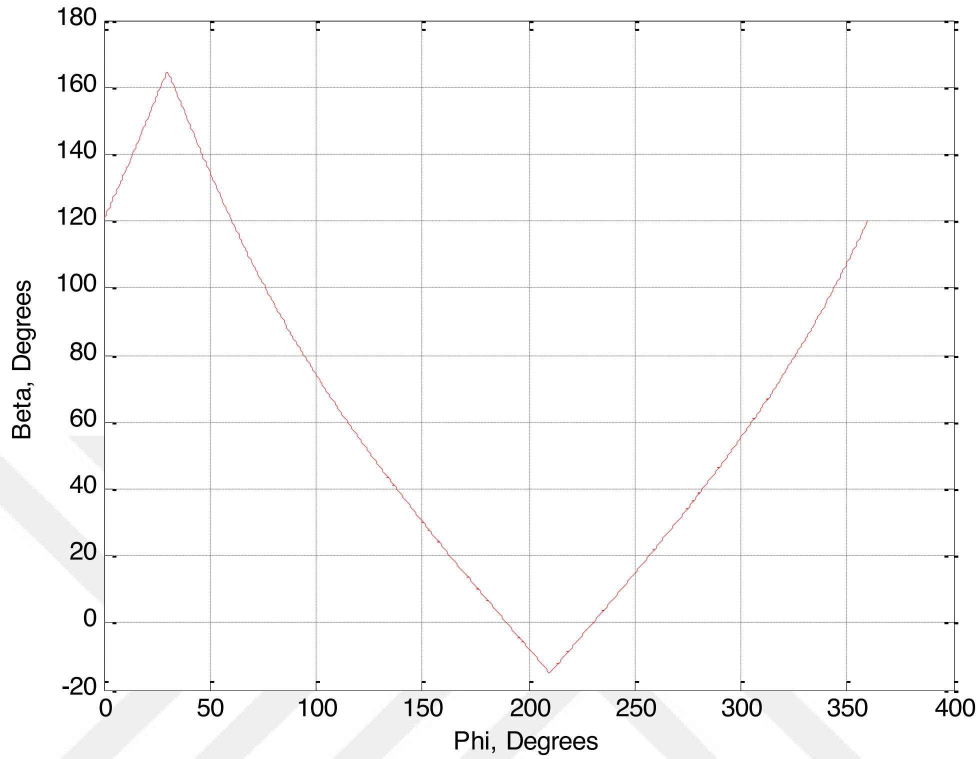

Figure 40 β versus φ graph for $\varphi'=\pi/3$.

To obtain smooth varying curve we need to alter this graph by means of unit step functions. This is necessary for preventing the abrupt changes in the transmitted, reflected, or both transmitted and reflected field plots. By doing this we obtain,

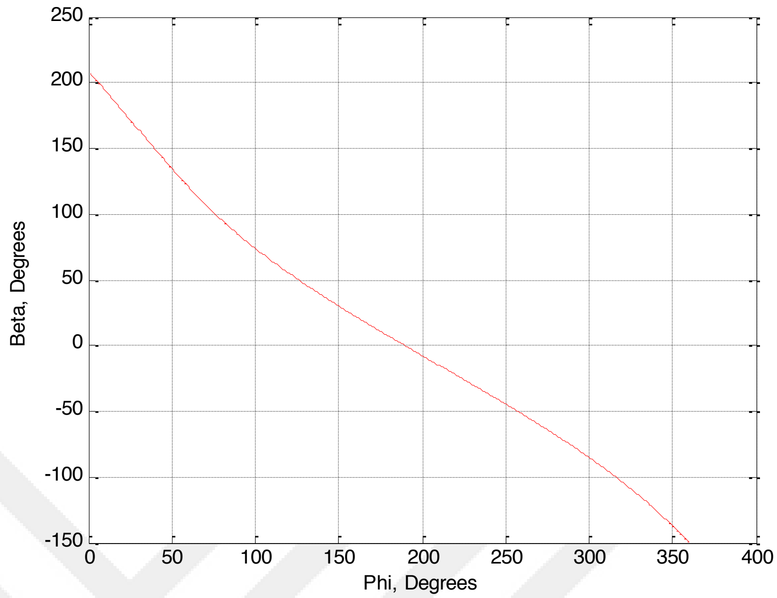

Figure 41 Altered β versus φ graph for φ'=π/3.

For various φ' values we obtain the curves shown in Fig. 42 below. Any of these can be used for the expressions containing β.

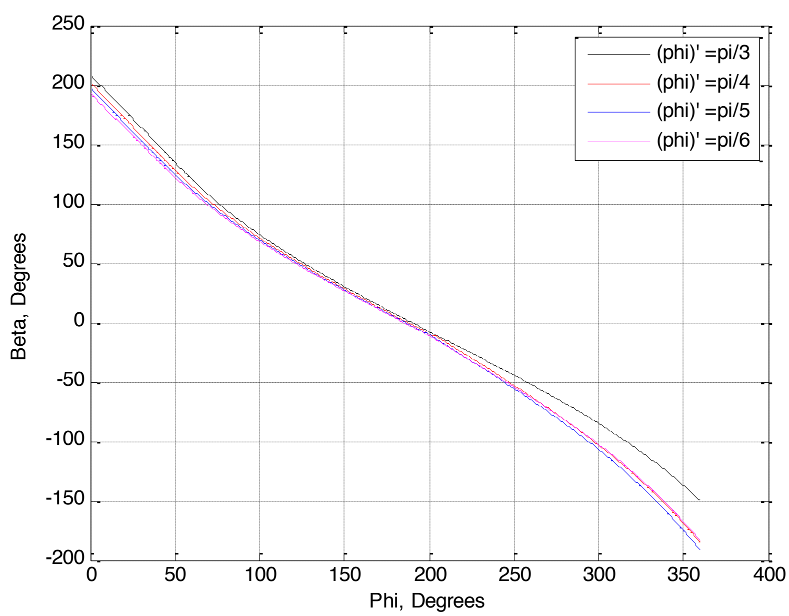

Figure 42 Revised beta versus φ variations.

Fig. 43 is plotted by using the total electric field [61] given by Eq. (5.59). It shows the total scattered field whose transmitted and reflected field components are the right and left lobes respectively.

$$E_s = \frac{kexp(j\pi/4)}{2\pi}\int_{-\varphi_e}^{\varphi_e}[\cos((\beta+\alpha)/2) + \sin((\beta-\alpha)/2)]\frac{exp\{-jk[\rho\prime\cos(\varphi'-\varphi_0)+R]\}}{\sqrt{kR}}\frac{\rho\prime}{\cos(\varphi\prime/2)}d\varphi' \tag{5.59}$$

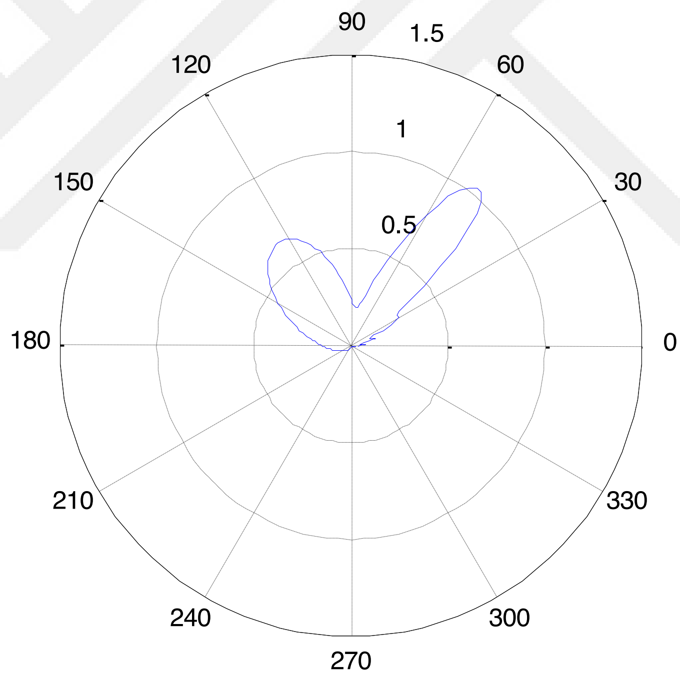

Figure 43 Total scattered field with respect to φ.

For the incident angle of the form "a + j b" where 'a' and 'b' are constants, the scattered field varies with respect to 'b', keeping 'a' constant, as in Fig. 44 below.

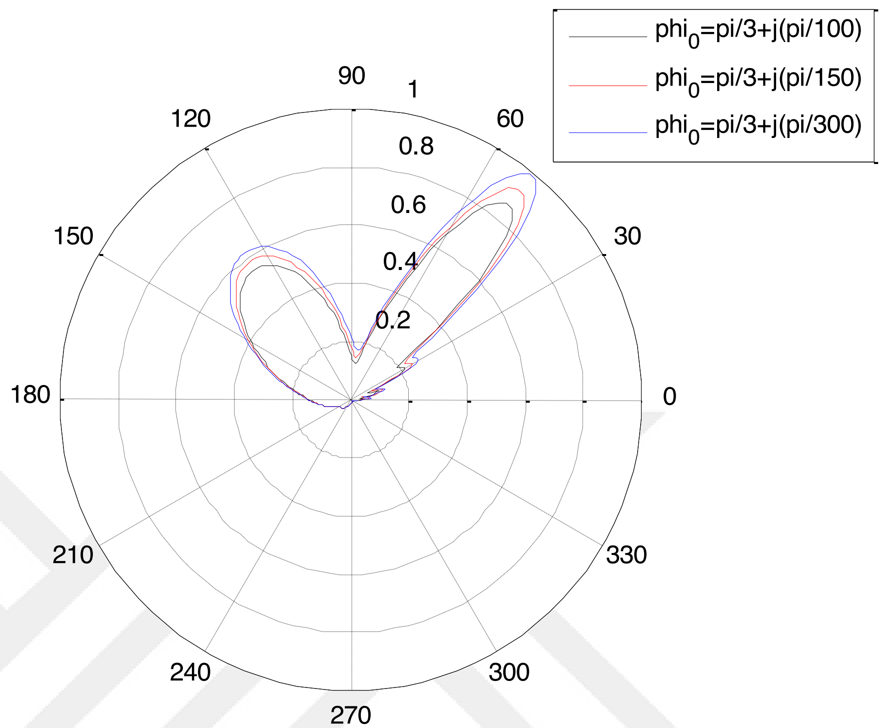

Figure 44 Total scattered field variations with respect to φ for φ_0 = a + j b values.

As the φ_i approaches to zero, the beam amplitude increases. On the contrary, as imaginary part of the incident angle having the form of "a-j b" approaches to zero, the beam amplitude decreases as shown in Fig. 45.

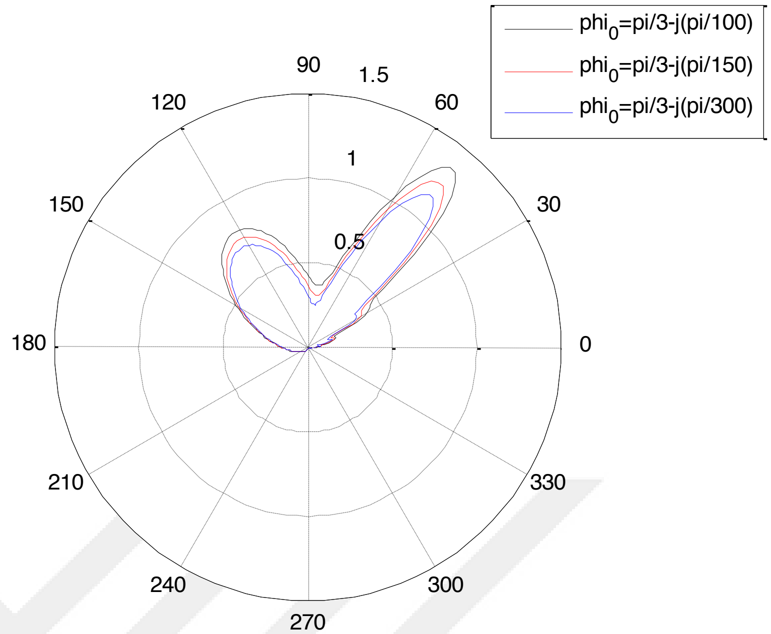

Figure 45 Total scattered field variations with respect to φ for φ_0 = a-j b values.

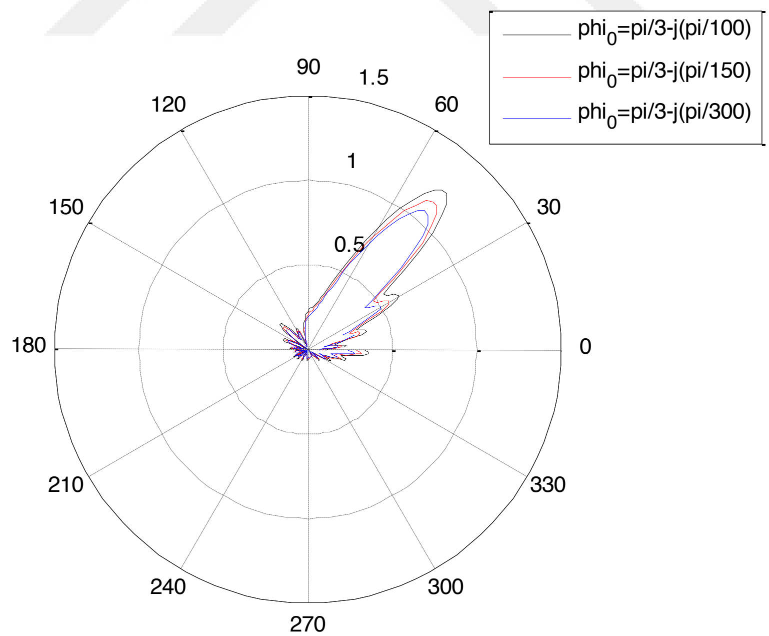

Figure 46 Transmitted field variations with respect to φ for φ_0 = a-j b values.

Fig. 46 and 47 show the variations of the transmitted and reflected beam amplitudes with respect to the imaginary part of the complex angle of incidence respectively.

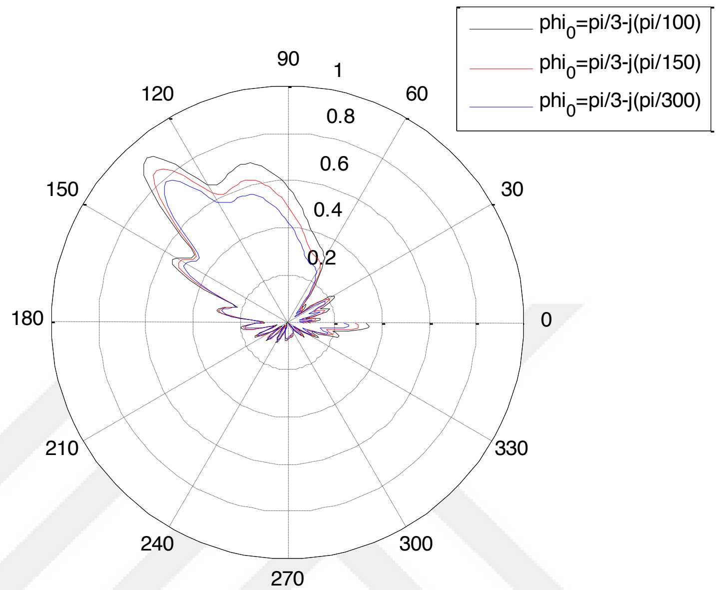

Figure 47 Reflected field variations with respect to φ for φ_0 = a-j b values.

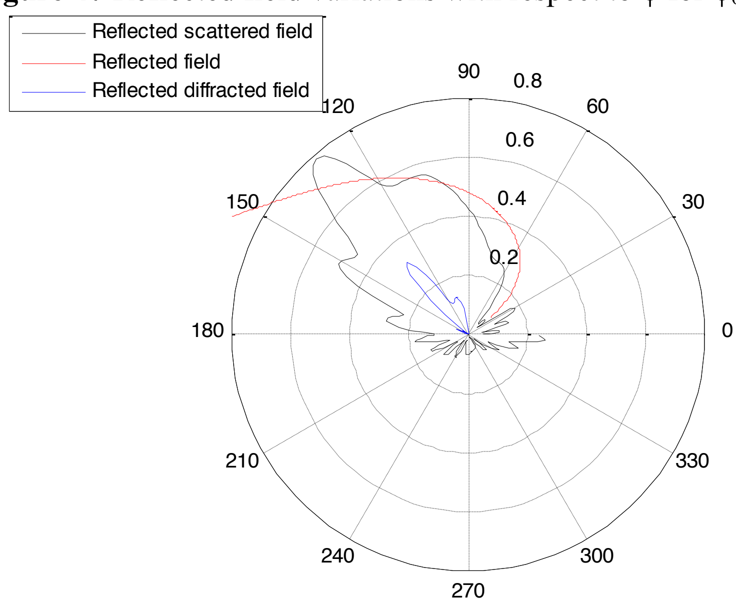

Figure 48 Reflected scattered field and its components.

In Fig. 48, reflected scattered, reflected and reflected-diffracted fields are shown all together on the same plot. Reflected field which is obtained by the stationary phase point method is subtracted from the reflected-scattered field and the reflected-diffracted field is obtained.

5.4 Diffracted waves

Diffracted field can be written as [61],

$$E_d \cong \frac{1}{jk}\left[\frac{f(\varphi_e)}{g\prime(\varphi_e)}\exp\big(-jkg(\varphi_e)\big) - \frac{f(-\varphi_e)}{g\prime(-\varphi_e)}\exp\big(-jkg(-\varphi_e)\big)\right], \tag{5.60}$$

where,

$$f(\varphi_e) = \frac{ke^{j\frac{\pi}{4}}}{\sqrt{2\pi}}\frac{\rho_e}{\sqrt{kR_e}\,cos\frac{\varphi_e}{2}} \ , \tag{5.61}$$

and

$$g(\varphi_e) = \rho_e\cos(\varphi_e - \varphi_0) + R_e \ . \tag{5.62}$$

Eq. (5.60) is obtained as,

$$E_d = \frac{e^{-j\frac{\pi}{4}}e^{jkR_e}e^{jk\rho_e\cos(\varphi_e-\varphi_0)}}{\sqrt{2k\pi R_e}}\left[\frac{\cos\left(\varphi_0-\frac{\varphi_e}{2}\right)}{\sin\left(\varphi_0-\frac{\varphi_e}{2}\right)-\sin\beta_{e1}} - \frac{\cos\left(\varphi_0+\frac{\varphi_e}{2}\right)}{\sin\left(\varphi_0+\frac{\varphi_e}{2}\right)-\sin\beta_{e2}}\right], \tag{5.63}$$

where,

$$R_e^2 = \rho^2 - \rho_e^2 - 2\rho\rho_e\cos(\varphi - \varphi_e). \tag{5.64}$$

Using the identity of,

$$\sin a - \sin b = 2\cos\frac{a+b}{2}\sin\frac{a-b}{2}\,, \tag{5.65}$$

For the upper edge,

$$E_d = \frac{e^{-j\left(\frac{\pi}{4}\right)} e^{jkR_e} e^{jk\rho_e \cos(\varphi_e-\varphi_0)}}{2\sqrt{2k\pi R_e}}\left[\frac{A}{\cos\frac{\varphi_0-\frac{\varphi_e}{2}+\beta_{e1}}{2}}+\frac{B}{\sin\frac{\varphi_0-\frac{\varphi_e}{2}-\beta_{e1}}{2}}\right]. \tag{5.66}$$

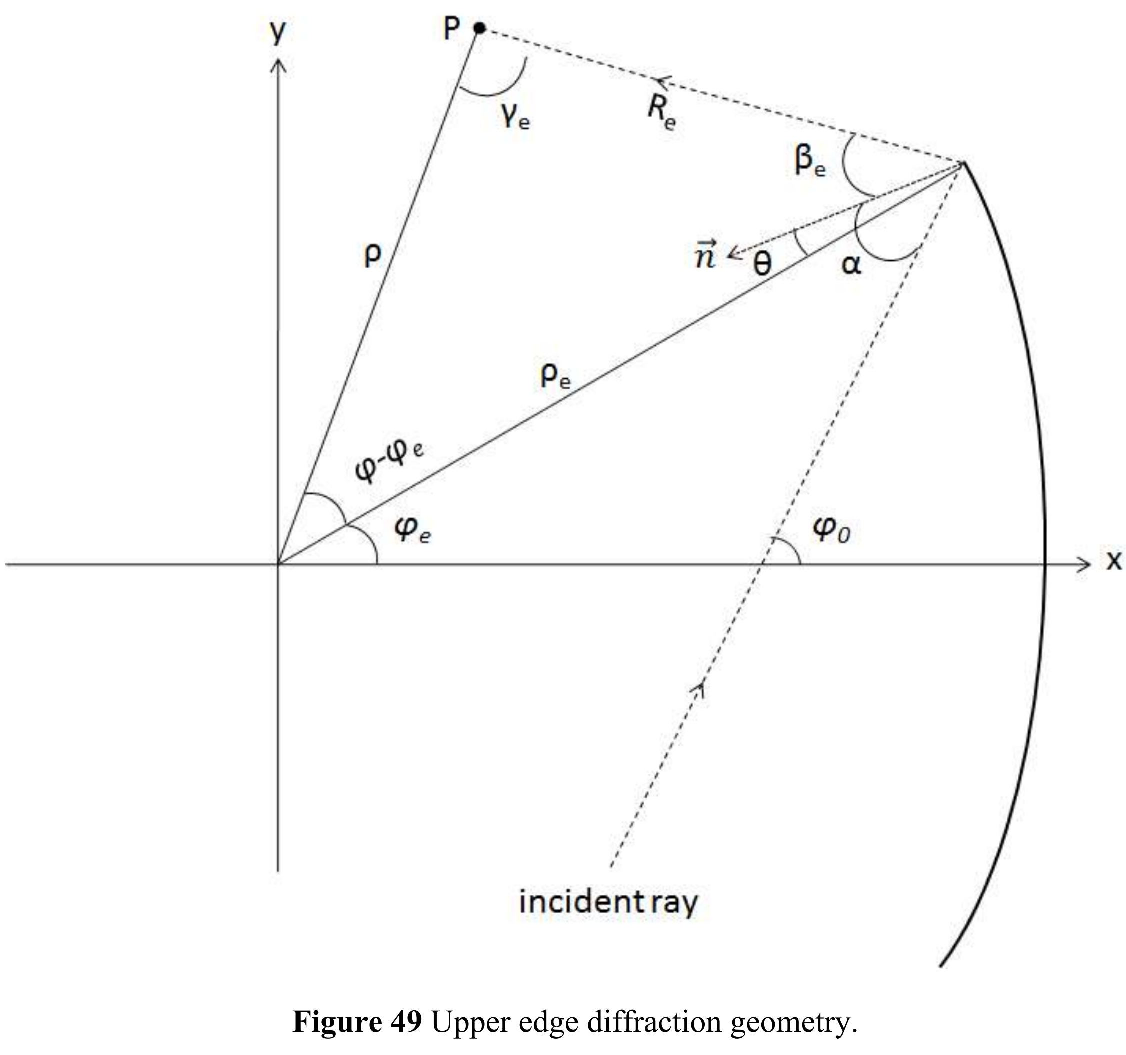

Figure 49 Upper edge diffraction geometry.

By the approach used in [93, 94] if we let,

$$t_1 = -\sqrt{2kR_e}\, cos\left(\frac{\varphi_0 - \frac{\varphi_e}{2} + \beta_{e1}}{2}\right), \tag{5.67}$$

we obtain,

$$kR_e = 2kR_e cos^2\left(\frac{\varphi_0 - \frac{\varphi_e}{2} + \beta_{e1}}{2}\right) - kR_e\, cos\left(\varphi_0 - \frac{\varphi_e}{2} + \beta_{e1}\right). \tag{5.68}$$

Reflected part of Ed can be written as,

$$E_{d1} = -sgn(t_1)F[|t_1|]\, cos\left(\varphi_0 - \frac{\varphi_e}{2}\right) Ae^{jkR_e\, cos\left(\varphi_0 - \frac{\varphi_e}{2} + \beta_{e1}\right)}, \tag{5.69}$$

where,

$$sgn(t_1)F[|t_1|] = \frac{e^{-j\frac{\pi}{4}}}{2\sqrt{\pi}} \frac{e^{-jt_1^2}}{t_1}. \tag{5.70}$$

Similarly, for

$$t_2 = -\sqrt{2kR_e}\, sin\left(\frac{\varphi_0 - \frac{\varphi_e}{2} - \beta_{e1}}{2}\right), \tag{5.71}$$

we can obtain,

$$kR_e = 2kR_e sin^2\left(\frac{\varphi_0 - \frac{\varphi_e}{2} - \beta_{e1}}{2}\right) + kR_e\, cos\left(\varphi_0 - \frac{\varphi_e}{2} - \beta_{e1}\right). \tag{5.72}$$

Transmitted part of E_d is obtained as,

$$E_{d2} = -sgn(t_2)F[|t_2|]\, cos\left(\varphi_0 - \frac{\varphi_e}{2}\right) Be^{jkR_e\, cos\left(\varphi_0 - \frac{\varphi_e}{2} - \beta_{e1}\right)}. \tag{5.73}$$

Diffracted field can be concluded as,

$$E_{d1} + E_{d2} = -sgn(t_1)F[|t_1|]\,cos\left(\varphi_0 - \frac{\varphi_e}{2}\right)Ae^{jkR_e\,cos\left(\varphi_0 - \frac{\varphi_e}{2} + \beta_{e1}\right)}$$
$$- sgn(t_2)F[|t_2|]\,cos\left(\varphi_0 - \frac{\varphi_e}{2}\right)Be^{jkR_e\,cos\left(\varphi_0 - \frac{\varphi_e}{2} - \beta_{e1}\right)}\,.$$

where A and B are the undetermined coefficients. (5.74)

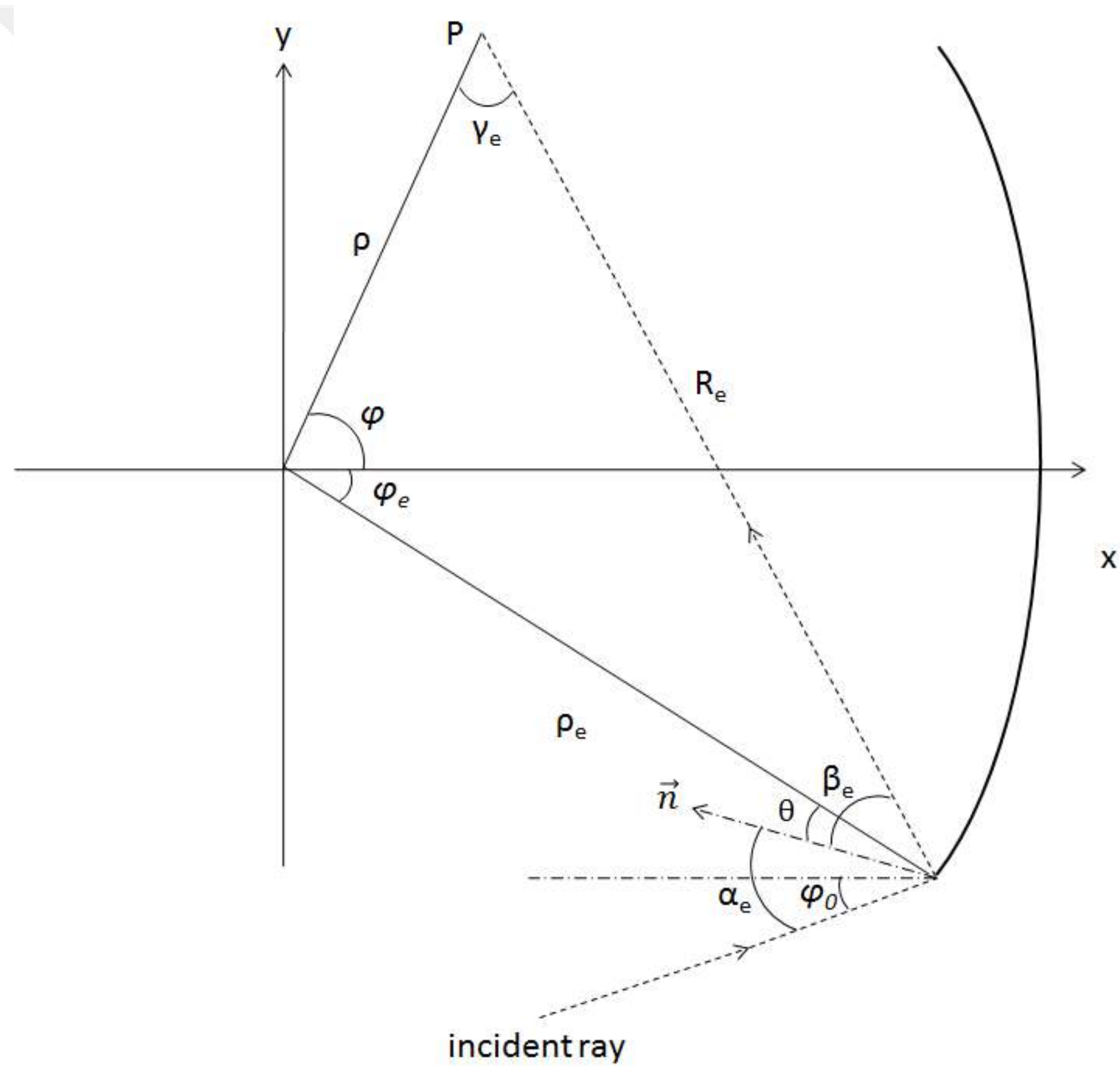

Figure 50 Lower edge diffraction geometry.

In a similar manner, diffracted field for the lower edge can be found as,

$$E_{d1} + E_{d2} = -sgn(t_3)F[|t_3|]\cos\left(\varphi_0 + \frac{\varphi_e}{2}\right) Ce^{jkR_e \cos\left(\varphi_0 + \frac{\varphi_e}{2} + \beta_{e2}\right)} -$$

$$sgn(t_4)F[|t_4|]\cos\left(\varphi_0 + \frac{\varphi_e}{2}\right) De^{jkR_e \cos\left(\varphi_0 + \frac{\varphi_e}{2} - \beta_{e2}\right)}, \qquad (5.75)$$

where C and D are the undetermined coefficients, and

$$t_3 = -\sqrt{2kR_e}\cos\left(\frac{\varphi_0 + \frac{\varphi_e}{2} + \beta_{e2}}{2}\right), \qquad (5.76)$$

and

$$t_4 = -\sqrt{2kR_e}\sin\left(\frac{\varphi_0 + \frac{\varphi_e}{2} - \beta_{e2}}{2}\right). \qquad (5.77)$$

5.5. Numerical results for the diffracted fields

The following plots between Fig. 51. and Fig. 59 are obtained for the upper edge of the

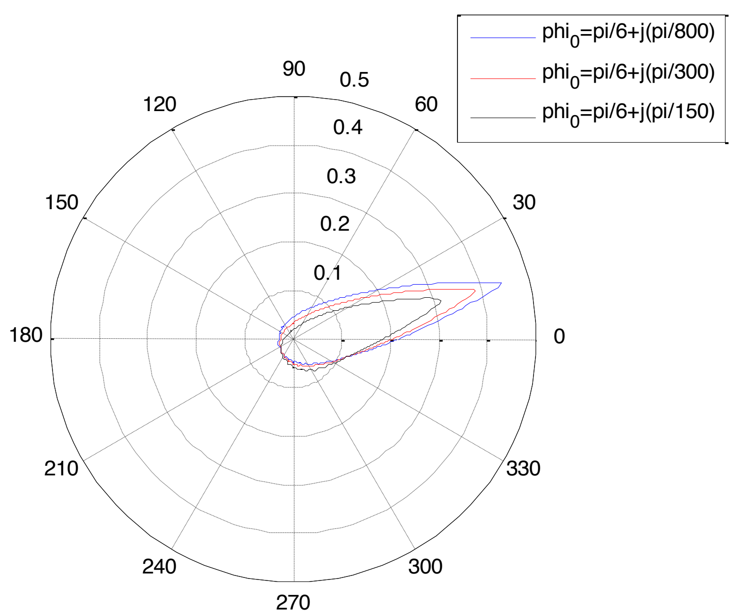

Figure 51 Upper edge transmitted field for positive φ_i values.

reflector. As can be seen in Fig. 51 and Fig. 52, the positive imaginary part φ_i of the incident angle and the beam amplitude are inversely proportional.

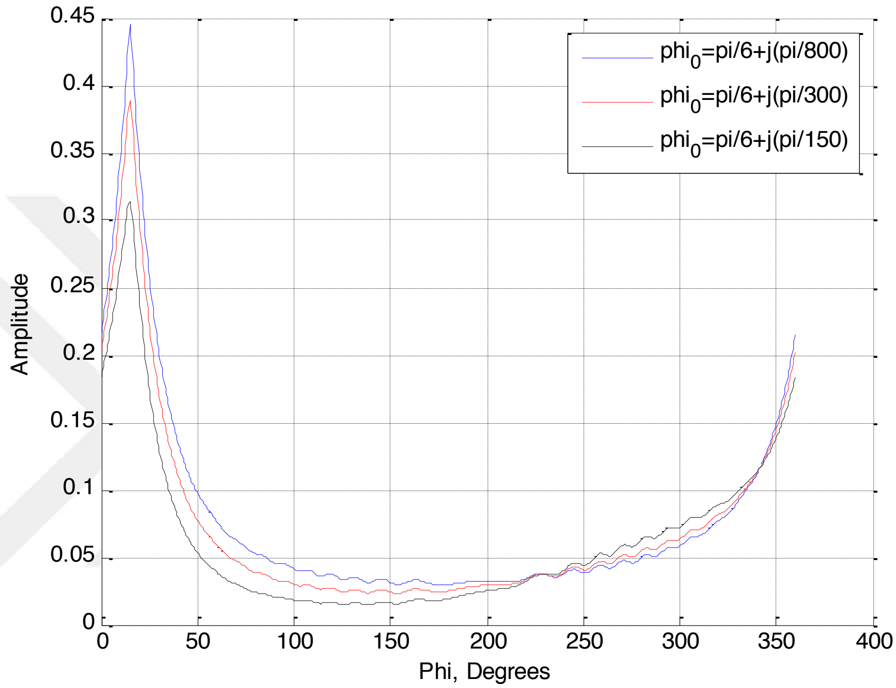

Figure 52 Upper edge transmitted field for positive φ_i values.

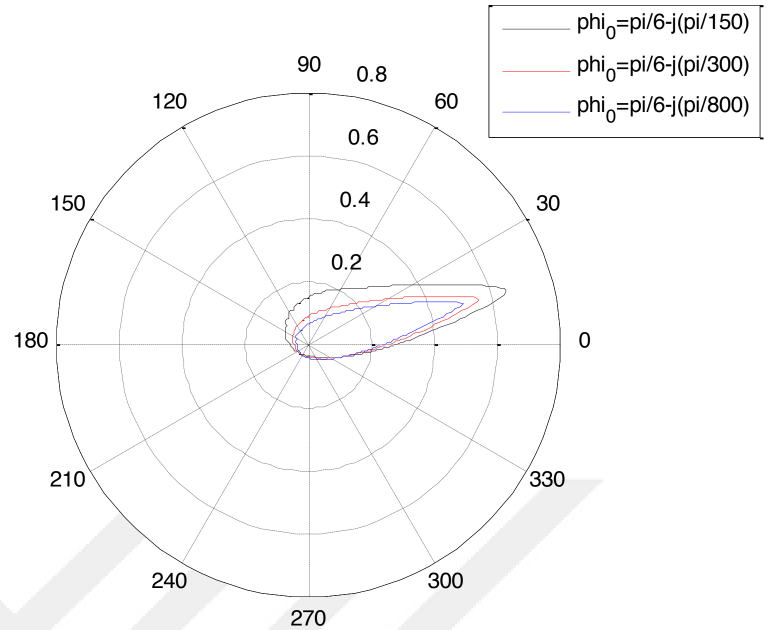

Figure 53 Upper edge transmitted field for negative φ_i values.

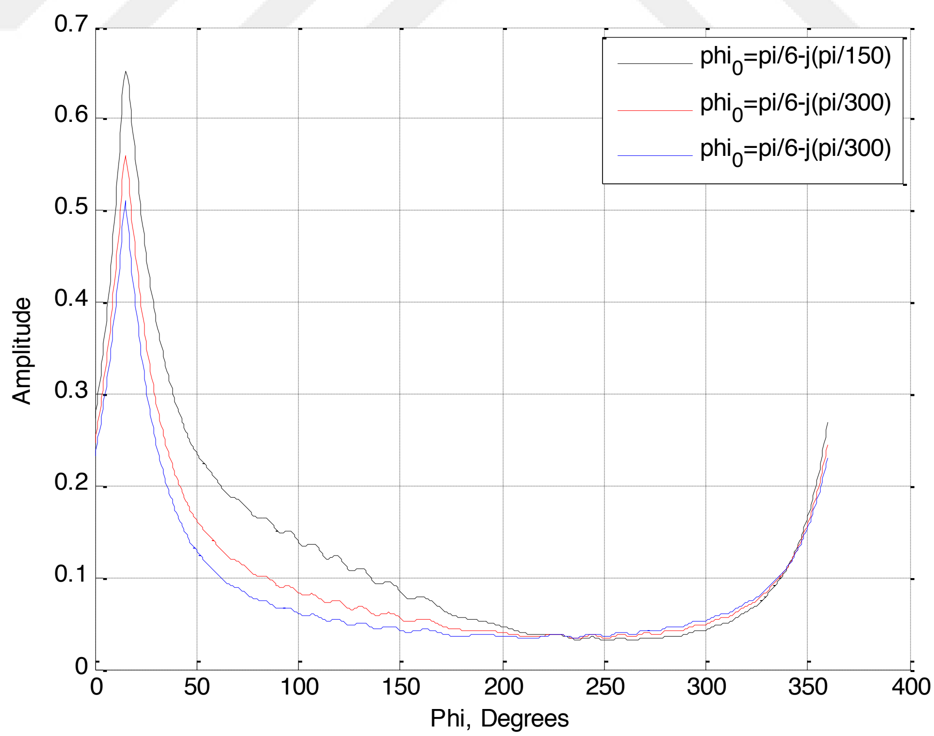

Figure 54 Upper edge transmitted field for negative φ_i values.

In Fig. 53 and Fig. 54, the negative imaginary part of the incident angle and the beam amplitude are directly proportional. Fig. 55 and Fig. 56 depict reflected part of the scattered field for the incident angle having a constant real part and various positive imaginary parts while Fig. 57 and Fig 58 are having the same conditions except that they have negative imaginary components below. For the positive imaginary components their magnitudes are inversely proportional to the beam magnitudes whereas for the negative ones they are directly to the beam magnitudes.

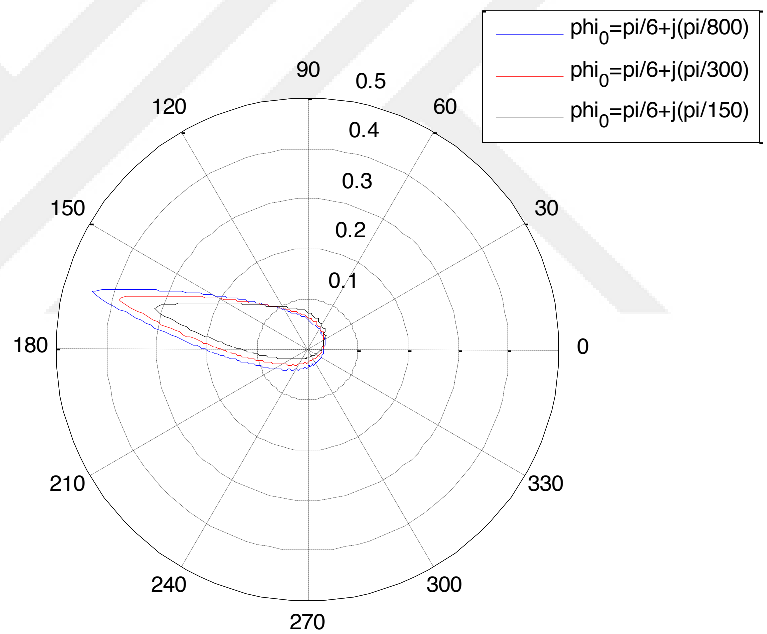

Figure 55 Upper edge reflected field for positive φi values.

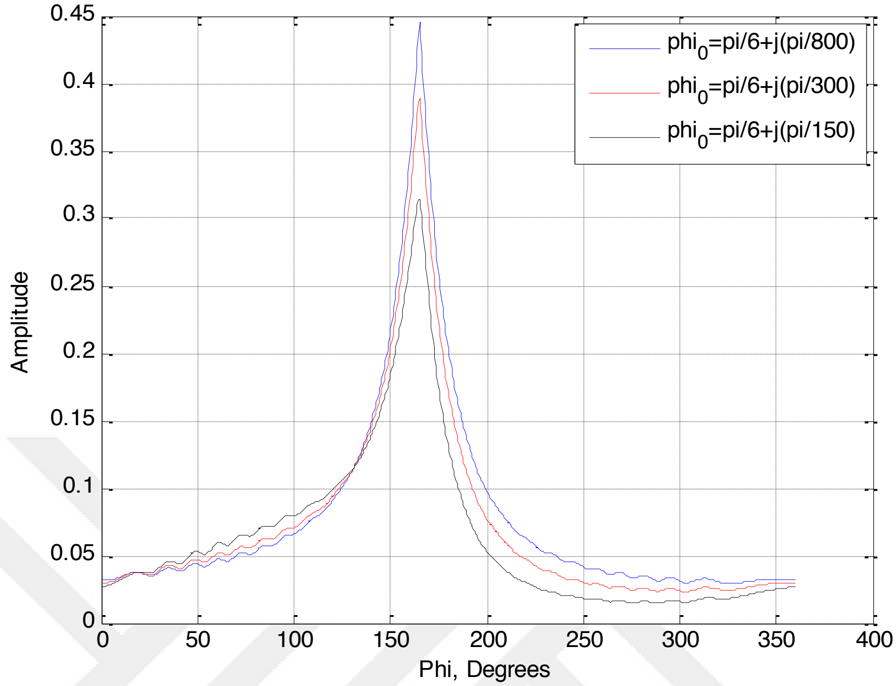

Figure 56 Upper edge reflected field for positive φ_i values.

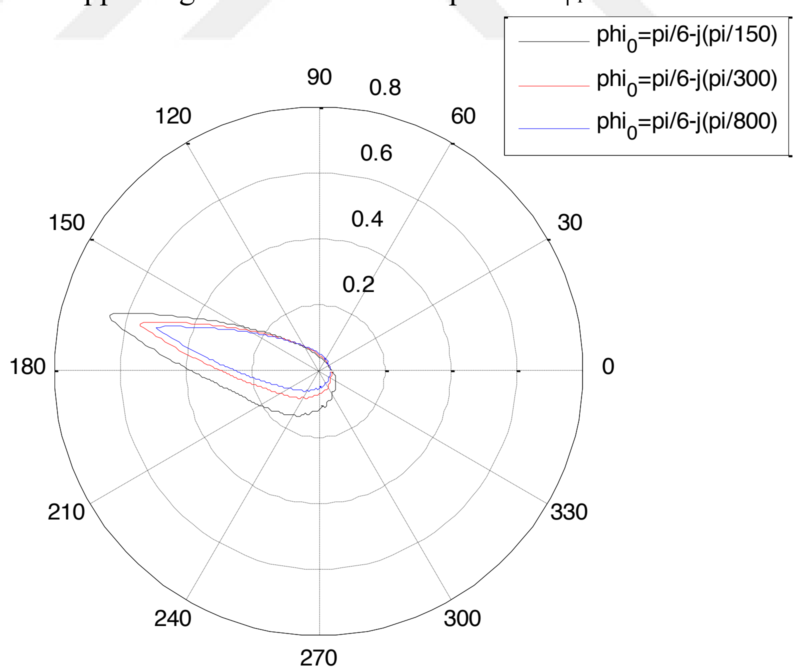

Figure 57 Upper edge reflected field for negative φ_i values.

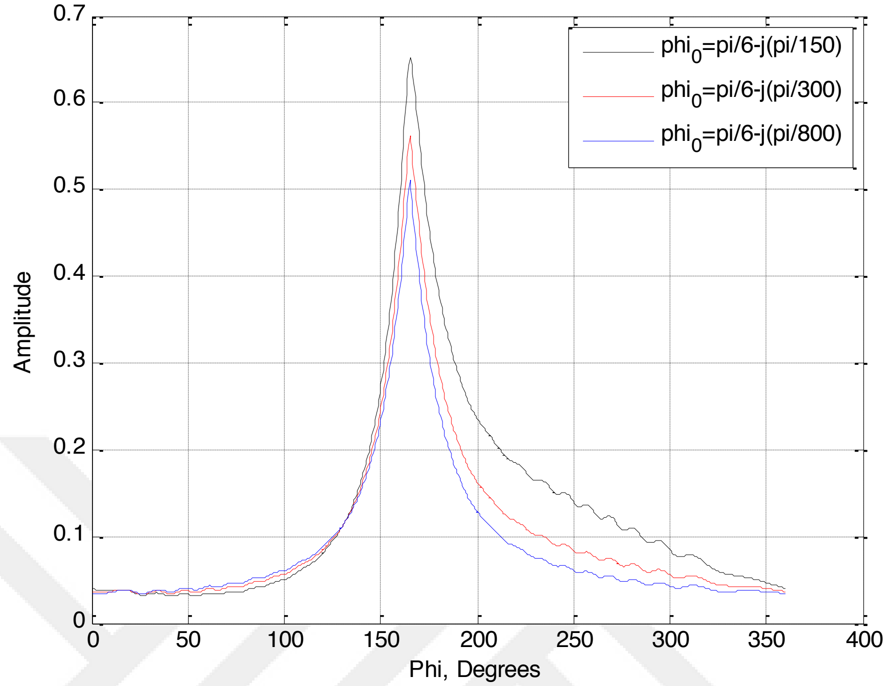

Figure 58 Upper edge reflected field for negative φ_i values.

We can conclude that for the negative imaginary components of the incident angle, beam amplitude and the absolute value of the imaginary part are directly proportional, for the positive imaginary components they are inversely proportional.

In addition, symmetry axis of the beam varies by changing the imaginary component value. It is remarkable to note that when the imaginary part of the incident angle vanishes, the beam becomes symmetrical with respect to an axis which connects the origin and vertex of the beams shown in Fig. 59 below.

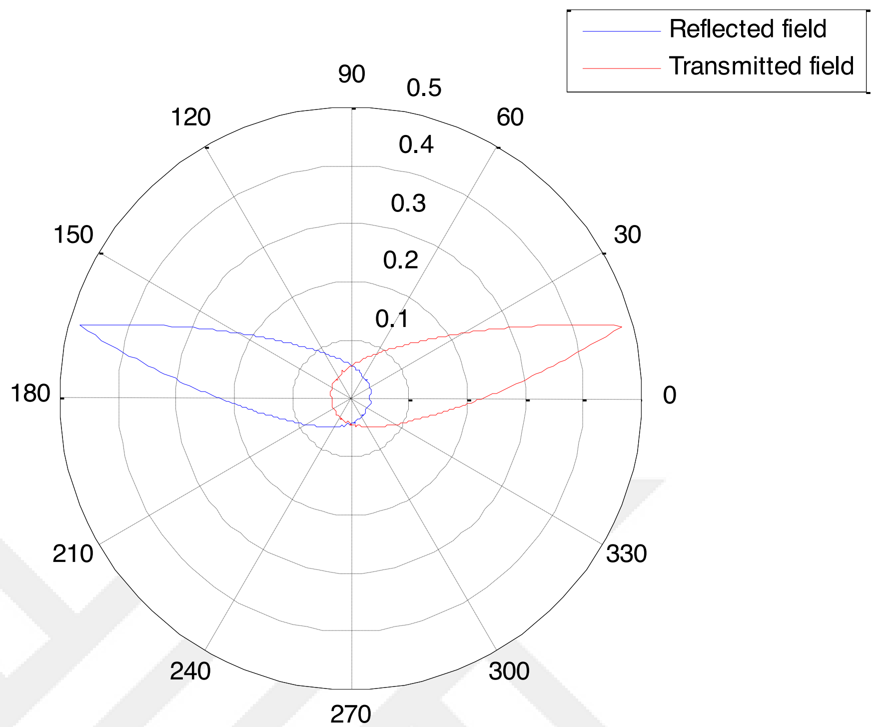

Figure 59 Upper edge reflected and transmitted fields for φ_0 =pi/6.

The following plots Fig. 60 through Fig. 67 are obtained for the lower edge of the reflector. The first four figures belong to the reflected field, whereas the last four ones represent the transmitted field. Fig. 60 and Fig. 61 show the changes in the beam amplitudes for the positive imaginary values (φ_i) of the incident angle. We see that amplitude decreases with the increasing values of φ_i.

Fig. 62 and Fig 63 show the effect of complex conjugate of incident angles used in Fig. 60 and Fig. 61. It is seen that the beam amplitude and φ_i are directly proportional for this case. In Fig. 64 and Fig. 65 the beam amplitude and φ_i are inversely proportional whereas in Fig. 66 and Fig. 67 they are directly proportional.

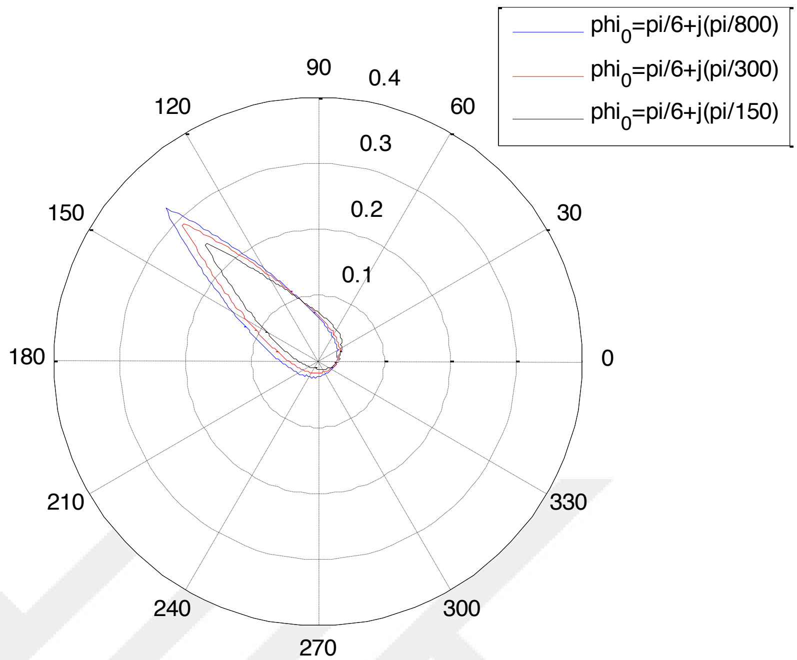

Figure 60 Lower edge reflected field for positive φ_i values.

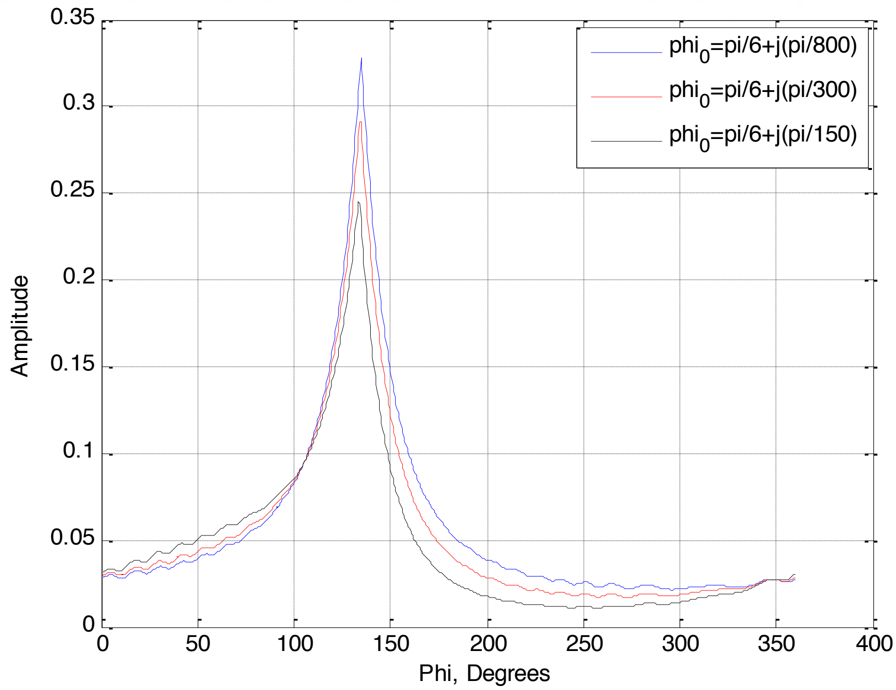

Figure 61 Lower edge reflected field for positive φ_i values.

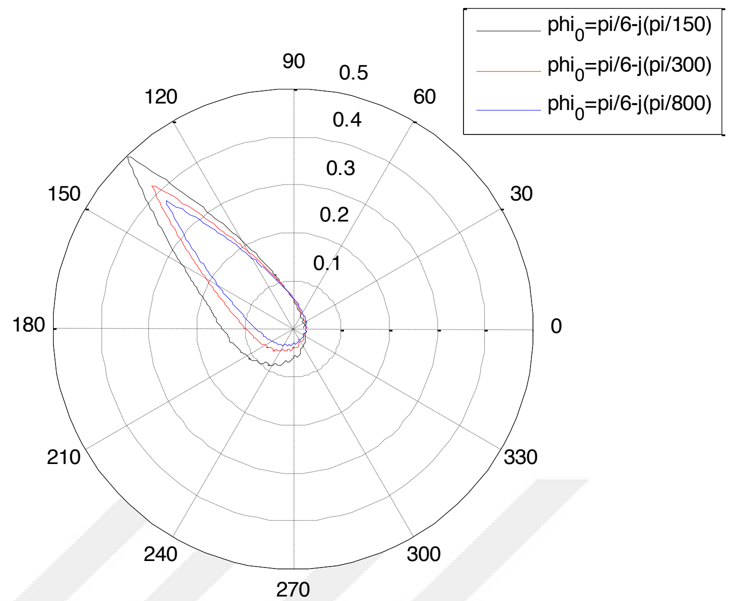

Figure 62 Lower edge reflected field for negative φ_i values.

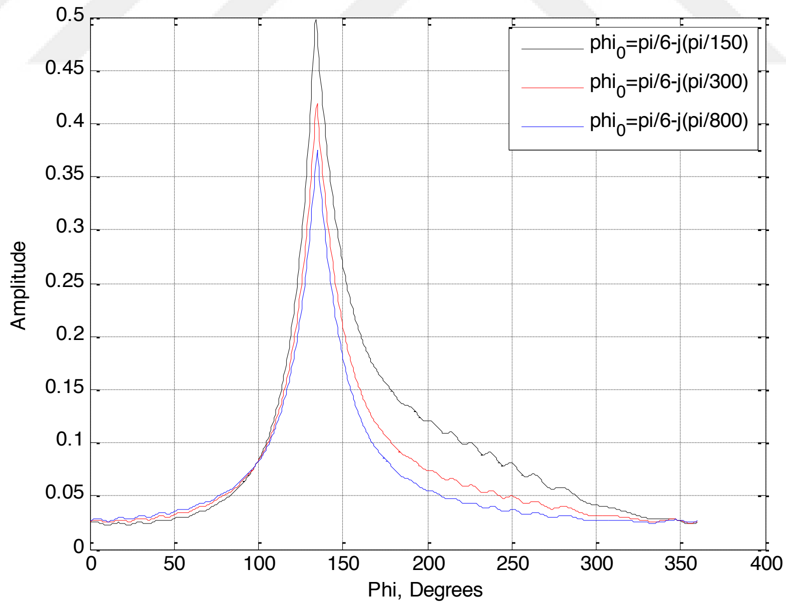

Figure 63 Lower edge reflected field for negative φi values.

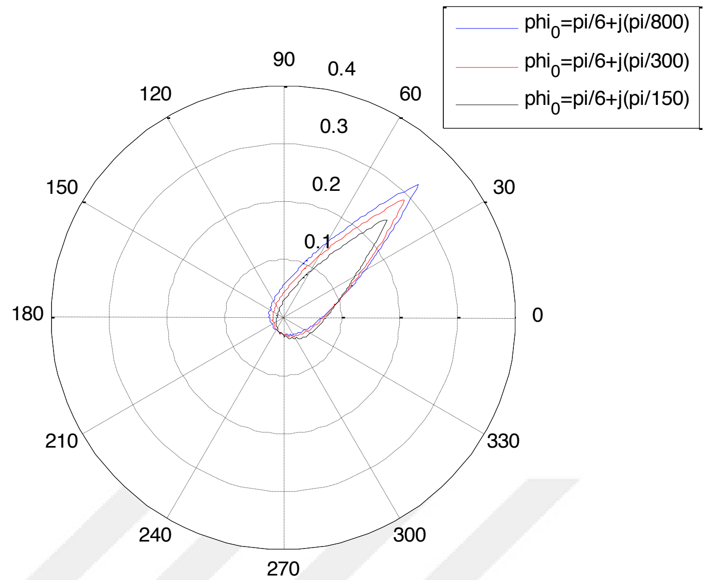

Figure 64 Lower edge transmitted field for positive φ_i values.

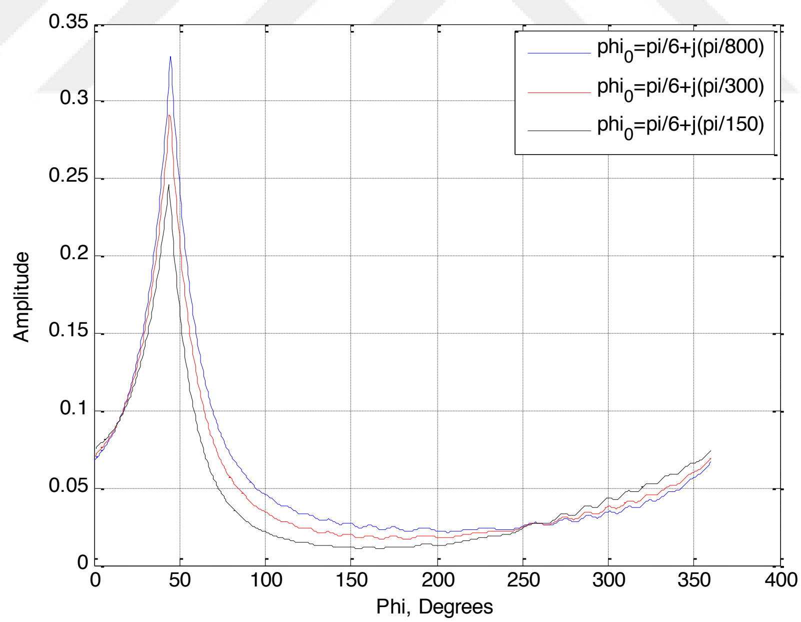

Figure 65 Lower edge transmitted field for positive φi values.

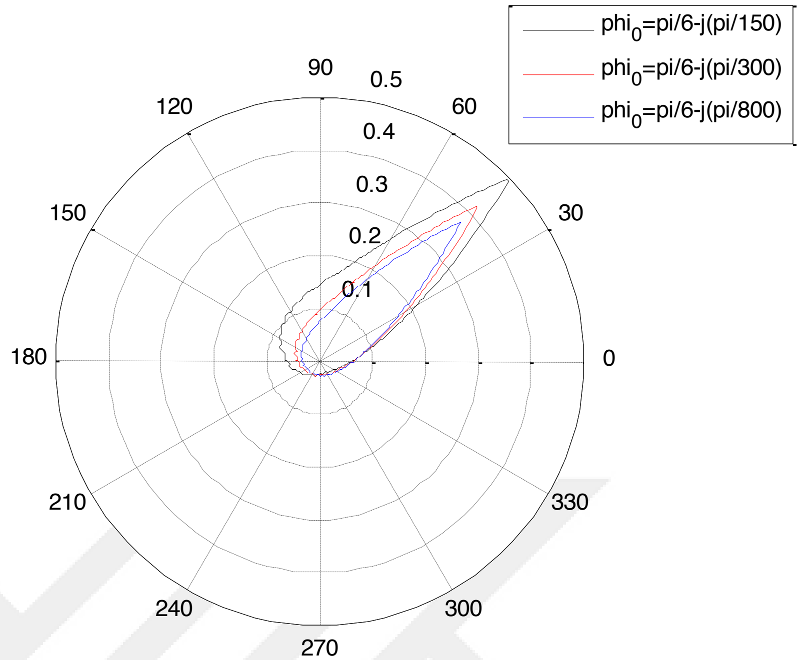

Figure 66 Lower edge transmitted field for negative φ_i values.

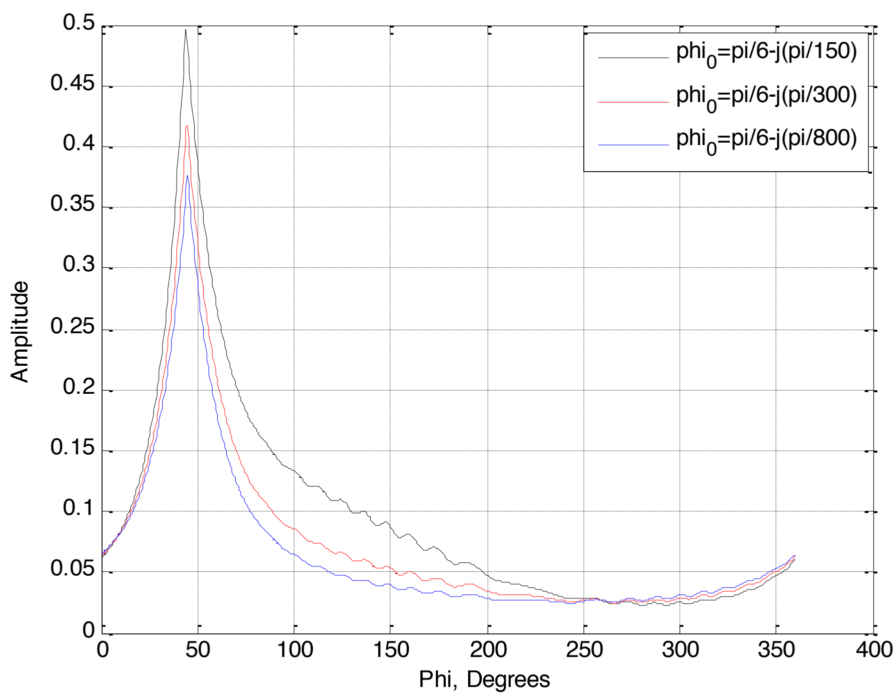

Figure 67 Lower edge transmitted field for negative φ_i values.

CHAPTER 6

CONCLUSION

In this study, evanescent waves are reviewed, and as the subclasses of these waves, inhomogeneous plane waves and Gaussian beams are derived. Also, for these two subclasses numerical analyses are carried out to figure out the behavior of these waves. The diffraction theory is discussed briefly and Kirchhoff's diffraction integral on which many diffraction problem solutions are based is derived. A non-uniform diffracted field expression encountered at the end of asymptotic evaluations had to be solved to get a uniform field expression. Otherwise diffracted field would approach to infinity at the reflection and shadow boundaries due to the asymptotic high-frequency characteristics of the obtained field expression. To obtain a uniform expression, a feature of Fresnel function is utilized. The uniform field expressions for both upper and lower edges of the reflector are obtained.

Inhomogeneous wave is obtained as the multiplication of two exponential terms, one representing the phase or propagation direction, and the other the amplitude of it. It is observed that the wave amplitude decreases with the decreasing imaginary component of the incident angle meaning that they are directly proportional. Complex conjugate of incident angle resulted in a field that is 180 degrees out of phase with the former one. Also, an incident angle with no real component resulted in beam radiation directed to –

$\pi/2$ or $\pi/2$ depending to the polarity of the imaginary component of the incident angle. To verify the theory, an incident angle with no imaginary component is applied and a plane wave radiation which is a circle is obtained. Besides, it is observed that when the real component is changed and the imaginary component is kept constant in the incident angle, a phase shift in the beam direction with the same amount as the change in the real component occurs. For the Gaussian beams all the necessary calculations to obtain the ultimate expression are performed and the plots of Gaussian beams for its parameters are implemented. In the last stage that is the main part of this study, the asymptotic evaluation of the scattering integral based on the MTPO is carried out. We used the surface integrals of MTPO to express the scattering integral for a cylindrical parabolic PEC reflector on which a plane wave is incident with an arbitrary angle. Asymptotic evaluations of the scattering integrals are obtained by some approximation methods. For the reflected and diffracted fields, we used the stationary phase method, and the edge point method respectively. Reflected and edge diffracted waves are plotted numerically for some parameters. It is observed that the fields that are obtained and plotted are reasonable and consistent. Also, by taking the incident angle as a complex parameter, evanescent waves are obtained for both reflected and diffracted fields. The behavior of evanescent waves is observed and compared to the theory. The results obtained complied with the theoretical derivations.

REFERENCES

1. **Stutzman, W. L., Thiele, G. A. (1998)** "Antenna theory and design", John Wiley & Sons, Second edition.

2. **Felsen, L. B., Marcuwitz, N., (1994)** "Radiation and Scattering of Waves", John Wiley & Sons.

3. **Kouyoumjian R. G. and Pathak P. H., (1974),** "A Uniform Theory of Diffraction for Edge in A Perfectly Conducting Surface", Prog. IEEE, vol.62 no. 11, pp. 1448-1461.

4. **Keller J. B., (1962),** "Geometrical Theory of Diffraction", J. Opt. Soc. Am., vol. 52, pp.116-130.

5. **McDonald H. M., (1913),** "The Effect Produced by an Obstacle on A Train of Electric Waves", Phil. Trans. R. Soc. Lond., Ser. A., Math. Phys. Sc., vol. 212, pp. 299-337.

6. **Pathak P.**, **(1979),** "An Asymptotic Analysis of the Scattering of Plane Waves by A Smooth Convex Cylinder", Radio.Sci., vol.14, pp. 419-435.

7. **Umul Y. Z., Yalcin U., (2003).** "Asymptotic Evaluation Of The Edge Diffraction In Cylindric Paraboloidal Reflector Antennas," Math. Comput. Appl. Int. J. **8**, 143-150.

8. **Franz W., (1954),** “Über die Green’she Funktion des Zylinders und der Kugel”, Z. Naturforsch., vol. 9a, pp.705-716.

9**. Borghi F., Santarsiero M., Frezza F., Schettini G., (1996),** “Plane-wave Scattering by A Perfectly Conducting Circular Cylinder Near A Plane Wave Surface: Cylindrical-Wave Approach”, J. Opt. Soc. Am., vol. 13, pp. 483-493.

10. **Umul Y. Z., (2012)** “Diffraction of Plane Waves by The Interface Between Black and Soft/Hard Semi-Planes,” Optik -Int. J. Light Electron Opt. **123**, 624-628

11. **Umul Y. Z., (2010)** “Diffraction of Plane Waves by A Black Wedge,” Opt. Laser Technol. **42**, 32-36.

12. **Umul Y. Z., (2009)** “Closed Form Series Solution of the Diffraction Problem of Plane Waves By An Impedance Half-Plane,” J. Opt. A: Pure Appl. Opt. **11**, 045709 (7 pp.).

13. **Umul Y. Z., (2007)** “Diffraction of Evanescent Plane Waves by A Resistive Half-Plane,” J. Opt. Soc. Am. A **24**, 3226-3232.

14 **Ufimtsev P. Ya., (2007),** “Fundamentals of The Physical Theory of Diffraction”, Wiley, New Jersey.

15. **Ufimtsev P. Ya., (2007),** “Fast Convergent Integrals for Nonunifrom Currents on Wedge Faces”, J. Electromagnetics, vol. 18, pp. 289-313.

16. **Ufimtsev P. Ya., (1989),** “Theory of Acoustical Edge Waves”, J. Acoust. Soc. Am., vol. 86, pp. 463-474.

17. **Ufimtsev P. Ya., (2006),** “Improved Theory of Acoustic Elementary Edge Waves”, J. Acoust. Soc. Am, vol. 120, p. 631.

18. **Ufimtsev P. Ya., (1991),** “Elementary Edge Waves and The Physical Theory of Diffraction”, J. Electromagnetics, vol. 11, pp. 125-160.

19. **Ufimtsev P. Ya., (2006),** “Improved Physical Theory of Diffraction: Removal of the Grazing Singularities”, IEEE Trans. Antennas Propagat., vol. 54, pp. 2698-2702.

20. **Umul Y. Z., (2004)**, “Modified Theory of Physical Optics,” Opt. Express, vol.12, no. 20, pp.4959–4972.

21. **Umul Y. Z., (2005)** “Modified Theory of Physical Optics Approach to Wedge Diffraction Problems,” Opt. Express 13, 216-224.

22. **Umul Y. Z., (2006)** “Modified Theory of the Physical-Optics Approach to The Impedance Wedge Problem,” Opt. Lett. 31, 401-403.

23. **Umul Y. Z., (2006)** "Modified Theory of Physical Optics Solution of Impedance Half Plane Problem," IEEE Trans. Antennas Propag. 54, 2048-2053.

24. **Umul Y. Z., (2005)** "Diffraction by A Black Half Plane: Modified Theory of Physical Optics Approach," Opt. Express 13, 7276-7287.

25. **Umul Y. Z., (2008)** "Uniform Version of the Modified Theory of Physical Optics Based Boundary Diffraction Wave Theory," J. Mod. Opt. 55, 2797-2804.

26. **Umul Y. Z, (2008)** "MTPO Based Potential Function of the Boundary Diffraction Wave Theory," Opt. Laser Technol. 40, 769-774.

27. **Umul Y. Z., (2011)** "Physical Optics Theory for The Diffraction of Waves by Impedance Surfaces," J. Opt. Soc. Am. A 28, 255-262.

28. **Umul Y. Z., (2011)** "Physical Optics Theory for The Scattering of Waves by An Impedance Strip," Opt. Commun. 284, 1760-1765.

29. **Umul Y. Z., (2011)** "Physical Optics Scattering of Waves by A Half-Plane with Different Face Impedances," IEEE Antennas Wireless Propag. Lett. 10, 21-24.

30. **Umul Y. Z., (2011)** "The Physical Optics of Phase-Conjugate Mirrors: Scalar Theory," Opt. Commun. 284, 2687-2689.

31. **Umul Y. Z., (2012)** “Physical Optics Theory Of Resistive Surfaces,” Opt. Laser Technol. 44, 357-361.

32. **Umul Y. Z., (2012)** “Physical Optics Integral of Creeping Waves,” J. Electromagn. Waves Appl. 26, 1203-1214.

33. **Pathak P.**, **(1979),** “An Asymptotic Analysis of the Scattering of Plane Waves by A Smooth Convex Cylinder”, Radio.Sci., vol.14, pp. 419-435.

34. **Kouyoumjian R. G., (1965)**, “Asymptotic High-Frequency Methods”, Proc. IEEE, vol.53, pp.864-876.

35. **Borghi F., Santarsiero M., Frezza F., Schettini G.**, **(1996),** “Plane-Wave Scattering by A Perfectly Conducting Circular Cylinder Near a Plane Wave Surface: Cylindrical-Wave Approach”, J. Opt. Soc. Am., vol. 13, pp. 483-493.

36. **Keller J. B.**, **(1956),** “Diffraction by A Convex Cylinder”, IRE. Trans. On Antennas and Propagation, vol. AP-4, pp. 312-321.

37. **Rayliigh L., (1881),** “On The Electromagnetic Theory of Light”, Phill. Mag. (GB), vol.12, pp. 81-101.

38. **Epstein P. S., (1914),** “Ph.D. Dissertation”, Munich, Germany.

39. **Debye P., (1908),** "Das Electromagnetisch Feld um einen Zylinder und Die Theorie des Regenbogens", Phys. Z., vol.9, pp.775-779.

40. **Riblet H. J., (1959),** "Second Order Geometric Optic Currents on A Cylinder", in Proc.McGill Symp. On Microwave Optics, pt. II Bedford, Mass.: Electronics Research Directorate, AF Cambridge Research Center, pp. 215-225.

41. **Wetzel L., (1957),** "High Frequency Current Distributions on Conducting Obstacles", Cruft Lab., Harvard University, Cambridge, Mass., Scientific Rept. 10, Contract AF 19, pp.604-786.

42. **Waith J. R., (1959),** "Electromagnetic Radiation from Cylindrical Structures", Pergamon, New York, Based on NBS Rept. 5553, 1958.

43. **Lawrence D. E., Sarabandi K., (2002**), "Electromagnetic Scattering from A Dielectric Cylinder Buried Beneath A Slightly Rough Surface", IEEE Trans Antennas and Propagation, vol. 50, no. 10.

44. **Yalçın U., (2007)**, "Scattering from A Cylindrical Reflector: Modified Theory of Physical Optics Solution", J. Opt. Soc. Am. A., vol. 24, no.2, pp.502-506.

45. **Borghi R., Gori F., Santarsiero M., Frezza F., Schettini G., (1996),** “Plane Wave Scattering by A Perfectly Conducting Circular Cylinder Near A Plane Surface: Cylindrical-Wave Approach”, J. Opt. Soc. Am. A., vol. 13, no.3, pp.483-493.

46. **Büyükaksoy A., Uzgören G., (1988),** “Diffraction of High Frequency Waves by A Cylindrically Curved Surface with Different Face Impedance”, IEEE Transactions on Antennas and Propagation, vol. 36, no.5, pp.592-600.

47. **Umul Y. Z., Yengel E., Aydın A., (2003),** “Comparison of Physical Optics Integral and Exact Solution for Cylinder Problem”, in Proceedings of ELECO 2003, Third International Conference on Electrical and Electronics Engineering, Bursa, Turkey, pp.245-248, 31-34.

48. **Syed H. H., Volakis J. L., (1996),** “PTD Analysis of Impedance Structures”, IEEE Trans. Antennas Propagat., vol. 7, pp. 983-988.

49. **Michaeli A., (1993),** “Application of Physical Optics and Physical Theory of Diffraction to A Smooth Convex Surface”, J. Electromagnetic Waves App., vol. 7, pp. 1623-1631.

50. **Rubinowicz A., (1957),** “Thomas Young and the Theory of Diffraction”, Nature, vol. 180, pp. 4-162.

51. **Maggi G.A., (1888),** "Sulla Propagazione Libre e Perturbata Delle Onde Luminose in un Mezzo Izotropo", Ann. Mat., vol. 16, pp. 21-48.

52. **Rubinowicz A., (1917),** "Die Beugungswelle in der Kirchoffschen Theorie der Beugungserscheinungen", Ann. Phys., vol. 4, pp. 78-257.

53. **Umul Y. Z. (2013)** "A New Representation Of The Kirchhoff's Diffraction Integral,"Opt. Commun.

54. **Umul Y. Z., (2008)** "Modified Diffraction Theory of Kirchhoff," J. Opt. Soc. Am. 25, 1850-1860.

55. **Ganci S., (1995),** "A General Scalar Solution for The Half-Plane Problem", J. Mod. Opt., vol. 42, pp. 11-1707.

56. **Ganci S., (1996),** "Half Plane Diffraction in Case of Oblique Incidence", J. Mod. Opt., vol. 43, pp. 51-2543.

57. **Ufimtsev P. Ya., (1971),** "Method of Edge Waves in The Physical Theory of Diffraction", Air force system command, foreign tech. div. document ID No. FTD-HC-23-259-71 (Translation from the Russian version published by Soviet Radio House, Moscow, 1962).

58. **Umul Y. Z., (2009),** “Rigorous Expressions for The Equivalent Edge Currents”, Progress in Electromagnetic Research B., vol. 15, pp. 77-94.

59. **Büyükaksoy A., Uzgören G., (1987**), “High-Frequency Scattering from The Impedance Discontinuity on A Cylindrical Curved Impedance Strip”, IEEE Trans. Antennas. Propagat., vol. 35, pp. 234-236.

60. **Akduman I., Büyükaksoy A., (1995),** “Asyyptotic Expressions for The Surface Currents Induced on A Cylindrically Curved Impedance Strip”, IEEE Trans. Antennas. Propagat., vol. 43, pp. 453-463.

61. **Umul Y. Z., (2008),** “Scattering of A Line Source by A Cylindrical Parabolic Impedance Surface”, J. Opt. Soc. A., vol. 25, pp. 1652-1659.

62. **Hacıvelioğlu F., Sevgi L., Ufimtsev, P. Ya., (2011),** “Electromagnetic Wave Scattering from A Wedge with Perfectly Reflecting Boundaries: Analysis of Asymptotic Techniques”, IEEE Antennas Propogat. Mag., vol. 53, pp. 232-253.

63. **Michaeli, A. (1989)** “Transition Functions for High-Frequency Diffraction by A Curved Perfectly Conducting Wedge. I. Canonical Solution for A Curved Sheet”, IEEE Trans. Antennas and Propag., Vol.37, pp.1073-1079.

64. **Serbest, A. H., Büyükaksoy, A., and Uzgoren, G. (1989)** "Diffraction of High-Frequency Electromagnetic Waves by Curved Strips", IEEE Trans. Antennas and Propag., Vol.37, pp.592-600.

65. **Molinet, F. A. (2005)** "Edge-Excited Rays On Convex and Concave Structures: A Review", IEEE Antennas and Propag., Vol.47, pp.34-46.

66. **Idemen, M. and Felsen, L. B. (1981),** "Diffraction of A Whispering Gallery Mode By The Edge Of A Thin Concave Cylindrically Curved Surface", IEEE Trans. Antennas and Propag., Vol.AP-29, pp.571-579.

67. **Yalçın U., Sarnik M. (2013),** "Uniform Diffracted Fields from A Cylindrical Reflector with Modified Theory of Physical Optics", The Sci. Word J., vol. 2013, pp. 1-6.

68. **Keller, J. B., Lewis, R. M., Seckler, B. D. (1956)** "Asymptotic Solution of Some Diffraction Problems", Cornrnun. Pure. Appl,. Math, Vol. 9, pp. 207-265.

69. **Büyükaksoy, A., Uzgören, G. (1987)** "High-Frequency Scattering from The Impedance Discontinuity On A Cylindrically Curved Surface", IEEE Trans. Antennas Propag., Vol. 35, pp. 234-236.

70. **Umul Y. Z., (2008),** "Fringe Waves Radiated by A Half-Plane for The Boundary Conditions of Neumann", App. Phys. B., vol. 93, 885-889.

71. **Syed H., Volakis J. L., (1996),** "PTD Analysis of Impedance Structures", IEEE Trans. Antennas. Propogat., vol. 44, pp. 983-988.

72. **Casciato M. D., Sarabandi K., (2001),** "Scattering from A Land-Sea Transation", IEEE Antennas Propogat. Symp., vol. 1, pp. 452-455.

73. **Casciato M. D., (2001),** "Radio Wave Diffraction and Scattering Models for Wireless Channel Simulations", Ph.D. Thesis. , Univ. of Michigan.

74. **Corona P., D'Ambrosio G., Franceschetti G., (1979**), "Scattering Properties of Satellite-Borne Solar Cell Panels", IEEE Trans. Antennas. Propogat., vol. 27, pp. 496-499.

75. **Bucci O. M., Francesschetti G., (1976),** "Electromagnetic Scattering by A Half-Plane with Two Face Impedance", Radio. Sci., vol. 11, pp. 49-59.

76. **Shevernev, V. I. (2005)** "Diffraction of An Inhomogeneous Plane Wave By A Half Plane", Radiophys. Quantum Electron, Vol. 19, pp. 1285-1291.

77. **Bertoni, H. L., Green, A. C., Felsen, L. B. (1978)** "Shadowing an Inhomogeneous Plane Wave by an Edge", J. Opt. Soc. Am., Vol. 68, pp. 983-989.

78. **Deschamps, G. A., Lee, S. W., Gowan, Fontana, E. T. (1979)** "Diffraction of an Evanescent Plane Wave by A Half Plane", Wave Motion, Vol. 1, pp.25-35.

79. **Kouyoumjian, R. G., Manara, G., Nepa P., Taute, B. J. E., (1996)** "The Diffraction of an Inhomogeneous Plane Wave by A Wedge", Radio Sci., Vol. 31, pp.1387-1397.

80. **Manara, G., Nepa P., Kouyoumjian, R. G., Taute, B. J. E., (1998)** "The Diffraction of an Inhomogeneous Plane Wave by an Impedance Wedge in A Lossy Medium", IEEE Trans. Antennas Propag., Vol. 46, pp. 1753-1755.

81. **Keller, J. B., Streifer, W., (1971)** "Complex Rays with an Application to Gaussian beams", J. Opt. Soc. Am., Vol. 61, pp. 40-43.

82. **Choudary, S., Felsen, L. B., (1973)** "Asymptotic Theory for Inhomogeneous Waves", IEEE Trans. Antennas Propag., Vol. 21, pp. 827-842.

83. **Wang, W. D., Deschamps, G. A., (1974)** "Application of Complex Ray Tracing to Scattering Problems", Proc. IEEE, Vol. 11, pp. 1541-1551.

84. **Felsen, L. B., (1976)** "Evanescent waves", J. Opt. Soc. Am., Vol. 66, pp. 751-760.

85. **Umul, Y. Z., (2007)** "Uniform Theory for The Diffraction of Evanescent Plane Waves", J. Opt. Soc. Am., Vol. 24, pp. 2426-2430.

86. **Ronchi, L., Russo V., Francia, G. T. D., Zaccagnini, C., (1961)** "Scattering of Evanescent Waves by Cylindrical Structures", Opt. Acta, Vol. 8, pp. 281-299.

87. **Jackson, J. D. (1962)** "Classical Electrodynamics", John Wiley & Sons, New York.

88. **Umul, Y. Z., (2014)** "Diffraction of Waves by a Resistive Half-Plane", Optics Communications, pp. 6-12.

89. **Umul, Y. Z., (2007)** "Diffraction of HOMOGENEOUS and Inhomogeneous Plane Waves By A Planar Junction Between Perfectly Conducting And Impedance Half Planes", Journal of Optical Society of America, Vol. 24, pp. 1786-1792.

90. **Saleh, B. E. A., Teich, M. C., (2007)** "Fundamentals of Photonics", John Wiley & Sons, Second edition.

91. **Green, A. C., Bertoni, H. L., Felsen, L. B. (1979)** "Properties of the Shadow Cast by a Half-Screen when Illuminated by a Gaussian Beam", Journal of Optical Society of America,503.

92. **Umul, Y. Z., (2007)** “Edge-Dislocation Waves in The Diffraction Process By An Impedance Half-Plane”, J. Opt. Soc. Am., Vol. 24, pp. 507-511.

93. **Umul, Y. Z., (2012)** “Boundary Diffraction Wave Theory of Junctions Between Two Surfaces with Different Face Impedances, Optics & Laser Technology, Vol. 44, pp. 1312-1317.

94. **Umul, Y. Z., (2011)** “Boundary Diffraction Wave Theory of Resistive Surfaces With Edge Discontinuities”, Optics Communications, Vol. 284, pp. 5269-5274.

APPENDICES

A.1 The Stationary Phase and Edge Point Methods

A.1.1 Stationary phase point method [78]

Radiation integrals consist of an amplitude function times a phase function. In many cases an asymptotic evaluation is employed if the amplitude function varies slowly whereas the phase function varies rapidly. For our problem we consider the integral,

$$I = \int_a^b f(x)\, e^{j\beta\gamma(x)} dx\ , \tag{A.1}$$

where f(x) and γ(x) are real functions, and β is a large number. The integral endpoints can be infinite. If f(x) is slowly varying and βγ(x) is rapidly varying functions over the interval of integration due to β being large, the main contribution to the integral comes from the stationary phase point. If there exist more than one stationary points, the contribution of all these stationary points will be summed up. A stationary phase point is defined as a point where the first derivative of the phase function γ is equal to zero:

$$\frac{d\gamma}{dx} = 0, \tag{A.2}$$

meaning that the function $\gamma(x)$ is maximum at x_0. If $\gamma(x)$ is multiplied by β, the difference between the maximum-valued γ and any other x-valued γ will rapidly increase resulting in a rapid exponential growth of the integrand. Therefore, the significant contribution to the integral will come from the points that are close to x_0.

If we expand the phase function in a Taylor series around the stationary phase point, the following expression can be written:

$$\gamma(x) \cong \gamma_0 + (x - x_0)\gamma_0' + \frac{1}{2}(x - x_0)^2\gamma_0'' + \cdots \ , \qquad \text{(A.3)}$$

where γ_0' and γ_0'' represent the derivatives of γ with respect to x, evaluated at x_0. Now γ_0' is assumed as zero by definition in the neighborhood of the point of stationay phase the quantity (x-x_0) is small and therefore the high-order terms (i.e., order 3 and higher) in Eq. (A.2) may be neglected. If there is only one stationay point x_0 in the interval from a to b, and x_0 is not close to either a or b, the Eq. (A.1) can be written as,

$$I = \int_{x-\delta}^{x+\delta} f(x)e^{j\beta\gamma_0}e^{j\beta(x-x_0)^2\gamma_0''/2}dx, \qquad \text{(A.4)}$$

when $\gamma_0'' \neq 0$ where δ represents a small number. By doing this we reduce the range of integration to a small neighborhood about the stationary phase point. If f(x) is slowly varying, it can be approximated over this small interval. In this case Eq. (A.3) becomes,

$$I_0 = f(x_0)e^{j\beta\gamma_0}\int_{-\infty}^{\infty} e^{j\beta(x-x_0)^2\gamma_0''/2}dx, \qquad \text{(A.5)}$$

$$I_0 = f(x_0)e^{j\beta\gamma_0}\int_{-\infty}^{\infty} e^{j\beta z^2\gamma_0''/2}dz, \qquad \text{(A.6)}$$

where (x-x0)=z. For convenience, the limits of integration are changed to infinity. This causes a little error which can be neglected. In other regions, the rapid phase variations will cancel each other because of the slowly varying characteristics of f(x). Now let us consider the integral

$$\int_{-\infty}^{\infty} e^{jaz^2} dz. \tag{A.7}$$

Eq. (A.7) can be written via the Euler's formula as,

$$\int_{-\infty}^{\infty} (\cos az^2 + j \sin az^2) dz. \tag{A.8}$$

By solving this equation we obtain,

$$\sqrt{\frac{\pi}{|a|}} e^{j\frac{\pi}{4} sgn(a)} \quad , \tag{A.9}$$

where,

$$sgn(a) = \begin{cases} -1, & a < 0 \\ 1, & a > 0 \end{cases} . \tag{A.10}$$

To evaluate Eq. (A.4), Eq. (A.5) is used and as a result the stationary phase approximation results in,

$$I = \int_{x-\delta}^{x+\delta} f(x) e^{j\beta\gamma(x)} dx \approx f(x_0) e^{j\beta\gamma(x_0)} \sqrt{\frac{2\pi}{\beta|\gamma_0''|}} e^{j\frac{\pi}{4} sgn(x_0)} . \tag{A.11}$$

If more than one stationary phase points exist in the integration interval and there is no coupling between them, the total value of the integral is obtained by summing the contributions of all these stationary points. Eq. (A.9) is invalid if the second derivative of the phase function is zero at the stationary phase point. In that case, the third-order term in Eq. (A.2) is used. In addition, Eq. (A.9) becomes invalid if one of the limits of integration is close to the stationary phase point. For this case we can express the integral in the form of a Fresnel integral. One more problem arises if there exist two or more stationay points close together in the integration range. To obtain the endpoint contribution, it is reasonablet to write Eq. (A.1) as,

$$I = \int_{-\infty}^{\infty} f(x)e^{j\beta\gamma(x)}dx - \int_{b}^{\infty} f(x)e^{j\beta\gamma(x)}dx - \int_{-a}^{\infty} f(-x)e^{j\beta\gamma(-x)}dx, \qquad \text{(A.12)}$$

or

$$I = I_0 - I_b - I_a, \qquad \text{(A.13)}$$

Evaluation of I_0 has been done in Eq. (A.9). I_b, for instance, can be evaluated via integration by parts with the wave number to be complex and to have a small amount of loss (i.e., small α) so that the contribution to the integral by the upper limit at infinity vanishes, and then letting the wave number to be approximated by β,as before. Thus,

$$I_b \cong -\frac{1}{j\beta}\frac{f(b)}{\gamma'(b)}e^{j\beta\gamma(b)}. \qquad \text{(A.14)}$$

A similar expression can be found for I_{-a}. Eq. (A.12) is valid when the limit value “b” is not near or coupled to x_0. When the stationary point is coupled to the endpoint, it is written that,

$$I_b \cong u\big(-sgn(b - x_0)\big)I_0 + sgn(b - x_0)\times f(b)e^{j\beta\gamma(b)\mp jv^2}\sqrt{\frac{2}{\beta|\gamma_0''|}}F_{\pm}(v), \qquad \text{(A.15)}$$

where,

u is the unit step function

$F_{\pm}(v)$ is the Fresnel integral

$$\gamma''(b) \neq 0, \tag{A.16}$$

and

$$v = \sqrt{\frac{\beta}{2|\gamma_0''(b)|}}|\gamma_0''| \,. \tag{A.17}$$

A.1.2 Edge Point Method

For the edge diffraction this method is employed. The integral,

$$\int_a^\infty f(x)exp\big(-jkg(x)\big)dx, \tag{A.18}$$

can be written as,

$$\int_a^\infty f(x)\frac{g'(x)}{g'(x)}exp\big(-jkg(x)\big)dx. \tag{A.19}$$

If the method of integration by parts,

$$\int_a^b udv = uv - \int_a^b vdu, \tag{A.20}$$

is applied by assuming,

$$u = \frac{f(x)}{g'(x)}\,, \tag{A.21}$$

we write,

$$du = \frac{f'(x)g\prime(x) - f(x)g\prime\prime(x)}{[g\prime(x)]^2}, \tag{A.22}$$

and,

$$dv = g'(x)exp\big(-jkg(x)\big). \tag{A.23}$$

By assuming,

$$v = -\frac{1}{jk}exp\big(-jkg(x)\big), \tag{A.24}$$

the integral becomes as,

$$\int_a^\infty f(x)\frac{g\prime(x)}{g\prime(x)}exp\big(-jkg(x)\big) = \left[\frac{f(x)}{g\prime(x)}\left(-\frac{1}{jk}\right)exp\big(-jkg(x)\big)\right]_a^\infty -$$

$$\int_a^\infty -\frac{1}{jk}exp\big(-jkg(x)\big)\left[\frac{f'(x)g'^{(x)} - f(x)g''^{(x)}}{\left[g'^{(x)}\right]^2}\right]dx. \tag{A.25}$$

If the integration by parts method is used for the integral term on the right hand side of the equality, this will result in terms having k^2 or in the denominators which make the integral negligible due to the high value of “k” at high frequencies. As a result, the integral will be approximately as,

$$\int_a^\infty f(x)\frac{g\prime(x)}{g\prime(x)}exp\big(-jkg(x)\big)dx \cong \left[\frac{f(x)}{g'^{(x)}}\left(-\frac{1}{jk}\right)exp\big(-jkg(x)\big)\right]_a^\infty. \tag{A.26}$$

This approach is known as the Edge Point Method.

A.2 CURRICULUM VITAE

PERSONAL INFORMATION

Surname, Name: KARA, Mustafa
Date and Place of Birth: Sept. 25, 1967 - Trabzon
Email: mustafa.kara@odu.edu.tr

EDUCATION

M.Sc., Çankaya University Electronic and Communication Engineering, 2008.
B.Sc., Middle East Technical University Electrical and Electronics Engineering, 1991.

WORK EXPERIENCE

1993-2006,	Karadeniz Technical University Ordu MYO, Electronic Communication Department, Instructor, Ordu / Türkiye.
1993-1994,	Delaware Technical & Community College, Visiting Instructor, Dover / Delaware / USA.
2006- Now,	Ordu University TBMYO, Electronics & Automation Department, Instructor, Ordu / Türkiye.

FOREIGN LANGUAGES

Upper Intermediate English

PUBLICATIONS

1. Paketimsi ve Kırınmayan Işınların Atmosferde Bir Engel Tarafından Kırınması, Çankaya University Journal of Science and Engineering, Vol. 8, No:1, May 2011.
2. Scattering of a Plane wave by a Cylindrical Parabolic Perfectly Electric Conducting Reflector, Optik, Vol. 127, Issue 10, pp. 4531-4535, May 2016.